Leaching kinetics of carbonatite and silicate based chalcopyrite minerals

B Barlow

orcid.org/ 0000-0001-9338-0732

Dissertation accepted in fulfilment of the requirements for the degree *Master of Engineering in Chemical Engineering* at the North West University

Supervisor: Prof. E Fosso-Kankeu

Co-supervisor: Prof. F.B Waanders

Graduation: May 2020

Student number: 25030973

Higher Degrees Administration

SOLEMN DECLARATION AND PERMISSION TO SUBMIT

Solemn declaration by student

I, Brad Barlow

declare herewith that the thesis/dissertation/mini-dissertation/article entitled (**exactly as registered/approved title**),

Leaching kinetics of carbonatite and silicate based chalcopyrite minerals

which I herewith submit to the North-West University is in compliance/partial compliance with the requirements set for the degree:

MEng Chemical Engineering

is my own work, has been text-edited in accordance with the requirements and has not already been submitted to any other university.

LATE SUBMISSION: If a thesis/dissertation/mini-dissertation/article of a student is submitted after the deadline for submission, the period available for examination is limited. No guarantee can therefore be given that (should the examiner reports be positive) the degree will be conferred at the next applicable graduation ceremony. It may also imply that the student would have to re-register for the following academic year.

Ethics number: ENG-2019-128

ORCID: 0000-0001-9338-0732

Signature of Student: Brad Barlow — Digitally signed by Brad Barlow Date: 2019.11.21 19:53:26 +02'00'

University Number: 25030973

Signed on this 21 day of November of 2019

Permission to submit and solemn declaration by supervisor/promoter

The undersigned declares that the thesis/dissertation/mini-dissertation complies with the specifications set out by the NWU:

- with regards to A-rules (PhD students shoud have at least one paper on aspects of the thesis submitted for review in an accredited scientific journal) Yes ○ No ○ Not applicable (n/a) ●
- with regards to faculty rules on submission or acceptance by an accredited scientific journal: Yes ● No ○ n/a ○
- with regards to faculty rules on peer reviewed conference proceedings: Yes ○ No ○ n/a ○
- the student is hereby granted permission to submit his/her mini-dissertation/ dissertation/thesis: Yes ● No ○
- that the student's work has been checked by me for plagiarism (by making use of Turnitin software for example) and a satisfactory report has been obtained: Yes ● No ○

and that the work was language edited before submission for examination.

Signature of Supervisor/Promoter

Elvis Fosso-Kankeu — Digitally signed by Elvis Fosso-Kankeu Date: 2019.11.22 06:06:54 +02'00'

Date 22/11/2019

Original details: Marietjie Ackermann(10512187) P:\Support docs\SOLEMN DECLARATION AND PERMISSION TO SUBMIT.docm 28 July 2017
File reference: 7.1.11.3.2

ACKNOWLEDGEMENTS

I would like to give special thanks to the North West University for this opportunity as well as the use of the laboratory at the School of Chemical and Minerals Engineering & the University of Johannesburg for the use of their laboratory equipment. I want to acknowledge PMC and Ruashi holdings for supplying the material on which the study is based. A special thanks goes to Prof Elvis Fosso-Kankeu and Mr J. Kolela Nyembwe for their guidance, advice and support of which without the study would not have been a success. I would further like to convey a special thanks to my family, friends and other colleagues who provided additional support, love and assistance during the course of the study.

ABSTRACT

Copper (Cu) is a widely used metal with high thermal and electrical conductivities, which is primarily extracted from the low-grade Cu sulphide mineral, chalcopyrite. Hydrothermal extraction is the preferred process for leaching this mineral; however, recovery is typically low, as a passivation layer is formed on the mineral surface. This study investigated carbonate minerals from Phalaborwa, South Africa, and siliciclastic minerals from Katanga, Democratic Republic of Congo, by applying chemical leaching with ferric sulphate in a sulphuric acid medium, where pH evolution was allowed to occur. This was done in accordance with the aim of the study, which was the comparative evaluation of the leaching behaviour of various chalcopyrite minerals for Cu recovery determination. The objectives of the study were to evaluate the leaching behaviour of the minerals at different temperature conditions, and the effect of the mineral species formed; four temperatures were considered (25℃, 45℃, 65℃, 85℃). Magnetite was also investigated as a potential additive for enhancing leaching behaviour. To investigate the mineralogical and chemical compositions of the minerals, X-ray Diffraction and X-ray fluorescence were used, respectively. To predict the mineral species present in the aqueous solution of the observed minerals, PHREEQC simulation software with input parameters of pH, ORP, acidity, alkalinity, Cl^- and SO_4^{2-}, was used. The carbonatite associated with calcite-magnesium and dolomite displayed acid-consuming behaviour – rise in temperature was concurrent with rise in pH levels, thereby promoting alkaline conditions; retardation of the Cu recovery rate was observed under these alkaline conditions, likely due to the mineral's surface being covered by a matrix mixture of gypsum and hematite, as well as ferric salts that restrict the transport of electrons from the mineral surface. The highest rates, albeit low, were observed at lower temperatures, were the formation of insoluble Cu species and the formation of gypsum reduced. Magnetite was identified as an effective additive during the mineral dissolution of both carbonatite minerals: 12.84% for run of mine and 20.94% for tails where achieved after 12 hours dissolution at 85℃; acidic conditions (pH 1-2) were promoted by the inclusion of magnetite, which promoted Cu solubility and, by extension, improved recovery behaviour. The silicate mineral associated with various silica species of quartz displayed characteristics of acid attack, which intensified with temperature increase, as pH was maintained at low levels (pH 1-2). Recovery of Cu was favoured under these conditions, as it allowed for the minimisation of ferric salt species (19.49% recovery at 85℃). The presence of pyrite also enhanced leaching through galvanic interactions with chalcopyrite. Cu extraction was not as effective (15.78%) when the silicate mineral was treated with magnetite, as low pH conditions (pH<1) favourable to ferric salt formation of jarosite was present, along with the formation of gypsum. With lower accumulation of pyrite, the effects of the Galvanox process was also reduced. It can be concluded that the recovery rate of copper from chalcopyrite host ores, in ferric sulphate solution, was enhanced at conditions where siliciclastic host ores, providing acidic conditions, were leached at high temperatures. The extraction behaviour of copper from the carbonate mineral was greatly affected by the host ores' inability to naturally provide low pH levels, as a result of

high concentration of alkaline earth species. Lastly, improved recovery from the carbonite dominant mineral could be achieved by the inclusion of magnetite as it was identified as a positively enhancing agent for the extraction of copper from the host ore with an intrinsic high-pH affinity.

Keywords: chalcopyrite, magnetite, mineralogy, sulphate media, tails, temperature

PRESENTATIONS AND PUBLICATIONS

Results linked to this study were submitted and presented in conference proceedings, and were submitted for publication in a peer-reviewed journal.

Conference proceedings:

[1] Barlow, B., Nyembwe, K., Fosso-Kankeu, E. & Waanders, F.B, November 2018. *Prediction of dissolution of copper from a chalcopyrite carbonatite ore of South Africa*. 10th International Conference on Advances in Science, Engineering, Technology and Natural Resources. Cape Town

[2] Barlow, B., Fosso-Kankeu, E., Nyembwe, K., Waanders, F.B. & Malenga E.N., November 2019. *The Kinetic Dissolution of Copper from Chalcopyrite-containing Carbonatite Tailings Samples in Sulphate Media.* 11th International Conference on Advances in Science, Engineering, Technology and Natural Resources. Johannesburg

Journal publications

[1] Barlow, B., Fosso-Kankeu, E., Nyembwe, K. & Waanders, F.B., *Leaching kinetics of copper from different chalcopyrite ores (Silicates & Carbonatites) Part 1: Effects of Temperature and varying Mineralogy.* Submitted to journal for publication

[2] Barlow, B., Fosso-Kankeu, E., Nyembwe, K. & Waanders, F.B., *Leaching kinetics of copper from different chalcopyrite ores (Silicates & Carbonatites) Part 2: Effects of additives (Magnetite) and carbonate tailings investigation.* Submitted to journal for publication

TABLE OF CONTENTS

LIST OF ABBREVIATIONS AND ACRONYMS

CAC	Central African Copper-belt
COD	Chemical oxygen demand
Cr	Carbonatite run of mine
Cr_mag	Carbonatite run of mine treated with magnetite
Ct	Carbonatite tailings
Ct_mag	Carbonatite tailings treated with magnetite
DRC	Democratic Republic of the Congo
ICP-OES	Inductively coupled optical-emission spectroscopy
ORP	Oxidation redox potential
ROM	Run of mine
SEM	Scanning electron microscopy
SEM-EDS	Scanning electron microscopy with energy dispersive spectroscopy
Sr	Silicate run of mine
Sr_mag	Silicate run of mine treated with magnetite
XPS	X-ray photoelectron microscopy
XRD	X-ray diffraction
XRF	X-ray florescence spectroscopy

LIST OF FIGURES

LIST OF TABLES

Dissertation structure

Chapter 1: Background and motivation

This chapter provides an introduction into the study, as well as the motivation and reasoning behind the study. The problem statement, linked to the motivation, is also discussed, as are the aims and objectives that were pursued for successful completion of the study.

Chapter 2: Literature review

In this chapter, the literature relevant to this study is discussed. This includes information on the different leaching processes, these being pyrometallurgical and hydrometallurgical extraction, different leaching mediums, an in-depth discussion of the passivation mechanism, relevant causes, and information linked to desirable conditions for dissolution of chalcopyrite. The minerals of focus for this study is also discussed and elaborated on further.

Chapter 3: Behavioural observation of the leaching kinetics of copper from different chalcopyrite bearing ores with regards to change in temperature and varying mineralogical background. This chapter contains a comparative evaluation of the leaching performance of copper from chalcopyrite contained in carbonatite and silicate host ores during leaching under different temperature conditions.

Chapter 4: Determination of the effects of additives on the leaching performance of copper from different chalcopyrite-bearing host ores.

This chapter contains an evaluation of the leaching performance of the different chalcopyrite-bearing ores at optimal temperature range, under the effects of magnetite addition as an additive.

Chapter 5: Conclusion and recommendations

In this chapter, the conclusion of the study is discussed, along with all recommendations for future investigations.

Chapter 1: Background and motivation

1.1 Introduction

Copper (Cu) has been used for thousands of years, due to it being one of the few elements to occur in nature in its metallic form (native copper), and because of its range of malleable and conductive properties (Copper Development Association, 2004). These days, most copper is present in combination with other elements within an ore body, and is mined using open-pit as well as underground mining techniques. The amount of copper that exists is vast, with approximations of $10^{\wedge 14}$ tons in the top kilometres of the Earth's crust. Copper is used in electric wiring and electronics (accounting for nearly 65% of its use) due to its high thermal and electrical conductivity, which is second only to silver (Cotton & Wilkinson, 1980). Copper is corrosion-resistant and can be used as an antifouling agent, making it very effective in the line parts of ships where it prevents the growth of barnacles and mussels (Jerabek et al., 2016). Additionally, copper is ductile and malleable, which means it can be shaped and moulded without the metal breaking; it is also an excellent alloy, and it is used to form brass and bronze when combined with zinc and tin, which are both harder and stronger than copper (Stanley, 2013). Copper's recycling rate is higher than any other engineering metal, as the metal retains its chemical and physical properties after being recycled, thus, copper can be recycled perpetually (Copper Development Association, 2004).

Ore deposits of copper are present on every continent and have been mined for more than 10 000 years; however, it is estimated that 95% of copper in circulation was mined in the last 100 years (Stanley, 2013). In the 21st century, most copper mining facilities are open-cast mines from which copper is usually extracted from oxide and sulphide minerals. Extraction processes differ for oxide and sulphide-copper-containing ores, as the chemistries of these ore bodies differ; the extraction processes are hydrometallurgy and pyrometallurgy, respectively. Copper is also present in carbonate ores such as malachite, and silicate ores such as chrysocolla. The biggest producer of copper in the world is Chile, with reserves estimated at 210 million metric tons in 2015; Australia and Peru are second, with both countries producing 13% of the world's copper supply (Jamieson, 2016).

South Africa's leading copper producer is the Rio Tinto Copper Mine in Phalaborwa, Limpopo, of which the majority of shares is held by Rio Tinto plc (Beale, 1985a). The mine is also a major producer of vermiculite and zirconium oxide minerals, as well as one of the largest open-pit mines in the world. The open-pit mining operations that started in 1964 ceased in 2002, when the mine reached its final economically feasible depth. Since then, the mine has started underground mining operations to extend the mine's lifespan by a further 20 years (Palabora Mining Company, 2012). The copper ore body at the Rio Tinto Copper Mine is hosted in a carbonatite, in which the highest concentrations (1.0%) are present at the core. The carbonatite complex is geologically unique, as it

is the only carbonatite complex in the world that contains sufficient amounts of copper sulphide minerals for the operations to be economically feasible (Heinrich, 1970). Due to the low grade of copper within the carbonate complex, current operations first leach the ROM to a concentrate before extracting copper from the chalcopyrite-containing mineral.

The Democratic Republic of the Congo (DRC) and Zambia are the biggest producers of copper on the African continent. This feat is due to Central African Copper-belt (CAC), of which the greatest portion lies in the DRC (Lydall & Auchterlonie, 2011). The CAC contains approximately 40% of the world's copper reserves, making it the second largest global reserve. The Lufilian Arc, a major geological structure within the CAC, contains extensive high-grade copper minerals. Grades of copper in this region have been reported to reach as high as 7-8% (Lydall & Auchterlonie, 2011). Operations in this region typically report copper grades of 1-4%. The CAC comprises more siliciclastic sediments on the Zambian side, to more evaporitic-carbonate-rich sediments on the DRC side of the copperbelt (Theron, 2013). The copperbelt contains silicate sediments from which copper is extracted from the chalcopyrite host mineral; though carbonate-rich sediments are also present within the copperbelt. The copper is leached straight from the feed stream samples (ROM) of these high copper grades that are found within the silicate minerals.

Copper is found in various ore bodies, which each face their own challenges regarding the extraction process. Chalcopyrite, which accounts for 70% of all copper-bearing minerals, faces various challenges that hinder the leaching process (Schaming, 2011). Most industrial applications make use of pyrometallurgical methods (80-85% of copper extracted from chalcopyrite), although it is not considered to be eco-friendly (Li et al., 2013). Though hydrometallurgical methods are both more economical and more environmentally friendly than pyrometallurgical methods, they are not widely applied in industry, as current methods deliver lower extraction than the latter (Li et al., 2013). Compared to other sulphide-copper-bearing minerals, such as chalcocite, chalcopyrite delivers lower extraction rates. The low extraction rate is believed to the result of a passivation film forming on the chalcopyrite surface (Biegler & Swift, 1979; Schaming, 2011).

1.2 Problem statement

The challenge affecting the extraction of copper from chalcopyrite, as opposed to other copper-sulphide ores, such as chalcocite, is the low extraction rate, which is believed to be due to a passivation film forming on the mineral surface (Barlow et al., 2018). Passivation refers to the state at which a material is considered to become passive, i.e., when a material is described as being less affected or corroded by the surrounding environment. During passivation, an outer layer is said to form on the surface of the material due to chemical interactions with other substances (Roll, 2014). Passivation is not always desired, for instance, in the case of chemical leaching of chalcopyrite. During the treatment of chalcopyrite, a passivation film is formed, which decreases the effects of the

lixiviant on the ore body, thereby acting as a shield to substantially decrease the rate at which copper is leached from the surface of the ore body, and subsequently preventing interaction of the lixiviant with the surface (Schaming, 2011). The formation of elemental sulphur, which is produced during the ferric leaching of chalcopyrite, as well as polysulphides that form as a result of solid-state changes, have both been assumed to be the cause of the passivation film (Tshilombo, 2004; Li et al., 2010). Metal-deficient layers that build up progressively during mineral dissolution on the mineral surface have also been theorised to be a main cause, though this theory has been disproven (Holmes & Crundwell, 2013).

Although the cause of passivation has not been identified thus far, various factors that influence the dissolution rate of copper from the chalcopyrite ore body have been identified and studied; among which particle size, temperature, pH levels, mineral ore bodies and additive (such as pyrite) addition. For the scope of this study, the effects of temperature, varying mineralogical background and the effects of additive addition during pH evolution, were investigated. By allowing pH evolution to occur, the effects of the gangue species within the different host ores could be observed. Previous studies indicated that leaching performance depends on the interaction of the solids contained within the host rock, with lixiviant, as well as the associated gangue species, present within the host rock (Vilca, 2013). The carbonatite ore body of Rio Tinto and the siliciclastic ore from the DRC both contain chalcopyrite, which is the main copper-bearing mineral. Carbonatite, by definition, comprises more than 50% carbonate minerals, whereas the ore body from the DRC contains silica as the hosting gangue. Cu recovery rates have been observed to improve in the presence of certain minerals, such as pyrite, which reacts in solution to sulphuric acid, leading to increased dissolution of Cu from chalcopyrite, as it is believed to be an acid-consuming reaction (Aydogan et al., 2006). Previous geological studies of the carbonatite ore from Rio Tinto identified pyrite as a trace mineral within the geological complex (Beale, 1985b) whereas the silicate host ore from the DRC contained large quantities of pyrite (Lydall & Auchterlonie, 2011). It is also known that the chemical reaction rates of minerals tend to improve at higher temperatures (Schaming, 2011). In this study, the kinetics and chemistry of Cu dissolution from these two different chalcopyrite bearing ores were examined in ferric sulphate media at varying experimental conditions of temperature, with the intent to outline the effect of gangue-related mineral, leaching pH and temperature and, lastly, to support the existing Cu recovery method employed in the two distinctive copper-bearing mines. In addition, the effects of additives during dissolution were examined with the intent of outlining the effect of the added mineral phases on the behaviour of the gangue-related species in the ferric sulphate media and leaching pH, as a means of determining if the addition of magnetite, as an additive, would aid the dissolution rate of copper from these chalcopyrite-containing mineral ores.

1.3 Aim and objectives

1.3.1 Aim

The aims of the study were as follows:

- The comparative determination of the dissolution behavior and the impact of passivation formation during the leaching of copper from different chalcopyrite bearing ores.
- The observation of dissolution behavior of different plants stream samples within the same carbonatite complex under the effect of different gangue species within the samples streams.

1.3.2 Objectives

The aims were achieved by pursuing the following objectives:

- To determine the physicochemical and mineralogical properties of chalcopyrite bearing minerals
- To assess the dissolution kinetics of chalcopyrite bearing minerals.
- To elucidate on the formation and mechanism of the kinetic barriers.
- To propose optimum parameters for efficient copper dissolution kinetics.

1.4 Hypothesis

The leaching behaviour of Cu is variable, depending on the composition of the chalcopyrite hosting ore. Gangue minerals within the host ore play an important role during diffraction of minerals into the leaching solution, as well as in the evolution of pH, which influences the mineral speciation in solution. The evolution of pH during carbonatite leaching is likely to result in alkaline conditions, as high concentrations of alkaline earth metals are present in the mineral. The silicate solution will likely be of an acidic nature, as higher concentrations of sulphide species are present. As solubility of metals is enhanced under acidic conditions, the likelihood of greater Cu recoveries during mineral dissolution of the clastic mineral are high. Kinetic leaching behaviour is also expected to change when a solution is exposed to different temperatures, with behaviour still being affected by the gangue species present.

References

Aydogan, S., Ucar, G. & Canbazoglu, M., 2006. Dissolution kinetics of chalcopyrite in acidic potassium dichromate solution. *Hydrometallurgy,* 81(1), pp. 45-51.

Barlow, B., Nyembwe, K., Wanders, F. & Fosso-Kankeu, E., 2018. *Prediction of dissolution of copper from a chalcopyrite carbonatite ore of South Africa.* CapeTown, South Africa, s.n., pp. 99-103.

Beale, C., 1985a. Copper in South Africa-Part I. *Journal of the South African Institute of Mining and Metallurgy,* 85(3), pp. 73-80.

Beale, C., 1985b. Copper in South Africa: Part II. *Journal of the South African Institute of Mining and Metallurgy,* 85(4), pp. 109-124.

Biegler, I. & Swift, D., 1979. Anodic electrochemistry of chalcopyrite. *Journal of Applied Electrochemistry,* 9(5), pp. 545-554.

Copper Development Association, 2004. *Copper and copper alloys; Composition, applications & properties.* Hertfordshire: s.n.

Cotton, F. & Wilkinson, G., 1980. 10.1016/j.hydromet.2008.04.015. In: *Advanced inorganic chemistry: A comprehensive text.* 4th ed. s.l.:Interscience Publishers, pp. 798-821.

Heinrich, E., 1970. *The Palabora Carbonatitic Complex: A Unique Copper Deposit,* s.l.: s.n.

Holmes, P. & Crundwell, F., 2013. Polysulfides do not cause passivation: Results from the dissolution of pyrite and implications for other sulphide minerals. *Hydrometallurgy,* Volume 139, pp. 101-110.

Jamieson, S., 2016. *5 Top Copper Reserves by Country.* [Online] Available at: https://investingnews.com/daily/resource-investing/base-metals-investing/copper-investing/most-copper-reserves-by-country/
[Accessed 14 March 2018].

Jerabek, A., Wall, K. & Stallings, C., 2016. *A practical application of reduced-copper antifouling paint in ,arine biological research,* s.l.: s.n.

Li, J. et al., 2010. Chalcopyrite leaching: the rate controlling factors. *Geochimica et Cosmochimica Acta,* 74(10), pp. 2881-2893.

Li, Y. et al., 2013. A Review of the Structure, Fundamental Mechanisms and Kinetics of the Leaching of Chalcopyrite. *Advances in Colloid and Interface Science,* 197-198(September), pp. 1-32.

Lydall, M. & Auchterlonie, A., 2011. *The Democratic Republic of the Congo and Zambia: A Growing Global Hotspot for Copper-Cobalt Mineral Investment and Exploitations,* s.l.: s.n.

Palabora Mining Company, 2012. *About Palabora.* [Online] Available at: http://www.palabora.com/palabora.asp [Accessed 12 May 2018].

Roll, D., 2014. *Passivation and the Passive Layer*, s.l.: s.n.

Schaming, J., 2011. *An investigation of leaching chalcopyrite ores.* Kingston, Ontario: Queen's University.

Stanley, J., 2013. *Development of a copper mining and processing educational module for a tribal community college*, s.l.: s.n.

Theron, S., 2013. *The origin of the Central African Copperbelt: in a nutshell.* s.l., s.n.

Tshilombo, A., 2004. *Mechanism and kinetics of chalcopyrite passivation and depassivation during ferric and microbial leaching*, s.l.: Vancouver: University of British Columbia.

Vilca, A., 2013. *Studies on the curing and leaching kinetics of mixed copper ores.* Vancouver: The University of British Columbia.

Chapter 2: Literature review

2.1 Introduction

The following general background information that relates to this study will be represented in this chapter: Background on the extraction methods for chalcopyrite leaching, different leaching mediums associated with hydrometallurgical extraction, as well as the properties of chalcopyrite; passivation phenomena associated with chalcopyrite, along with general presumed causes; effect of temperature and pH on the leaching mechanism; using various oxidizing agents during the leaching of chalcopyrite; and information on the chalcopyrite bearing minerals, carbonatite and silicate.

2.2 Chalcopyrite as a copper sulphide ore

2.2.1 General information

The majority of the world's copper production involves porphyry copper deposits that consist primarily of three types of copper minerals separated by depth. Copper oxides are present on the shallow surface zone, chalcocites and other secondary copper-bearing minerals are on a larger supergene enrichment zone, and low-grade chalcopyrite ($CuFeS_2$) ores are found beneath, in the hypogene zone (Schaming, 2011). Due to high demand for copper, the shallower depth zones are depleting and the mining industry is compelled to mine the hypogene zone, which is rich in low-grade copper ores. Chalcopyrite, present on the hypogene zone, accounts for 70% of the world's copper reserves and 80% of the world's copper production. In the industry today, pyrometallurgy is the dominant treatment method used for extracting copper from $CuFeS_2$ (80-85%), although this process is not optimal, due to high SO_2 emissions (Sokic et al., 2009). Hydrometallurgical treatment of chalcopyrite ores are attractive, as it provides both more economical and environmentally friendly benefits (with easier control of waste) than those of pyrometallurgy. However hydrometallurgical treatment only accounts for approximately 18% of copper extracted from $CuFeS_2$, due to low extraction rates associated with this extraction process (Cordoba et al., 2008a; Li et al., 2010; Barlow et al., 2018)

2.2.2 Pyrometallurgical extraction process

After receiving the feed stream samples from mining, the first step in the pyrometallurgical extraction process is crushing and grounding the ore. Flotation is then used to concentrate the crushed run of mine (ROM) samples to a 20-30% range. A simultaneous process then follows, with the dry concentrate material fed to the flash smelter along with flux (typically used for chemical reaction with unwanted impurities and, in this case, for the formation of slag), where partial roasting and smelting occurs (Khoshkhoo, 2014). During the process, sulphur dioxide (SO_2) bearing off-gas is

produced and must be controlled before it can be released into the atmosphere; this is done by capturing the gas as sulphuric acid produced through oxidative reactions (Schlesinger et al., 2002) . Matte smelting occurs in the flash smelter at 1 250°C, at which iron (Fe) and sulphur (S) are oxidised from $CuFeS_2$ to produce matte (copper-enriched molten sulphur faze). During the process, the matte and the slag separate in the flash furnace. The copper-rich sulphide matte (45-70% Cu) is transferred to a converting oven in which oxidation occurs to form blister copper (98-99% Cu). Fire and electro-refining take place afterwards, for removing the remaining O_2 and to produce copper cathodes with 99.99% purity (Habashi, 1998; Khoshkhoo, 2014). A more detailed process for extracting copper from chalcopyrite using pyrometallurgical extraction procedures is illustrated in Figure 2-1 (Schlesinger et al., 2002).

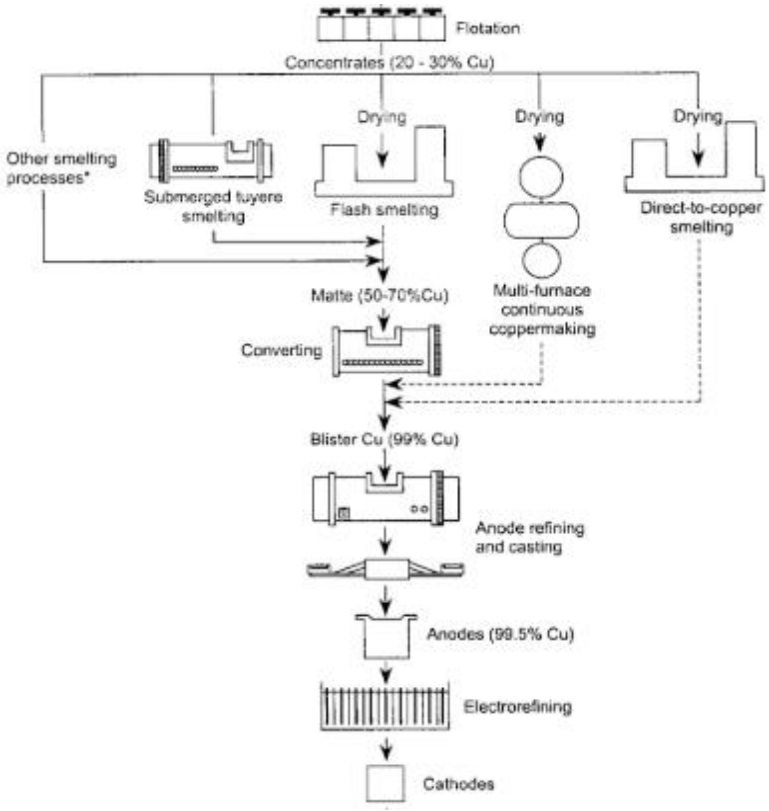

Source: (Schlesinger et al., 2002)

Figure 2-1: Principal pyrometallurgical process for copper production

2.2.3 Hydrometallurgical extraction process

The extraction process can be characterised by considering lixiviants, of which chloride and sulphate are the most common (Hackl et al., 1995); other systems including ammonium, cyanide, nitrate, mixed sulphate, such as nitrous-sulphate, and mixed nitrates, such as ferric-nitrate, also exist (Roman & Benner, 1973; Venkatachalam, 1991; Moyo, 2016). The hydrometallurgical process for extracting

copper from chalcopyrite is less complex and better understood than pyrometallurgical techniques. Most (sulphite-based) methods consist of three main processes: leaching the raw feed stream material to a concentrate, then solvent extraction (SX), and electrowinning (EW) (Khoshkhoo, 2014). Sulphate based leaching of chalcopyrite is not very difficult to implement and is, therefore, widely used as a hydrometallurgical copper extraction process. The sulphate-based process makes use of either bioleaching, ferric sulphate leaching or oxygen leaching to extract copper (Hackl et al., 1995). For all three sulphate-based leaching processes, the overall reaction chemistry is alike. The sulphate-based systems have a disadvantage, as ferric sulphate leaching delivers slow and incomplete extraction rates, similarly, leaching rates are low for oxygen leaching at low temperatures (Li et al., 2013). Chloride-based leaching has proven to be effective for copper dissolution from chalcopyrite, as leaching kinetics are improved due to increased metal solubility associated with chloride solutions. Unlike the sulphate-based system, the oxidation of elemental sulphur to sulphuric acid is also minimised (Cheng & Lawson, 1991; Chiluiza & Donoso, 2016). Current chloride processes for chalcopyrite leaching include the Cuprex process, the Intec process and the BioCOP process, among others (Wang, 2005). The disadvantage of chloride leaching is that it is less economically feasible, as chloride is a corrosive material that generally increases reactor costs, because more expensive material is needed for construction. There are also certain difficulties during electrowinning and solvent extraction of copper from the chloride-based solution (Khoshkhoo, 2014). Sulphate-based hydrometallurgical leaching is the most attractive, as the economic feasibility is better than that of the other leaching methods. It can also be easily integrated into existing electrowinning and solvent extraction procedures and concentrate leaching can also be easily integrated with other leaching techniques, such as heap leaching. Current sulphate based processes for chalcopyrite leaching include the Activox process where ultrafine milling and low-temperature oxidation are used in a combination for Cu extraction (Palmer & Johnson, 2005; Paphane et al., 2013), the Mt Gordon process using ferric leaching technology in which a single stage SAG/cyclone milling circuit along with low temperature and pressure autoclave oxidation is used (Shaw et al., 2004) and the Mintek process in which high temperature heap bioleaching for Cu extraction is used (Wang, 2005).

2.2.4 Crystal structure

Burdick and Ellis (1917), determined the crystal structure of the copper sulphide mineral and called it chalcopyrite. The crystal structure of the sulphide-based mineral is isostructural, with the zinc blend structure of sphalerite (ZnS). Chalcopyrite is also determined to be a covalent copper sulphide (Edelbro et al., 2003; Tshilombo, 2004). The crystal structure of the copper bearing chalcopyrite mineral is illustrated in Figure 2-2.

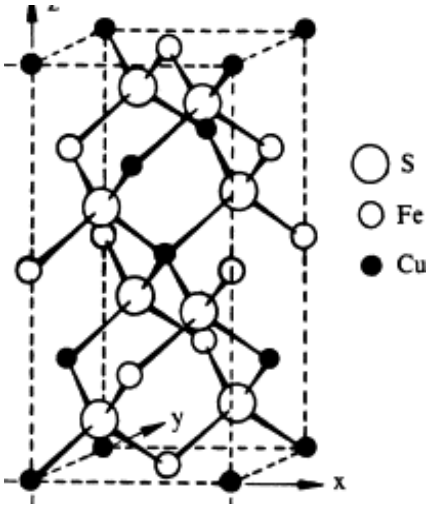

Figure 2-2: Chalcopyrite crystal structure

Chalcopyrite has a tetragonal unit cell, with four copper (Cu), four iron (Fe) and eight sulphur (S) atoms being present. The metal atoms of both metals are coordinated by a tetrahedron of S atoms, whereas the sulphur atoms are coordinated by a tetrahedron of two atoms of each metal (Liu et al., 2008; Khoshkhoo, 2014). This structural configuration of the unit cell makes the chalcopyrite mineral the most stable of the copper sulphide minerals, which along with its abundance, promotes the extraction of copper from this mineral (Wang, 2005). The dimensional unit cell lattice constants of chalcopyrite are given as a = b = 5.2988 and c = 10.434 (Hiskey, 1993) with the Cu-S, Fe-S and S-S bond lengths being 0.230, 0.225 and 0.368 nm, respectively (Hall & Stewart, 1973).

2.3 Chalcopyrite passivation film

Hydrometallurgical extraction of copper from chalcopyrite offers better waste management strategies, as well as monitory benefits, as the capital cost for smelters and refinery complexes needed to treat chalcopyrite pyrometallurgically is very high. Furthermore, although the hydrometallurgical treatment is able to provide onsite extraction via small-scale leaching plants, as opposed to treatments that involve additional transport costs for sending material to refineries, it currently makes up only 18% of total copper production, as leaching rates are very low due to a passivation layer forming on the surface of the mineral (Stott et al., 2000). Numerous studies have focused on identifying the cause of the formation of the passivation film, but, as yet, there is no generally accepted theory about the mechanism of formation (Cordoba et al., 2008a; Li et al., 2010). It has been suggested that the film is a poor electrical conductor with low permeability. Some of the most popular candidates for the formation of the passivation film will be discussed next.

2.3.1 Elemental sulphur

The formation of elemental sulphur during leaching with ferric sulphate is one of the presumed causes of the formation of a passivation film, and the one that has received the most attention. Studies found that, although sulphate is also formed during ferric leaching of chalcopyrite, elemental sulphur is observed to be the main sulphidic product formed (Dutrizac, 1989). It is implied that, during leaching, the mineral surface becomes enveloped in a thick layer of elemental sulphur, thereby hindering contact of reactants with the surface of the mineral and decreasing the speed of electron transfer (Gomez et al., 1996).

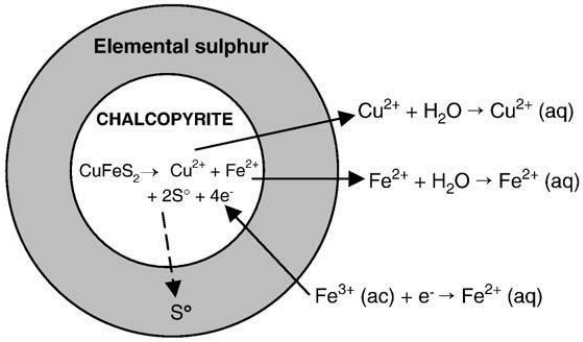

Source: (Munoz et al., 1979)

Figure 2-3: Formation of elemental sulphur

The shape of the sulphur formed – either dense or porous – is said to have an effect on whether the elemental sulphur will have an impact on the dissolution rate of copper. Other influential factors that have been identified are continuity and coverage of the sulphur. Studies have found that bulk sulphur that was produced in cases where the systems' redox potential was high (600 mV measured with a Ag/AgCl electrode), the bulk sulphur dispersed, instead of forming the thick, elemental sulphur layer around the particles (Fowler & Crundwell, 1998; Fowler & Crundwell, 1999); therefore, in these cases, the presence of elemental sulphur does not generally tend to have a significant impact on the dissolution kinetics (Khoshkhoo et al., 2014). Numerous other studies also observed the existence of elemental sulphur, but dismissed the possibility that its effects were the main cause of passivation (Hirato et al., 1987; Dutrizac, 1989). In cases where organic solvents were used to remove elemental sulphur, the leaching kinetics of chalcopyrite were still observed to occur slowly, indicating that other factors also influenced the dissolution of copper from the surface of chalcopyrite (Buttinelli et al., 1992).

2.3.2 Metal-deficient layer (polysulphides)

Another theory about the passivation layer is that it is a transformed surface phase consisting of metal-deficient sulphides (or polysulphides). Chalcopyrite is prone to non-stoichiometric leaching, as Fe is preferentially released into solution before Cu, to the extent that ratios of 4:1, and even 5:1

Fe to Cu are observed in solution (Khoshkhoo et al., 2014; Lu et al., 2016). As a result, a copper-rich phase, devoid of iron, is formed on the surface of the mineral (Biegler & Swift, 1979; Peterson & Dixon, 2006). The debate about the composition of this copper-rich phase has led to a number of surface compounds being identified and proposed: amorphous metal sulphides (Mikhlin et al., 2004), disulphides, such as copper sulphide and pyrite (CuS_2 & FeS_2) (Klauber et al., 2001), $Cu_{1-r}Fe_{1-s}S_{2-t}$ (Nava & Gonzalez, 2006) and sulphuric-rich polysulphides (S_n^{2-}), assumed to be CuS_n (with n>2). The exact nature of these copper-rich intermediate layers is a complex matter, and insufficient evidence has been found to link them to the slow leaching kinetics of copper (Holmes & Crundwell, 2013).

2.3.3 Jarosite

Researchers have also proposed that the formation of jarosite ($XFe^{3+}{}_3(OH)_6(SO_4)_2$) during ferric leaching of chalcopyrite slows the leaching kinetics by restricting mass transfer of ions from the surface of the mineral. Additionally, the jarosite layer prevents ferric ion (Fe^{3+}) from contacting the chalcopyrite mineral surface, further hindering dissolution. Many studies have found that ferric ion enhances dissolution of chalcopyrite (although only at low concentrations) (Dutrizac et al., 1969; Cordoba et al., 2008a). In the presence of Fe^{3+} and sulphate ion (SO_4^{2-}), jarosite formation is said to occur according to the following reaction:

$$\boldsymbol{3Fe_2(SO_4)_3 + X_2SO_4 + 12H_2O \rightarrow 2XFe_3(SO_4)_2(OH)_{6(s)} + 6H_2SO_4} \qquad \textbf{Eq 1}$$

Where X = H_3O^+, K^+, Na^+ or NH_4^+, depending on the cations available in the system (Li et al., 2013). In another study, jarosite was partially (70%) removed through bioreduction of ferric ion, however, no significant improvement in the kinetic leaching rate of chalcopyrite was observed (Stott et al., 2000). Although many authors suggest that jarosite retards the leaching rate of copper from the surface of the chalcopyrite mineral, it is doubtful if jarosite alone is responsible for the slow leaching kinetics observed for chalcopyrite (Tshilombo, 2004).

2.4 Factors effecting chalcopyrite leaching kinetics

Although the formation and mechanism of the passivation film is still disputed and the studies that investigated the phenomenon could not present a generally accepted theory behind its formation, various studies have effectively identified certain parameters that are known to influence and/or improve the leaching kinetics of copper from the chalcopyrite host mineral. The acidity of the solution, reaction temperature, particle size distribution, mineralogical composition, redox potential, oxidant concentration and addition of additives are some of these influencing factors (Hackl et al., 1995; Antonijevic & Bogdanovic, 2004; Acero et al., 2009). For the purpose of this study, the effects of acid concentration, reaction temperature, mineralogical composition and additive addition were observed.

2.4.1 Effects of temperature

Various studies have shown that temperature has a strong influence on the copper leaching rate from chalcopyrite (Hackl et al., 1995; Cordoba et al., 2008a; Sokic et al., 2009). In order to obtain the activation energy of chalcopyrite, the leaching rate's temperature dependence must be understood; this will also determine the dominant leaching mechanism (Kaplun et al., 2011). Studies found that, for a case where the system is chemically controlled, the rate of leaching could be improved by increasing the temperature slightly (Parker et al., 1981). Activation energies lower than 40 kJ/mol imply diffusion-controlled leaching, whereas activation energies above 40 kJ/mol imply chemical controlled leaching. A number of authors have found high activation energies during chalcopyrite leaching with ferric sulphate: 84 kJ/mol (Munoz et al., 1979), 88 kJ/mol (Hirato et al., 1987), 130.7 kJ/mol (Cordoba et al., 2008a); as well as for ferric chloride: 60 kJ/mol (Hirato et al., 1986), 47 kJ/mol (Dutrizac, 1978). Effectively, high temperatures are also required to break down the bonds in the crystal lattice associated with these high activation energies (Cordoba et al., 2008a). Hackl et al. (1995) found that, during oxygen pressure leaching, kinetic reaction rates were slow at lower temperature rates (110-120°C, with copper extraction rates of 43-47%), and significantly increased at higher temperature rates (200-220°C), where copper dissolution was determined as 98.6% (200°C) and 99.3% (220°C), respectively (Hackl et al., 1995). Similar effects were observed by Sokic et al. (2009) using a 1.5 M H_2SO_4 solution in the presence of sodium nitrate ($NaNO_3$), where 28% copper extraction was observed after 120 minutes at 70°C, with an increase to 70% at 90°C (Sokic et al., 2009). During experimentation at a range of 35-68°C in ferric sulphate media, Córdoba et al. (2008a) found that extraction rates improved from less than 3% to more than 80%. For the purpose of this study, the effects of temperature in a ferric sulphate media at a range of 25-85°C was investigated to determine the impact on the leaching kinetics of chalcopyrite from different host ores (carbonatites and silicates).

2.4.2 Effects of pH

The acid concentration in solution and, by extension, the solution pH, are important factors to take into account when observing chalcopyrite dissolution kinetics. Previous studies observed that chalcopyrite leaching at solution pH 1-2 has proven to be beneficial in terms of the leaching rate (Dew et al., 1997; Halinen et al., 2009a). These low pH conditions are generally said to enhance the leaching rate, due to the acid associated with the low pH conditions, which prevents the hydrolysis and precipitation of ferric salts (Dutrizac et al., 1969). For pH conditions lower than 1, however, the kinetic leaching rate for chalcopyrite dissolution tends to be poor, as ferric ion can precipitate to form jarosite, which is known to have a detrimental effect on chalcopyrite dissolution; formation of this iron species is indicative of how readily ferric salts can hydrolyse (Lu et al., 2000; Cordoba et al., 2008a). Furthermore, studies found that pH lower than 0.5 provokes passivation, as ferric ion

hydrolyses and a surface layer devoid of Fe is formed as a result of competition between ferric and hydrogen ion (Antonijevic & Bogdanovic, 2004; Li et al., 2013). In turn, pH levels above 2 can have the same affect when ferric ion precipitates, as well as alkaline conditions promoting the formation of species such as gypsum gangue, which has also been known to hinder chalcopyrite leaching rates (Tshilombo & Ojumu, 2013). For this study, however, rather than keeping the pH stable during chalcopyrite leaching, the pH evolution of the solution was observed, to understand the effects and impact of the various mineralogical species present within the two different chalcopyrite hosting ores.

2.4.3 Effects of particle size

Particle size plays an important role during mineral dissolution of chalcopyrite as it is well known that smaller particles sizes tend to enhance the leaching kinetics of Cu (Munoz et al., 1979; Dutrizac, 1981). Studies found that because of its refractory nature, fine grinding of chalcopyrite promotes rapid leaching (Jeevaratnam, 2001); smaller particles provide a larger surface area for contact with the oxidant. In study conducted by Sokic et al. (2009), four different particle sizes were used during chalcopyrite leaching in a 1.5 M H_2SO_4 and 0.6 M $NaNO_3$ solution; +75, -75+50, -50+37, -37 μm (Sokic et al., 2009). From this investigation 69% Cu extraction was observed at -37 μm as compared to the 17% extraction observed at +75 μm. The addition of minerals, relative to the solution media, can also impact the effects of particle size in solution as in processes where pyrite was added during ferric sulphate leaching, the impact of particle size was enhanced below -75 μm compared to instances where pyrite was excluded at which no improvements were observed (Jones & Peters, 1976). In the absence of pyrite and below -75 μm, recovery improved in a ferric chloride media (Tshilombo, 2004). Similarly using a sulphuric acid media in the presence of $K_2Cr_2O_7$, copper extraction improved at particle sizes below 75 μm (Aydogan et al., 2006; Li et al., 2013). For the purpose of this study, the particle size is kept stable at -150 μm to better assess the effects of changing solution temperature, pH evolution, mineralogical composition and magnetite addition.

2.4.4 Leaching in the presence of an additive

2.4.4.1 Pyrite

Pyrite as an additive has been researched by numerous studies and has been observed to aid the dissolution rate of Cu from chalcopyrite during the galvanic reaction between the two minerals (Berry, 1978). Using ground pyrite has proven to be effective in this endeavour, as pyrite creates an alternative catalytic surface for ferric reduction, thereby attenuating the passive behaviour of the chalcopyrite mineral in a ferric sulphate media (Schaming, 2011). This behaviour has been identified at a concentration ratio of 4-2:1 pyrite to chalcopyrite. A higher mass concentration of pyrite to chalcopyrite aids in providing a bigger alternative surface for ferric reduction, thereby increasing the

dissolution rate. This method has been patented as the Galvanox process (Dixon, 2008), which is illustrated in Figure 2-4.

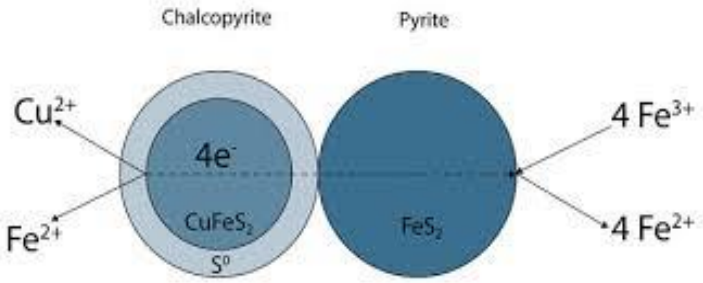

Figure 2-4: Schematic diagram of the Galvanox reaction

In this mixture of the two sulphide minerals, the resting potential of chalcopyrite is the lowest, and it subsequently acts as the anode, with oxidation occurring, whereas pyrite, with the higher resting potential, acts as the cathode and is galvanically protected as a result of the potential difference (Khoshkhoo, 2014). As mentioned, ferric reduction takes place on the surface of the pyrite mineral, subsequently increasing the rate of dissolution of copper from chalcopyrite (Tshilombo, 2004).

2.4.4.2 Silver

The addition of silver (Ag^+) during leaching has also proven to enhance the ferric leaching of chalcopyrite (Pawlek, 1976; Banerjee et al., 1990). In another study, the rate of chalcopyrite leaching during oxygen leaching was analysed in the presence and absence of silver. The study found that after 30 minutes of leaching, at 110°C, 40% copper dissolution was obtained in the absence of silver; by adding 0.75% dissolved silver by weight, under the same conditions, copper extraction reached 95%, indicating that silver can be used as an effective additive (Pawlek, 1976; Cordoba et al., 2008a). A different study, in which ferric leaching of chalcopyrite was conducted, found similar effects: after 180 minutes of leaching at 90°C, the extraction rate of 46%, improved to 90% extraction after the addition of small amounts of silver (50-500 mg/l) (Snell, 1975; Tshilombo, 2004). During ferric sulphate leaching of chalcopyrite in a sulphuric acid medium with the addition of silver, the leaching is said to take place according to the following reactions:

$$CuFeS_2 + 4Ag^+ \rightarrow Cu^{2+} + Fe^{2+} + 2Ag_2S \qquad \text{Eq 2}$$

$$Ag_2S + 2Fe^{3+} \rightarrow 2Ag^+ + 2Fe^{2+} + S \qquad \text{Eq 3}$$

As elemental sulphur is one of the causes of the retarding effect of chalcopyrite leaching, the addition of silver improves the leaching rate of copper, as a product layer of Ag_2S and sulphur is said to form, instead of a layer composed solely of sulphur. It is claimed that the porous silver-sulphate layer does not exert the same barrier effect found in the presence of the elemental sulphur layer, and provides

higher electrical conductivity, which improves the transport of electrons through the surface of the chalcopyrite mineral (Burkin, 1982; Prince & Warren, 1986).

2.4.4.3 Magnetite

Magnetite is an iron oxide (Fe_3O_4) and is generally magnetic. The chemical composition can also be written as $Fe^{2+}Fe^{3+}2O_4$, which implies that magnetite contains both ferrous (Fe^{2+}) and ferric ions (Fe^{3+}), making the mineral stable in environments where iron is present in reduced and oxidized states (Skinner & Jahren, 2003). The formation of magnetite can occur under a wide variety of conditions, from magmatic systems, where it crystallises in either silicate or sulphide melts at high temperatures, or hydrothermal systems, where it precipitates from hydrothermal fluids at lower temperatures (Dare et al., 2014). Magnetite from silicate melts are typically found in Fe-Ti-V-P deposits, whereas magnetite from sulphide melts are found in Ni-Cu- platinum group metal deposits (Dare et al., 2012; Boutroy et al., 2014).

Magnetite used in this study is from a magmatic system of silicates melts in the Bushveld Complex, the largest layered ingenious intrusion in the Earth's crust, which is situated in the northern part of South Africa. The formation of the magnetite in the Bushveld Complex is said to have crystallised under relative oxidising conditions, either before or concurrently with the iron-titanium oxide, ilmenite ($FeTiO_3$). The mineral is titanium rich, with in grades of 6-12 wt% (Toplis & Carroll, 1995; Namur et al., 2010). However, the magnetite that first crystallised in the layered intrusions were identified to be rich in vanadium (V), with concentrations of 0.14-0.8% by weight being present. Vanadium content is generally controlled through oxygen fugacity (Barnes et al., 2004; Dare et al., 2014).

Magnetite reacts with sulphuric acid to form ferrous sulphate, ferric sulphate and water, according to the following reaction:

$$Fe_3O_4 + 4H_2SO_4 = FeSO_4 + Fe_2(SO_4)_3 + 4H_2O \qquad \text{Eq 4}$$

This is significant as other studies found that chalcopyrite dissolution is strongly affected by ferric ion concentration (Cordoba et al., 2008a) and that a ferric sulphate concentration increase coincides with an increase in Fe^{3+} concentration, leading to increased dissolution (Hirato et al., 1987). However, this effect is limited to an iron concentration of 0.1 M – at high concentrations of ferric ion the effect is negligible (Dutrizac et al., 1969; Munoz et al., 1979). Leaching of chalcopyrite in the presence of ferric ion is shown by the following reaction equation (Dutrizac & MacDonald, 1974):

$$CuFeS_2 + 4Fe^{3+} + 3O_2 + 2H_2O \rightarrow Cu^{2+} + 5Fe^{2+} + 2H_2SO_4 \qquad \text{Eq 5}$$

Through this reaction, cupric ions are formed – a generally soluble species of copper – thereby increasing the leached concentration of copper in solution. It is assumed that chalcopyrite leaching

from the carbonatite hosting ore will be aided by the addition of magnetite, as the carbonatites mainly contain the alkaline earth metal, calcium (Ca), which is known to neutralise solution acidity and thereby lead to increased pH conditions (Lamar, 1961). As the dissolution of chalcopyrite is an acid-consuming reaction occurring at pH lower than 4, the addition of magnetite for further ferric sulphate formation will be significant, as the acid concentration will increase, which will work against the alkaline effects of the alkaline earth metal in the carbonatite hosting ore, as well as increasing the ferric ion concentration responsible for the formation of cupric ion. Furthermore, magnetite has not been sufficiently studied theoretically or from a practical point of view, and knowledge of its effects on chalcopyrite leaching in the presence of ferric sulphate will be of interest.

2.5 Mineral background

Even with the choice of lixiviant, whether sulphate- (ferric, oxygen, bioleaching), chloride- nitrate- or other solutions based, as well as the operating temperature range and oxidant/additive addition, another factor is at play in parameters affecting the chalcopyrite leaching rate, namely, that of the mineralogical composition of the host rock. As chalcopyrite is found in a range of different hosting ores, it is accompanied by various mineral species that could each impact the leaching behaviour in solution. For the purpose of this study, carbonate-rich hosting ores from Phalaborwa and silicate-rich hosting ores from the DRC were investigated.

2.5.1 South African carbonatitic chalcopyrite

2.5.1.1 Carbonatite overview

Carbonatite minerals are magmatic rock formations that contain more than 50 wt% primary carbonate species, as is defined by the International Union of Geological Science (Maitre, 2002). The formation and origin of carbonatites are believed to be as a result of either one or a combination of three main theorised instances: (a) low-degree primary mantle melts as a result of partial melting of carbonated peridotite (Wyllie & Huang, 1976; Eggler, 1978); (b) residual melts of crystal fractionated carbonated silicate magmas, such as nephelinite and kamafugites (Veksler & Lentz, 2006) and (c) immiscible melt fractions of carbonated-saturated silicate magmas (Kjarsgaard & Hamilton, 1989).

Carbonatite complexes can generally be divided into two groups, namely, alkaline-carbonatites and mineralised carbonatites. These complexes have gained much attention, as they are one of the main sources of rare earth elements (Simandl, 2014); alkaline-carbonatites complexes are of particular interest, as they are a noteworthy source of copper (Simandl & Paradis, 2018). Carbonatite can be divided further into calcite carbonatites, dolomite carbonatites, or ferro carbonatites, depending on the primary carbonate present within the mineral. In some instances, more than one carbonate mineral is present; then the term involves listing the carbonatite species in order of increasing model concentration (Simandl & Paradis, 2018). The International Union of Geological Science provides a

different strategy for classifying carbonatites into groups when the model classification method cannot be applied. Then, chemical classification is used to identify the type of carbonatite mineral based on weight percentage. This chemical classification divides carbonatites into calcio carbonatites, ferro carbonatites and magnesio carbonatites; special classification is also given to carbonatites with silicate quartz (SiO_2) contents above 20 wt%, which is termed silico carbonatites (Woolley & Kempe, 1989; Maitre, 2002). Figure 2-5 sets out the chemical classification of carbonatites.

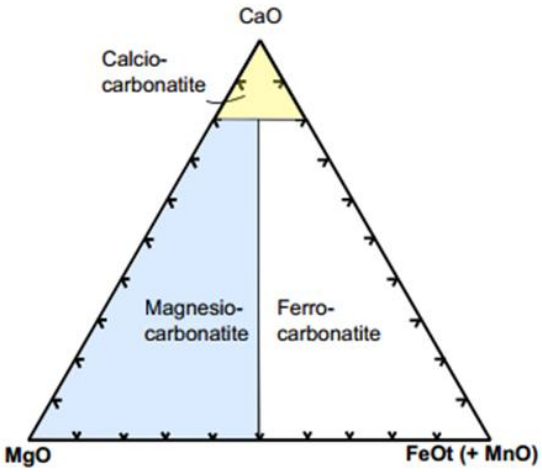

Figure 2-5: Carbonatite chemical classification diagram as proposed by Woolley and Kempe (1989)

2.5.1.2 Phalaborwa carbonatite complex: Brief history

The alkaline-carbonatite complex in Phalaborwa, South Africa, was mined from as early as 1 300 AD by indigenous African tribes, as it provided a source of copper and iron (Simandl & Paradis, 2018). The complex was rediscovered in 1912 by Hans Merensky, who identified large deposits of vermiculite, apatite and copper. As a result of the apatite discovery, Foskor, a state-owned company, established mining development in the area from which the town of Phalaborwa sprung (Cartwright, 1972). However, it was the discovery of the radioactive mineral, uranothorianite, that lead to the development of copper mining operations on Loolekop. The South African Atomic Energy Board, in search of the radioactive mineral, managed to succeed in establishing the widespread nature of the copper sulphide minerals in the carbonate-enriched complex (Beale, 1985b). As a result of these findings, the Newton Mining Cooperation, together with Rio Tinto, started a copper mining development in 1962 (Heinrich, 1970). From 1964 to 2002, the general mining procedure used at Loolekop was that of open-pit mining, until the final economical depth for open-pit procedures was reached. In order for operations to continue, the Phalaborwa Mining Company started underground mining to extend the mining operations by 20 years (Palabora Mining Company, 2012).

2.5.1.3 Phalaborwa carbonatite complex: Geology

The carbonatite complex is a bicentered ring complex, intruded as a vertical ovoid pipe into the Archean granite. There is a primary pipe with two subordinate pipes, of which the Loolekop subordinate pipe complex is of particular interest (Beale, 1985b). The Loolekop complex where the Phalaborwa Mine is situated, as seen in Figure 2-7, consists of three rock types: phoscorite dominant throughout the pipe, the older, transgressive carbonatites at the core of the pipe, of which the carbonatite is mainly composed of calcite-dolomite, and the younger, banded carbonatites, which are also composed of calcite and dolomite species, with calcite in excess (3:1) (Heinrich, 1970). Copper sulphides are consistent throughout the orebody, with only trace amounts of iron sulphide species, pyrite and pyrrhotite ($Fe_{(1-x)}S$) being present. It is in the transgressive carbonatite section that chalcopyrite (the main copper sulphide), and the other copper sulphides are most abundant within the complex, and also where the highest ore grades are found (1.0% copper); these chalcopyrite sediments are surrounded by bornite (Cu_5FeS_4) in the outlying phoscorite sediment (Beale, 1985b).

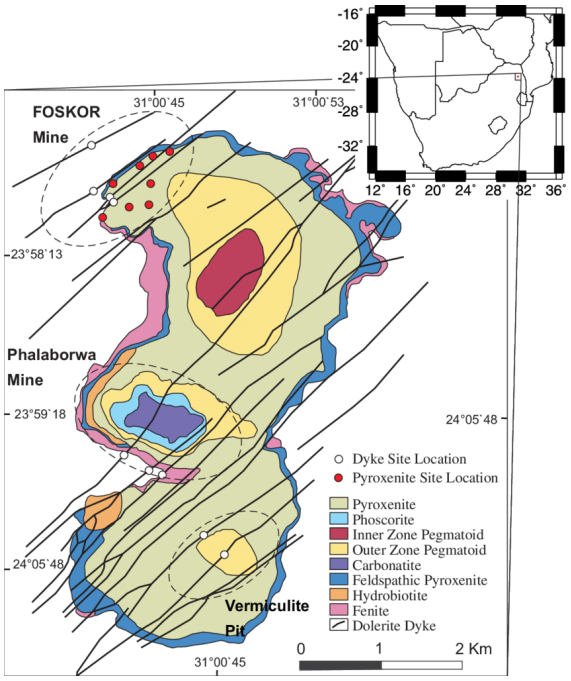

Source: (Letts et al., 2011)

Figure 2-6: Geological map of the Phalaborwa Complex

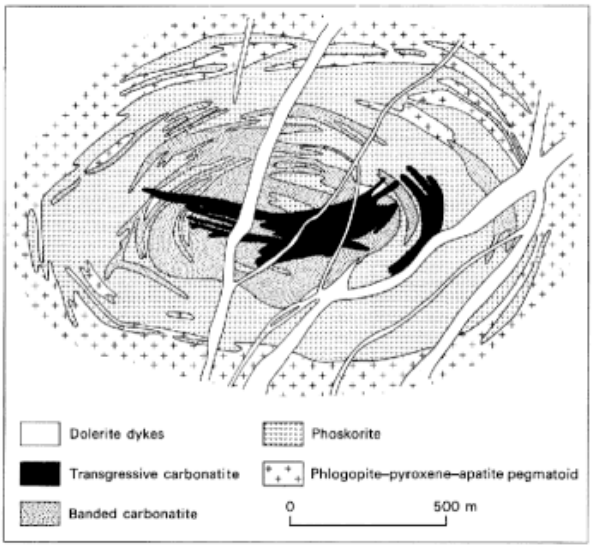

Figure 2-7: The Loolekop Complex

The carbonatite chalcopyrite ores from Phalaborwa were of interest for the purpose of the study as the complex is unique in its variety of sulphide minerals present, and a significant quantity of copper sulphides, making it the only carbonatite complex in the world that contains economically feasible deposits of copper. The trace amounts of pyrite are also important, as galvanic interaction of pyrite during chalcopyrite leaching has proven to complement leaching rates (Berry, 1978). The presence of valleriite in the complex ($(Fe^{2+}, Cu)_4(Mg, Al)_3S_4(OH,O)_6$) is also important, as it is believed that the copper-iron hybrid sulphide leads to retardation of the flotation process of sulphides it might be associated with (Heinrich, 1970).

2.5.2 Central African Copper-belt siliciclastic chalcopyrite

2.5.2.1 Overview: Sedimentary copper deposits

Sedimentary copper deposits are an important source of silver (Ag), and accounts for 15% of the world's copper resources (Boyle et al., 1989; Sillitoe, 2012). Sedimentary rocks can, generally, be divided into three subgroups: clastic (sometimes called detrital), chemical, and organic sedimentary rock types. Breccia, conglomerate, sandstone, siltstone and shale are common clastic or siliciclastic sedimentary rock species. Clastic sedimentary rock is formed from pre-existing rocks that have been mechanically eroded, whereas chemical sedimentary rock species consist of fluid precipitates (Mibei, 2014). Sedimentary copper deposits are said to form by fluid mixing in porous sedimentary and volcanic rock types. In this process, an oxidizing fluid (a copper-carrying chloride complex) and a reducing fluid are involved; generally four conditions have to be met for these sediments to form: (1) An oxidising source rock is required, (2) a source of brine must be available to mobilise the copper, (3) for copper precipitation, a source of reducing fluid is necessary to form the deposit, and (4) the conditions have to be favourable to allow for fluid mixing (Cox et al., 2007).

2.5.2.2 Central African Copper-belt: Geology

The Central African Copper-belt is of great importance, as it is the world's largest sedimentary copper deposit and the sedimentary province with the highest copper grades. It is estimated that the copper belt contains 200 Mt of copper deposits. In addition to its rich copper reserves, the CAC contains the world's largest reserves of cobalt (Co) (Cox et al., 2007; Lydall & Auchterlonie, 2011); and large enough reserves of nickel (Ni), uranium (U) and zinc (Zn) for these minerals to be significant (Unrug, 1988; Brouhton, 2014) . The Copper-belt extends over both the DRC and Zambia, and is hosted by Neoproterozoic rock of the Katanga supergroup (5-10 km thick) (Hitzman et al., 2012; Theron, 2013). The supergroup is divided into subgroups: Roan subgroup (mostly in Zambia), containing redbeds, overlaying mixed evaporitic carbonate and siliciclastic rocks and marine siliciclastic rocks, and Nguba and Kundelungu subgroups, in the DRC, with diamictite-carbonate-siliciclastic sequences (silicocarbonatites). The Zambian copper production/reserves of the CAC are estimated at 100 Mt, whereas the DRC's production/reserves are estimated at 180 Mt (Hitzman et al., 2012; Brouhton, 2014). The Congolese sections of the copperbelt are divided in three deposits (Kamoa, Kolwezi, and Tenke-Fungurume), and the Zambian section comprises six large deposits (Chambishi, Konkola-Musoshi, Nchanga-Chingola, Luanshya-Baluba, Mufilira and Nkana-Mindola); smaller deposits also exist. Generally, the Zambian side is dominated by siliciclastic sediments, whereas the Congolese side is dominated by chemical sediments (Theron, 2013). The Congolese- and Zambian copperbelt is shown in Figure 2-8.

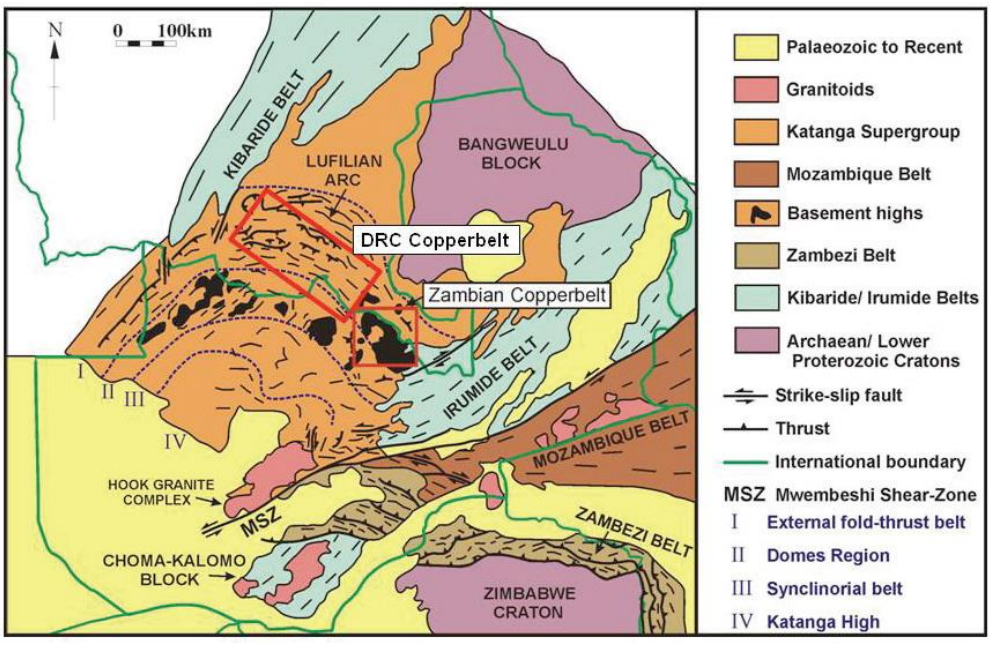

Figure 2-8: Geological overview of the Central African Copperbelt

The copper ore grades range from 0.5% (Samba deposit) to 4.26% (Chimbuluma deposit) in the Zambian copperbelt, averaging at 2.43%; ore grades of 2.32% (Kisanfu deposit) to 6.3% (Kipushi

deposit) are present in the Congolese copperbelt sediments of the CAC (Hitzman et al., 2005; Hitzman et al., 2012). Dolomite ($CaMg(CO_3)_2$) is identified as the dominant host lithology in mines of the subgroup located in the Congolese region (Jordaan, 1961) with carbonate-silicates (dolomitic siltstone, dolomitic schist) dominating certain regions of the Lower Roan Subgroup and clastic sedimentary quartzite dominant in other parts of the Lower Roan Subgroup (Coates et al., 2008) . The Roan Subgroup spans both the DRC and Zambia, with the biggest portion located in the Zambian copperbelt (Brouhton, 2014). The dominant sulphide species present within Zambian sediment subgroups is chalcopyrite, followed by bornite (Cu_5FeS_4), with subsidiaries of chalcocite and pyrite. The Congolese subgroups are also dominated by chalcopyrite, followed by bornite as the main sulphides, and also includes carrollite ($CuCo_2S_4$), chalcosite (Cu_2S), pyrite and sphalerite ((Zn,Fe)S) sulphides (Hitzman et al., 2005). The siliciclastic-chalcopyrite ores of the CAC (the highest grade sedimentary-copper deposits) were of interest to this report, as the cobalt quantities in the ore bodies are unique (the CAC is the world's largest Co deposit) and might have an influence on the leaching behaviour of the chalcopyrite mineral. Unlike the carbonatite-chalcopyrites of South Africa, the pyrite concentrations present in the CAC are significantly higher, which might lead to increased leaching kinetics due to the galvanic interactions between pyrite and chalcopyrite.

References

Acero, P., Cama, J., Ayora, C. & Asta, M., 2009. Chalcopyrite dissolution rate law from pH 1 to 3. *Geologica Acta,* 7(3), pp. 389-397.

Antonijevic, M. & Bogdanovic, G., 2004. Investigation of the leaching of chalcopyrite ore in acidic solutions. *Hydrometallurgy,* 73(2), pp. 245-56.

Aydogan, S., Ucar, G. & Canbazoglu, M., 2006. Dissolution kinetics of chalcopyrite in acidic potassium dichromate solution. *Hydrometallurgy,* 81(1), pp. 45-51.

Banerjee, P., Chakrabarti, B. & Das, A., 1990. Silver-catalysed hydrometallurgical extraction of copper from sulfide ores from Indian mines. *Hydrometallurgy,* 25(3), pp. 349-355.

Barlow, B., Nyembwe, K., Wanders, F. & Fosso-Kankeu, E., 2018. *Prediction of dissolution of copper from a chalcopyrite carbonatite ore of South Africa.* CapeTown, South Africa, s.n., pp. 99-103.

Barnes, S., Maier, W. & Ashwal, L., 2004. Platinum-group element distribution in the Main Zone and Upper Zone of the Bushveld Complex, South Africa. *Chemical Geology,* 208(1-4), pp. 293-317.

Beale, C., 1985b. Copper in South Africa: Part II. *Journal of the South African Institute of Mining and Metallurgy,* 85(4), pp. 109-124.

Berry, V., 1978. Galvanic interaction between chalcopyrite and pyrite during bacterial leaching of low grade waste. *Hydrometallurgy,* 3(4), pp. 309-326.

Biegler, I. & Swift, D., 1979. Anodic electrochemistry of chalcopyrite. *Journal of Applied Electrochemistry,* 9(5), pp. 545-554.

Boutroy, E. et al., 2014. Magnetite composition in Ni-Cu-PGE deposits worldwide and its application to mineral exploration. *Journal of Geochemical Exploration,* Volume 145, pp. 64-81.

Boyle, R. et al., 1989. Sediment-Hosted Stratiform Copper Deposits. In: *Understanding Mineral Deposits.* s.l.:Geological Association of Canada, pp. 539-572.

Brouhton, D., 2014. *Geology and ore deposits of the Central African Copperbelt,* s.l.: Colorado School of Mines.

Burkin, A., 1982. Composition and phase changes during oxidative acid leaching reactions. In: *Hydrometallurgical process fundamentals.* New York: Plenum Press, pp. 113-123.

Buttinelli, D. et al., 1992. Leaching by ferric sulphate of raw and concentrated copper-zinc comples sulphide ores. *International Journal of Mineral Processing,* 36(3-4), pp. 245-257.

Cartwright, A., 1972. *Phalaborwa: mining city of the furture.* Cape Town: Purnell.

Cheng, C. & Lawson, F., 1991. The kinetics of leaching chalcocite in acidic oxygenated sulphate-chloride solutions. *Hydrometallurgy,* 27(3), pp. 249-268.

Chiluiza, E. & Donoso, P., 2016. Chalcopyrite leaching in acidic chloride solution without sulphates. *Journal of the Mexican Chemical Society,* 4(60), pp. 238-246.

Coates, H., Anderson, W. & McGeorge, I., 2008. *Technical report on the Kakanda copper-cobalt project, Katanga Province, DRC,* s.l.: USGS.

Cordoba, E., Munoz, J., Blazquez, M. & Ballester, A., 2008a. Leaching of chalcopyrite with ferric ion Part I: General aspects. *Hydrometallurgy,* 93(3-4), pp. 81-87.

Cox, D. et al., 2007. *Sediment-hosted copper deposits of the world: deposit models and database,* s.l.: USGS.

Dare, S., Barnes, S. & Beaudoin, G., 2012. Variation in trace element content of magnetite crystallized from a fractionating sulfide liquid. *Geochim Cosmochim Acta,* Volume 88, pp. 27-50.

Dare, S. et al., 2014. Trace elements in magnetite as petrogenetic indicators. *Mineralium Deposita,* 49(7), pp. 785-796.

Dew, D., Lawson, E. & Broadhurst, J., 1997. The BIOX process for biooxidation of gold-bearing ores or concentrates. In: *Biomining.* Berlin: Springer, pp. 45-80.

Dixon, D., 2008. Galvanox: A novel galvanically-assisted atmospheric leaching technology for copper concentrates. *Canadian Metallurgical Quarterly,* 47(3), pp. 327-336.

Dutrizac, J., 1978. The kinetics of dissolutiom of chalcopyrite in ferric ion media. *Metallurgical Transactions B,* 9(3), pp. 431-439.

Dutrizac, J., 1981. The dissolution of chalcopyrite in ferric sulphate and ferric chloride media. *Metallurgy and Materials Transaction,* 12(2), pp. 371-378.

Dutrizac, J., 1989. Elemental sulphur formation during the ferric sulphate leaching of chalcopyrite. *Canadian Metallurgical Quarterly,* 28(4), pp. 337-344.

Dutrizac, J. & MacDonald, R., 1974. Ferric ion as a leaching medium. *Minerals Science and Engineering,* 6(2), pp. 59-100.

Dutrizac, J., MacDonald, R. & Ingraham, T., 1969. The kinetics of dissolution of synthetic chalcopyrite in aqueous acidic ferric sulfate solutions. *Transactions of the Metallurgical Society,* pp. 955-959.

Edelbro, R., Sandstrom, A. & Paul, J., 2003. Full potential calculations on the electron bandstructures of Sphalerite, Pyrite and Chalcopyrite. *Applied Surface Science,* 206(1-4), pp. 300-313.

Eggler, D., 1978. The effect of CO2 upon partial melting of peridotite in the systems Na2O-CaO-Al2O3-MgO-SiO2-CO2 to 35kb, with an analysis of melting in a peridotite-H2O-CO2 system. *American Journal of Science,* pp. 305-343.

Fowler, T. & Crundwell, F., 1998. Leaching of zinc sulphide by Thiobacillus ferrooxidans: Experiments with a controlled redox potential indicate no direct bacterial mechanism. *Applied and Environmental Microbiology,* Volume 64, pp. 3570-3575.

Fowler, T. & Crundwell, F., 1999. Leaching zinc sulphide by Thiobacillus ferooxidans: Bacterial oxidation of the sulphur poduct layer increases the rate of zinc sulphide dissolution at high concentrations of ferrous ions. *Applied and Environmental Microbiology,* Volume 65, pp. 5285-5292.

Gomez, C. et al., 1996. Electrochemistry of chalcopyrite. *Hydrometallurgy,* 43(1-3), pp. 331-344.

Habashi, F., 1998. *Handbook of Extractive Metallurgy.* 2nd ed. s.l.:Wiley-VCH.

Hackl, R., Dreisinger, D., Peters, E. & King, J., 1995. Passivation of chalcopyrite during oxidative leaching in sulfate media. *Hydrometallurgy,* 39(1-3), pp. 25-48.

Halinen, A., Rahunen, N., Kaksonen, A. & Puhakka, J., 2009a. Heap bioleaching of a complex sulfide ore: Part I: Effect of pH on metal extraction and microbial composition in pH controlled columns. *Hydrometallurgy,* 98(1-2), pp. 92-100.

Hall, S. & Stewart, J., 1973. The Crystal Structure of Chalcopyrite, CuFeS2. *Acta Crystallographica,* Volume 29, p. 579.

Heinrich, E., 1970. *The Palabora Carbonatitic Complex: A Unique Copper Deposit,* s.l.: s.n.

Hirato, T., Kinoshita, M., Awakura, Y. & Majima, H., 1986. The leaching of chalcopyrite with ferric chloride. *Metallurgical Trasactions B,* 17(1), pp. 19-28.

Hirato, T., Majima, H. & Awakura, Y., 1987. The leaching of chalcopyrite with ferric sulphate. *Matallurgical and Materials Transactions,* 18(3), pp. 489-496.

Hiskey, J., 1993. Chalcopyrite semiconductor electrochemistry and dissolution. *Extractive metallurgy of copper, nickel and cobalt,* Volume 1, pp. 949-969.

Hitzman, H. et al., 2012. The Central African Copperbelt: Diverse Stratigraphic, Structural, and Temporal Settings in the Wolrd's Largest Sedimentary Copper District. *Society of Economic Geologists,* Volume 16, pp. 457-514.

Hitzman, M. et al., 2005. The sediment-hosted stratiform copper ore system. *Society of Economic Geologists,* Volume 100, pp. 609-942.

Holmes, P. & Crundwell, F., 2013. Polysulfides do not cause passivation: Results from the dissolution of pyrite and implications for other sulphide minerals. *Hydrometallurgy,* Volume 139, pp. 101-110.

Jeevaratnam, E., 2001. *An Investigation into thr Ferric Leaching of Chalcopyirte - A Sub-Process in the Bioleaching of Chalcopyrite,* Cape Town: s.n.

Jones, D. & Peters, E., 1976. The leaching of chalcopyrite with ferric sulfate and ferric chloride . In: *Extractive metallurgy of copper.* s.l.:s.n., pp. 633-653.

Jordaan, J., 1961. *The geology of the Nothern Rhodesian Copperbelt,* London: s.n.

Kaplun, K., Li, J., Kawashima, N. & Gerson, A., 2011. Cu and Fe chalcopyrite leach activation energies and the effects of added Fe3+. *Geochim Cosmochim Acta,* 75(20), pp. 58765-5878.

Khoshkhoo, M., 2014. *Chalcopyrite Disolution in Sulphate-Based Leaching and Bioleaching Systems,* s.l.: s.n.

Khoshkhoo, M., Dopson, M., Schukarev, A. & Sandstrom, A., 2014. Electrochemical simulatoin of redox potential development in boileaching of a pyritic chalcopyrite concentrate. *Hydrometallurgy,* 14(7), pp. 144-145.

Kjarsgaard, B. & Hamilton, D., 1989. *The genesis of carbonatites by immiscibility,* London: Unwi Hyman.

Klauber, C., Parker, A., Bronswijk, W. v. & Watling, H., 2001. Sulphur speciation of leached chalcopyrite surfaces as determined by X-ray photoelectron spectroscopy. *International Journal of Minerals Processing,* 62(1-4), pp. 65-94.

Lamar, J. E., 1961. *Uses of Limestone and Dolomite,* Urbana: s.n.

Letts, S., Torsvik, T., Webb, S. & Ashwal, L., 2011. New Palaeoproterozoic palaeomagnetic data from the Kaapvaal Craton, South Africa. *The Geological Society,* 357(1), pp. 9-26.

Li, J. et al., 2010. Chalcopyrite leaching: the rate controlling factors. *Geochimica et Cosmochimica Acta,* 74(10), pp. 2881-2893.

Liu, Y., Zhou, M. & Zeng, G., 2008. Bioleaching of heavy metals from mine tailings by indigenous sulfur-oxidizing bacteria: Effects of substrate concentration. *Biosource Technology,* 99(10), pp. 4124-4129.

Li, Y. et al., 2013. A Review of the Structure, Fundamental Mechanisms and Kinetics of the Leaching of Chalcopyrite. *Advances in Colloid and Interface Science,* 197-198(September), pp. 1-32.

Lu, D. et al., 2016. Thermodynamic Analysis of Possible Chalcopyrite Dissolution Mechanism in Sulphuric Acid Aqueous Solution. *Metals,* 6(12), p. 303.

Lu, Z., Jeffrey, M. & Lawson, F., 2000. An electrochemical study of the effect of chloride ions on the dissolution of chalcopyrite in acidic solution. *Hydrometallurgy,* 56(2), pp. 145-155.

Lydall, M. & Auchterlonie, A., 2011. *The Democratic Republic of the Congo and Zambia: A Growing Global Hotspot for Copper-Cobalt Mineral Investment and Exploitations,* s.l.: s.n.

Maitre, R. L., 2002. *Igneous rocks: a classification and glossary of terms,* Cambridgeshire: Cambridge University Press.

Mibei, G., 2014. *Introduction to types and classification of rocks,* s.l.: s.n.

Mikhlin, Y. et al., 2004. Spectroscopic and electrochemical characterization of the surface layers of chalcopyrite (CuFeS2) reacted in acidic solutions.. *Applied Surface Science,* 225(1-4), pp. 395-409.

Moyo, T., 2016. *An Electrochemical and Leach Study of the Oxidative Dissolution of Chalcopyrite in Ammoniacal Solutions,* Cape Town: s.n.

Munoz, P., Miller, J. & Wadsworth, M., 1979. Reaction mechanism for the acid ferric sulfate leaching of chalcopyrite. *Metallurgical Transactions,* pp. 149-158.

Namur, O. et al., 2010. Crystallization sequences and magma chamber processes in ferrobasaltic Sept Iles layered intrusion, Canada. *Journal of Petroleum Science and Engineering,* 51(6), pp. 1203-1236.

Nava, D. & Gonzalez, I., 2006. Electrochemical characterization of chemical species formed during the electrochemical treatment of chalcopyrite in sulfuric acid. *Electrochemical Acta,* 51(25), pp. 5295-5303.

Palabora Mining Company, 2012. *About Palabora.* [Online] Available at: http://www.palabora.com/palabora.asp [Accessed 12 May 2018].

Palmer, C. & Johnson, G., 2005. The Activox (R) Process: Growing significance in the nickel industry. *The Journal of the Minerals, Metals & Materials Society,* 57(7), pp. 40-47.

Paphane, B., Nkoane, B. & Oyetunji, O., 2013. Kinetic studie on the leaching reactions in the autoclave circuit of the Tati Hydrometallurgical Demonstration Plant. *The Journal of The Southern African Institute of Mining and Metallurgy,* 113(6), pp. 485-489.

Parker, A., Paul, R. & Power, G., 1981. Electrochemistry of the oxidative leaching of copper from chalcopyrite. *Journal of Electroanalytical Chemistry and Interfacial Electrochemistry,* Volume 118, pp. 305-316.

Pawlek, F., 1976. The influence of grain size and mineralogical composition on the leachability of copper concentrates. In: *Extractive Metallurgy of Copper.* 2 ed. s.l.:s.n., pp. 690-705.

Peterson, J. & Dixon, D., 2006. Competitive bioleaching of pyrite and chalcopyrite. *Hydrometallurgy,* 83(1-4), pp. 40-49.

Prince, D. & Warren, G., 1986. The influence of silver ion on the electrochemical response of chalcopyrite and other mineral sulfide electrodes in sulfuric acid. *Hydrometallurgy,* 15(3), pp. 303-324.

Roman, R. & Benner, B., 1973. The Dissolution of Copper Concentrates. *Mineral Science Engineering.*

Schaming, J., 2011. *An investigation of leaching chalcopyrite ores.* Kingston, Ontario: Queen's University.

Schlesinger, M., King, M., Sole, K. & Davenport, W., 2002. *Extractive metallurgy of copper.* 4th ed. Amsterdam: Elsevier.

Shaw, D., Dreisinger, D. & Tomlinson, M., 2004. The commercialization of the FENIX iron control system for purifying copper electrowinning electrolytes. *The Journal of the Minerals, Metals & Materials Society,* 56(7), pp. 38-41.

Sillitoe, R., 2012. *Copper provinces: Society of Economic Geologists,* s.l.: s.n.

Simandl, G., 2014. Geology and market-dependant significance of rare earth element resources. *Mineral Deposita,* 49(8), pp. 889-904.

Simandl, G. & Paradis, S., 2018. Carbonatites: related ore deposits, resources, footprint, and exploration methods. *Applied Earth Science,* 127(4), pp. 123-152.

Skinner, H. & Jahren, A., 2003. Biomineralization. In: *Treatise on geochemistry.* s.l.:Elsevier, pp. 117-184.

Snell, G., 1975. *Sulfate leaching of copper ores using silver catalysts.* United States of America, Patent No. 886, 257.

Sokic, M., Markovic, B. & Zivkovic, D., 2009. Kinetics of chalcopyirte leaching by sodium nitrate in sulphuric acid. *Hydrometallurgy,* 95(3-4), pp. 273-279.

Stott, M., Wattling, H. & Franzmann, P., 2000. The role of iron-hydroxy precipitates in the passivation of chalcopyrite during bioleaching. *Minerals Engineering,* 13(10), pp. 1117-1127.

Theron, S., 2013. *The origin of the Central African Copperbelt: in a nutshell.* s.l., s.n.

Toplis, M. & Carroll, M., 1995. An experimental study of the influence of oxygen fugacity on Fe-Ti oxide stability, phase relations, and mineral-melt equilibria in ferro-basaltic systems. *Journal of Petroleum Science and Engineering,* 36(5), pp. 1137-1170.

Tshilombo, A., 2004. *Mechanism and kinetics of chalcopyrite passivation and depassivation during ferric and microbial leaching,* s.l.: Vancouver: University of British Columbia.

Tshilombo, O. & Ojumu, T., 2013. Investigation of the effect of pH operating conditions on bioleaching of low-grade chalcopyrite in column reactors. *Advanced Materials Research,* Volume 825, pp. 401-405.

Unrug, R., 1988. Mineralization controls and source of metals in the Lufilian fold belt, Shaba (Zaire), Zambia and Angola. *Economic Geology,* 83(6), pp. 1247-1258.

Veksler, I. & Lentz, D., 2006. Parental magmas of plutonic carbonatites, carbonate-silicate immiscibility and decarbonation reactions: evidence from melt and fluid inclusions. *Mineralogical Association of Canada,* Volume 36, pp. 123-149.

Venkatachalam, S., 1991. Treatment of chalcopyrite concentrates by hydrometallurgical techniques. *Minerals Engineering,* 4(7-11), pp. 1115-1126.

Wang, S., 2005. Copper leaching from chalcopyrite concentrates. *Journal of the Minerals, Metals and Materials Society,* 57(7), pp. 48-51.

Woolley, A. & Kempe, D., 1989. *Carbonatites: genesis and evolution,* London: Unwin Hyman.

Wyllie, P. & Huang, W., 1976. High CO2 solubilities in mantle magmas. *Geology,* 4(1), pp. 21-24.

Chapter 3: Leaching kinetics of copper from different chalcopyrite bearing ores: The effects of temperature and mineralogical composition

Abstract: The aim of the study was to determine the rate of Cu extraction from chalcopyrite ores of different mineralogical backgrounds, as well as to identify the rate of formation of passivation phenomena on the surface of the mineral. The objectives of the study were to observe the effects of temperature (25-85°C) on the extraction rate, as well as the effects of mineralogical composition on the dissolution rate and formation of the passivation layer. Experiments were conducted in sulphite media, with ferric sulphate as oxidant, and in which the solution pH was allowed to evolve. For mineralogical characterisation of the host rock samples (carbonatite and silicate ROM), X-ray florescence (XRF) was used. Speciation data was obtained using PHREEQC simulation software with input parameters of pH, oxidation redox potential (ORP), acidity, alkalinity, and chloride and sulphate ion concentrations obtained during chemical shake flask leaching. The carbonatite associated with calcite-magnesium and dolomite displayed acid consuming behaviour, as rise in temperature conditions were concurrent with rise in pH levels, promoting alkaline conditions; retardation of the copper recovery rate was observed under these alkaline conditions, probably due to the mineral's surface being covered by a matrix mixture of gypsum and hematite, as well as ferric salts restricting the transport of electrons from the mineral surface. The silicate mineral associated with various silica species (quartz, coesite quartz and rose quartz), followed by copper sulphide species, displayed characteristics of acid attack, which intensified with temperature increase, as pH was maintained at low levels (pH 1-2). Recovery of copper was favoured under these conditions, as it allowed for the minimisation of ferric salt species; the presence of pyrite also enhanced leaching through galvanic interactions with chalcopyrite.

Keywords: chalcopyrite, carbonatite, silicate, sulphate media, mineralogy, temperature

3.1 Introduction

Copper porphyry deposits account for the bulk of the World's copper extraction and production processes. These porphyry deposits are constituted of different depth layers, each containing different copper minerals. The first layer, the shallow surface zone, contains copper oxides minerals whereas the larger banded supergene zone is constituted of secondary Cu-bearing minerals; the hypogene zone, the deepest porphyry deposit, where chalcopyrite, accounting for 70% of the World's copper reserves, is deposited (Schaming, 2011; Li et al., 2013). Hydrometallurgical extraction of copper from chalcopyrite is the most desired extraction process as it does not contain the high SO_2 emissions (Sokic et al., 2009) associated with pyrometallurgical extraction. Lower process costs and better waste management also make hydrometallurgy a more attractive option. However 80-85% of Cu extracted from $CuFeS_2$ is obtained through pyrometallurgical techniques as current hydrometallurgical processes provide low leaching rates as a result of a passivation layer formed on the surface of the mineral during leaching (Stott et al., 2000). Elemental sulphur, copper-rich metal deficient layers, the existence of polysulphides as well as jarosite formation have all been hypothesised as the origin of the formed passivation layer (Tshilombo, 2004).

It is beyond the scope of this study to identify the exact cause of the passivation film, and this phenomenon will not be expanded upon further. Studies dedicated to finding the exact mechanism for the formation of the passivation film have fallen short; focus has rather been placed on studies associated with identifying specific parameters whereby the leaching kinetics of copper from chalcopyrite is said to improve. The use of additives, solution acidity, mineralogy of the host ore, reaction temperature and the use of specific lixiviants are some of these influencing parameters (Hackl et al., 1995; Antonijevic & Bogdanovic, 2004; Acero et al., 2009). Effects of acid concentration, reaction temperature and mineralogical compositions of the hosting ores were observed in this chapter.

Temperature conditions play an important role during chalcopyrite leaching as elevated temperatures provide desirable conditions for the extraction of copper (Schaming, 2011). Along with elevated temperatures (above 40°C), acid concentration in solution also effects the leaching rates; low solution pH (pH 1-2) has proven to be beneficial for Cu extraction as it prevents the precipitation of ferric salts, known to hinder Cu dissolution (Dutrizac et al., 1969; Acero et al., 2009; Joe et al., 2009). Mineralogical compositions is important as gangue species associated with the hosting mineral as well as interaction of solids contained within these minerals influence the leaching performance (Vilca, 2013; Barlow et al., 2018). The choice of lixiviant is also important as it might have different outcomes on the leaching performance depending on the associated host mineral composition.

3.2 Experimental setup and methodology

3.2.1 Materials

Solutions of the desired pH values were prepared using analytical reagent-grade sulphuric acid (H_2SO_4 98% ACE), ferric sulphate ($Fe_3(SO_4)$ X H_2O ACE), sodium hydroxide (NaOH pellets ACE) and distilled, deionised water (7.0 µs/cm). A pH meter and temperature probe (Hanna pH HI 8424) were used to measure pH, which was regularly calibrated with 4 and 7 standard buffer solutions, and the measured redox potential (Ag/AgCl) measurements were referenced to the Standard Hydrogen Electrode (SHE).

3.2.2 Chalcopyrite samples

The carbonatite samples that were used in the study was provided by the Phalaborwa Mining Company and received from their Rio Tinto mine in Phalaborwa, South Africa. Prior to use, the ROM samples required for experimentation were, first, crushed to +150 µm and then sieved to -150 µm, after which the sieved samples were stored in tightly sealed plastic containers, at room temperature conditions, until use. The silicates were provided by Ruashi Mine, which is located in the Katanga province of the DRC. As with the carbonatites, the silicates were crushed, then sieved to -150 µm and stored in a laboratory cabinet, at room temperature.

3.2.3 Chemical leaching of chalcopyrite ores

To leach the chalcopyrite feed stream samples of the silicate and carbonatite minerals, an incubator with a built-in orbital shaker (Labcon, South Africa) was used. The incubator acted as a containment chamber to prevent contamination of the solutions during experimentation, and maintained both the temperature and rotational speed. A volumetric flask holding 500 ml was used to prepare a 10% mass by volume solution; the liquid solution was prepared using distilled water, sulphuric acid and ferric sulphate, to produce a ferric sulphate solution of 0.1 M (Cordoba et al., 2008a). The experiments were carried out in triplicate with varying experimental conditions, and four sets of shake flask tests were conducted. Rotational speed for the orbital shaker was stable at 200 rpm, whilst temperature was set over a range of 25-85°C, increasing by a 20°C increment for each shake flask test. The solution for each shake flask test was prepared with a pH value of 0.5-1, after which the experiments were allowed to run under natural pH conditions for the duration of each 12-hour leaching test. The dissolution kinetic information was obtained on 30 ml samples, which were withdrawn from the leaching vessel hourly, and each was analysed for its dissolved metal content (Cu and Fe), using inductively coupled plasma optical emission spectroscopy (ICP-OES). Prior to that, the withdrawn slurry was filtered using 150 mm filtration paper. Lastly, the filtered residue was dried, stored in a desiccator and subjected to mineralogical characterisation using X-ray diffraction (XRD).

3.2.4 Equipment

The extracted slurry was filtered to obtain a clean leachate solution, of which a 1 ml sample was extracted and diluted by a factor of 10 using a 1% HNO_3 solution for standardisation. The samples were then stored in a laboratory fridge at 4°C until use. The standardised solutions were analysed for dissolved metal concentration (specifically Ca, Cu, Fe and Mg totals) through a use of ICP-OES (Agilent Technologies, USA). The iron content was determined by chromatometric titration using potassium dichromate ($K_2Cr_2O_7$). The solid residues were assessed for mineral content, optical phase identification and surface morphology by means of XRD, optical microscope and SEM–EDX, respectively. An XRD analysis using a Rigaku Ultima IV (operated at 40 kV and 30 mA) and PDXL analysis software was carried out; the instrument's detection limit was 2%. This technique enables the identification and quantification of the various mineral phases. The operating conditions of the diffractometer's copper radiation source were 30 kV and 25 mA. Data was recorded over the range $5° \leq 2\theta \leq 95°$. The samples were milled further, to 53 μm, and were scanned at 0.5°/min, with a step width of 0.01°. Tescan SEM (operated at 20 kV) with EDX analysis was used for grain morphology and chemistry. The leach residues were carbon coated prior to analysis. Lastly, the mineral identification was assessed using an optical microscope on samples mounted on epoxy resin.

3.2.5 Leachate analyses

Leachate samples obtained from filtering the chalcopyrite solutions were measured for pH, oxidation redox potential (ORP) and temperature. To measure pH, temperature and ORP (for each leachate solution), a portable pH meter with an analytical electrode HI8424 (Hanna Instruments Inc.) was used. Samples were also measured for sulphate ion concentration, chloride ion concentration, iron ion concentration, acidity and alkalinity. A Multiparameter Photometer HI 83099 was used for COD (chemical oxygen demand) and sulphate ion concentration of the selected samples.

3.2.6 Titration tests

3.2.6.1 Acidity

Using a 1 L volumetric flask, 1.06 g of sodium carbonate (Na_2CO_3) (0.02N) and 0.8 g of sodium hydroxide (NaOH) (0.02 N) were weighed off and diluted to 1 000 ml with distilled water. All the standard solutions for the titration procedure were diluted using distilled water, which had been boiled for 15 min and let cool to room temperature.

For the titration procedure, 3 ml of leachate was topped up with distilled water up to a 50 ml solution. Titration was carried out for solutions with pH values higher than 3.7. Titration with Na_2CO_3 was used as standardisation procedure. Thereafter, samples were titrated using NaOH solution until an endpoint pH value of 8.3 was achieved. Titration was conducted using a 50 ml burette.

3.2.6.2 Alkalinity

The alkalinity was measured with a titration method with 0.1 N sulphuric acid (H_2SO_4), prepared in a 1 L volumetric flask. Thereafter, 20 ml of leachate was topped up with distilled water to give a 100 ml solution. The solution was titrated from pH values lower than 8.3, to 4.5, using an indicator for clear endpoint visibility.

3.2.6.3 Chloride ion

Standard preparation was used for chloride titration: Silver nitrate crystals ($AgNO_3$) and potassium dichromate (K_2CrO_4) reagents were first dried in an oven at 100℃ for 2 hours, after which 2.395 g of $AgNO_3$ was weighed off and diluted to 1 000 ml with distilled water using a 1 L volumetric flask. A mass of 0.265 g sample of sodium chloride (NaCl) was weighed, transferred to a 100 ml volumetric flask and diluted using distilled water. Using distilled water, 10 g of K_2CrO_4 was weighed and diluted to 200 ml, after which $AgNO_3$ solution was added until a definite precipitation was formed. The K_2CrO_4 solution was then let stand for 12 hours.

A 50 ml NaCl solution was used to standardise the $AgNO_3$ titrant. Distilled water was used to top up 3 ml of leachate to obtain a 50 ml solution. The titration was carried out for a solution with pH values between 7 and 10. Sulphuric acid (H_2SO_4) and sodium hydroxide (NaOH) were used to adjust the pH if it was not in range. Before titrating with silver nitrate ($AgNO_3$) using a 50 ml burette, 1 ml of potassium chromate indicator (K_2CrO_4) was added. Titration continued until an orange-brown endpoint was reached.

3.2.6.4 Iron ion

The standard preparation for iron titration was as follows: 1.18 g of potassium dichromate (K_2CrO_4) was dried in an oven at 100℃ for a 2-hour period. The K_2CrO_4 was then transferred to a 250 ml volumetric flask and dissolved using distilled water to prepare a 0.02 M solution. Then, 3 g of ferrous ammonium sulphate ($(NH_4)_2Fe(SO_4)_26H_2O$) was weighed and transferred to a 250 ml flask, after which it was dissolved and diluted to 100 ml with boiled, deionised water and used to standardise potassium dichromate. After this, 30 ml of 50% sulphuric acid (H_2SO_4) and 10 ml of phosphoric acid (H_3PO_4), together with 8 drops of diphenylamine sulphonate indicator, were added. The solution was then titrated using K_2CrO_4 until a purple endpoint was reached.

For titration of the leachate sample, 1 ml of the leachate was extracted and diluted by a factor of 10 using distilled water, after which 2 ml of concentrated phosphoric acid (H_3PO_4) was added, as well as 2 to 4 drops of the indicator. The solution was then titrated with potassium dichromate (K_2CrO_4) until a purple endpoint was reached.

3.2.7 Speciation modelling

To determine the aqueous speciation of the major metal ions in the leachate of the chalcopyrite samples, AQUACHEM software was used, interfaced with PHREEQC (program version 3.3.12-12704) modelling software (Barlow et al., 2018). The PHREEQC database, Minteq.v4.dat was used for the purpose of this report. The ORP had to be adjusted with a correction factor before it could be used as input data. The correction factor was obtained from field measurements of oxidation-reduction potential (Stiggov, 2013). The corrected ORP value was then used to calculate the pe value using the following equation:

$$pe = E\_h/(0.059)$$

pe donates the negative logarithm of the electron activity

Eh donates the ORP of the sample

To predict the speciation of the major metals present within the leachate of the chalcopyrite-bearing minerals, the following input data was used within the PHREEQC workbench interface: acidity, alkalinity, pH, pe, temperature (°C), ICP data (metal ion concentrations), Cl^- and SO_4^{2-}.

3.3 Results and discussion

3.3.1 X-ray diffraction mineral investigation

The diffraction spectrum related to the different mineral phases present within the analysed ROM host ores, is presented in Figure 3-1.

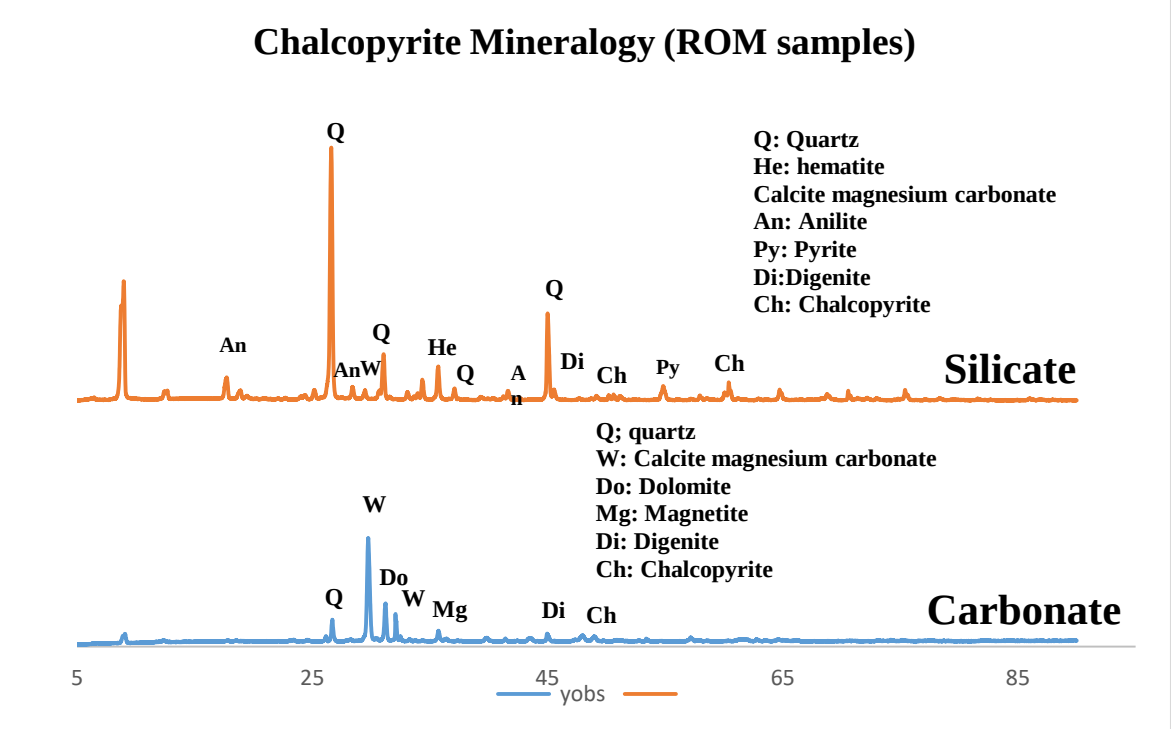

Figure 3-1: Diffraction spectrum of chalcopyrite-containing host rocks (XRD results)

The composition of the carbonate mineral and siliciclastic dominant minerals come from two very different geological complexes and, thus, mineralogical composition (and diffraction spectrum) of both host rocks are expected to be vastly different. In the carbonate samples, calcite magnesium (W) was identified as the major representative mineral (50%) present within the carbonatites, and quartz as the major mineral (20%) in the silicate sample. The XRF data displayed similar results for the elemental composition of Ca and Si (50% and 14.5% respectively). The other peaks displayed for quartz within the silicate host mineral, are the diffraction patterns for barium silicate, coesite quartz and rose quartz (13.3%, 11.5% and 3.5%, respectively). Dolomite displayed the second-highest carbonate diffraction spectrum, at 32%. The younger carbonatites formed at the Phalaborwa carbonatitic complex are described as being intrusive (Heinrich, 1970), which carbonate minerals are known to be principle constituent of, with approximately 60% of the world's intrusive carbonatites consisting of predominantly calcite, which corresponds with the concentration grade of calcite-magnesium and dolomite identified within the mineral (Chakhmouradian et al., 2016).

Furthermore, it can be said that the carbonatite host ore samples can be regarded as a calcite-rich silico-carbonatite, due to its high percentage of Ca and Si, which act as impurities (Nyembwe et al., 2019). Hematite (He) was also identified as a major constituent within the silicate mineral, at 9.5%. Chalcopyrite (Ch) was present within the silicate ore at 6.2% with the remainder of the copper sulphide minerals present being analite (An) and the secondary copper sulphide, digenite (Di) (6.8% and 6.2% respectively). Iron (Fe) is available within the iron oxide mineral magnetite (Mg) at 7%, whereas iron's presence within the silicate mineral was constituted by both iron oxide and iron sulphide minerals, hematite (He) and pyrite (Py), respectively. The presence of pyrite within the silicate host ore is of significance, as pyrite is known to aid the kinetic leaching of copper from chalcopyrite due to galvanic interaction between both minerals (Berry, 1978).

Table 3-1 presents the distribution of the identified minerals, in weight percentage, for the analysed host rock samples:

Table 3-1: Mineral composition of host rock samples

XRD RIR: observed phase quantification				
Observed phases		**Weight % in sample ores**		
Phase name	**Phase chemistry**	**Carbonatite**	**Silicate**	**Tails**
Analite	Cu_7S_4	****	6.76	****
Barium Silicate	Ba_2SiO_4	****	13.31	****
Calcite magnesium	$(Mg_{0.06}Ca_{0.94})\ (CO_3)$	48.20	****	73
Chalcopyrite	$CuFeS_2$	1.54	6.20	0.47

Coesite	SiO_2	****	11.47	****
Copper sulphide	Cu_2S	****	3.70	****
Digenite	Cu_9S_5	1.48	6.23	****
Dolomite	$CaMg\ (CO_3)_2$	32.34	****	****
Gehlenite	$Ca_2Al(Al,Si)_2O_7$	****	****	5.78
Hematite	Fe_2O_3	****	9.50	10.07
Lime	CaO	****	0.09	****
Magnetite	Fe_3O_4	7.02	****	****
Moganite	SiO_2	****	3.47	****
Periclase	MgO	5.64	9.10	****
Pyrite	FeS_2	****	6.89	****
Potassium oxide	K_2O	****	3.61	****

3.3.2 X-ray florescence elemental investigation

The bulk elemental chemistry of the chalcopyrite-containing host minerals of silicate and carbonatite is presented in Figure 3-2 and 3.3 respectively. Figure 3-2 shows the elemental compositions of the main elements, and Figure 3-3 those of the trace elements, as reported through XRF. Cr represents the carbonatite feed stream samples and Sr that of the silicate mineral.

Although it is not uncommon to find copper concentrations of 7-8% within the central African copper belt, most operations in the region, on average, report copper grades of between 1 and 4% (Lydall & Auchterlonie, 2011) which is observed for the silicate sample, which had a grade of 2.69%. The iron content was much higher in the carbonate samples than in that of the silicates; this occurrence could be due to the different iron mineral phases within the various host rocks – the former contains the iron oxide mineral, magnetite, which constitutes an important accessory that is not present in the latter (Beale, 1985a).

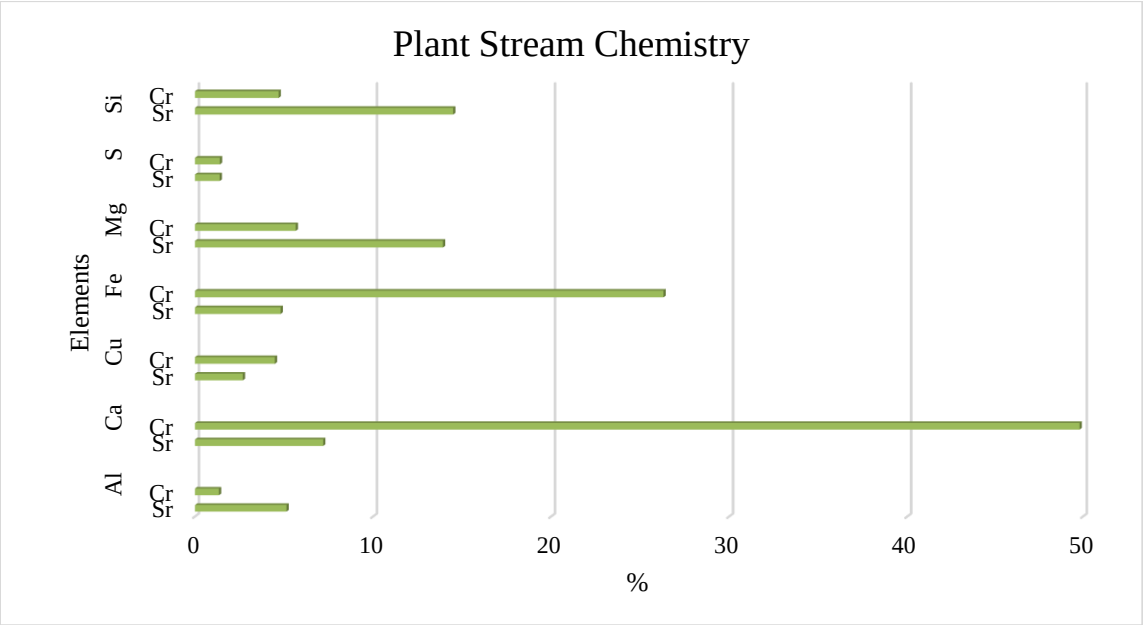

Figure 3-2: Bulk stream chemistry (main elements)

The main component of the Cr sample were identified as calcium (Ca), at 50%, whereas Ca only constituted 7% of the silicate run of mine (Sr) samples. Silica (Si) was identified as the main component of the Sr sample, but a relatively similar percentage was recorded for magnesium (Mg) (15% and 14%, respectively); with Si and Mg being present at only 5% and 6% in the carbonatite samples. The sulphur (S) content for both host rocks was relatively similar (1.4% and 1.39% respectively). Potassium (K) was also present at a high concentration (8%) in the silicate ore, as opposed to the trace amount (0.8%) identified within the carbonatite mineral.

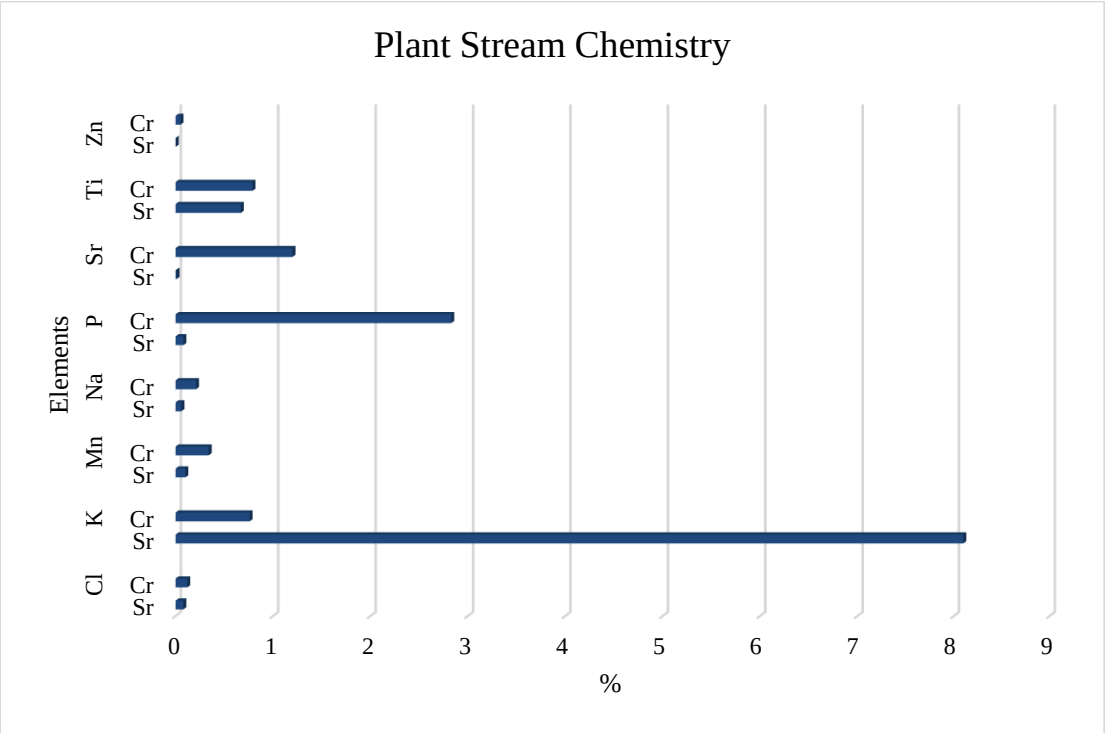

Figure 3-3: Bulk stream chemistry (trace elements)

3.3.3 pH Variation

The solution samples used during experimentation was initially prepared to a pH between 0.5 and 1 using sulphuric acid together with ferric sulphate, after which pH evolution was allowed to occur in order to analyse the effects of the gangue species within each of the hosting ores, on the acid concentration. Figure 3-4 displays the behavioural change in pH for both chalcopyrite-containing host ores during each of the various temperature runs conducted for the study.

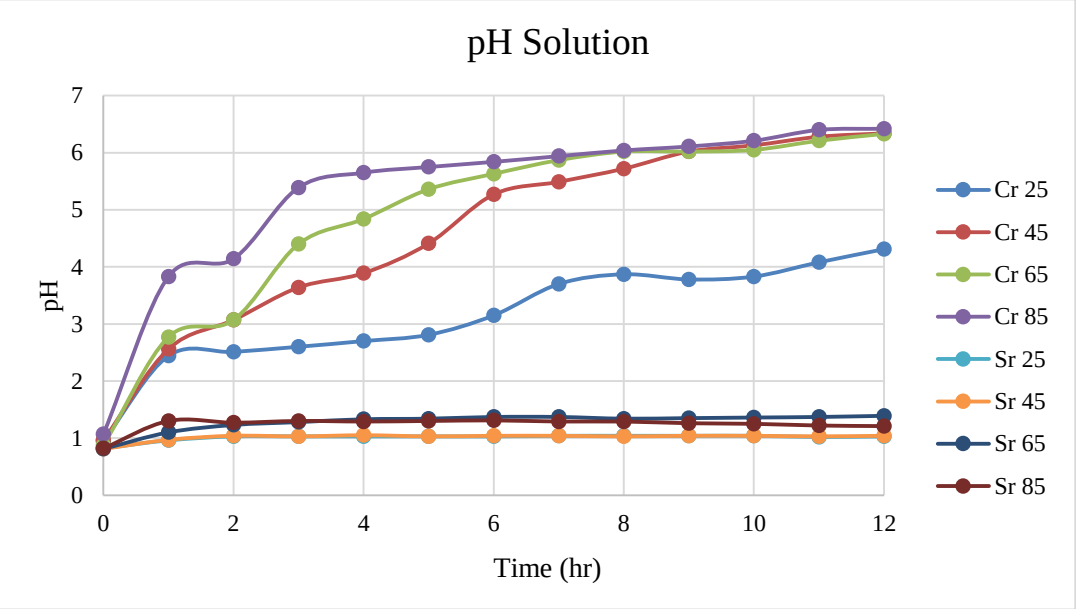

Cr: Carbonatite rom; Sr: silicate rom

Figure 3-4: pH behaviour at varying temperature conditions

For the carbonate samples, the lowest pH levels were observed for the experimental run conducted at 25°C, with the pH level, after the 12 hours dissolution period, being 4.31. For the experiments conducted at 45-85°C, the rate at which pH increased was in direct proportions to the increasing temperature, as shown in Figure 3-4. The high pH values observed during experimental runs conducted using the carbonate mineral is due to the acid in solution being neutralised by the high concentration of calcite-magnesium and dolomite minerals within the carbonate host rock, as observed from XRD analyses (Table 3-1). These minerals, in solutions, favour the formation of ionic species, such as Ca^{2+}, which replace hydrogen ions in solutions and, in doing so, effectively neutralise the solution acidity and promotes an increase in pH levels (Lamar, 1961). Furthermore, it can be said that, at lower temperatures (25°C), acid attack plays a vital role during mineral dissolution, as sulphuric acid promotes the formation of insoluble calcium salt species ($CaSO_4$) (Scrivener, 1998); competition with hydrogen ions is reduced, as less Ca^{2+} ions are formed, leading to acidic pH conditions.

The pH behaviour of the silicate host mineral displayed relatively stable changes in pH for each of the experimental runs over the whole temperature range, where a 0.4 change in value between highest and lowest final pH values were observed, compared to the carbonates, which displayed a 2.1 value increase between highest and lowest final pH values. From the observation, it can be said that the acid consumption during mineral dissolution of the silicate species is much lower than that observed for the carbonatite mineral. Oxidation of pyrite and other sulphide species leads to the formation of secondary sulphuric acid ($H_2SO_4^-$), which aided in replenishing the acid consumed during dissolution to stabilise the pH levels, as seen in Figure 3-4 (Fosso-Kankeu et al., 2017).

3.3.4 Effects of temperature

Figure 3-5 represents the dissolution curve of Cu from both chalcopyrite-containing host ores in acidified sulphate solution where pH evolution is allowed to occur naturally. Figure 3-6 represents the comparative dissolution curve of Cu and Fe for the dissolved Cu and Fe in solution of the carbonate host mineral, and Figure 3-7 that of the silicate.

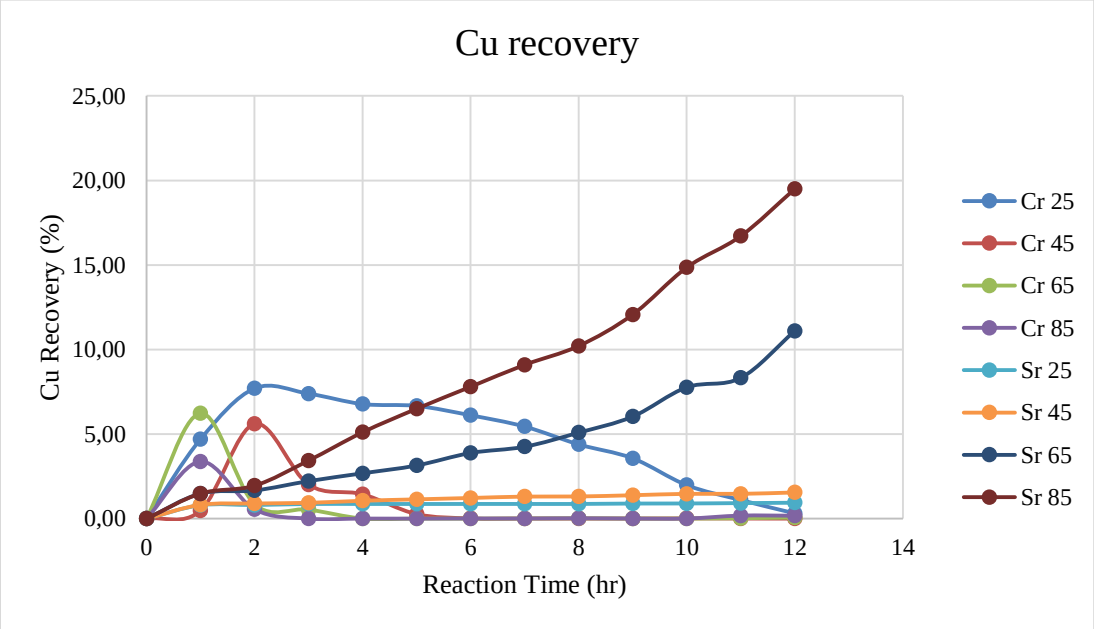

Cr: Carbonatite rom; Sr: silicate rom

Figure 3-5: Copper recovery for chalcopyrite-containing host ores in ferric sulphate media

The extraction of copper for the observed temperature range (25-85 °C) was carried out in a sulphate-based ferric sulphate medium. In the case of the carbonatite mineral dissolution, the recovery rate was enhanced at lower temperature conditions; at room temperature (25°C) conditions, the peak recovery rate of 7.7% was obtained after 2 hours of leaching, the recovery of Cu thereafter decreased to 0.3% recovery after 12 hours of dissolution. As temperature increased, the recovery rates slowly decreased, as peaks of 5.6% (after 2 hours at 45°C), 6.2% (after 1 hour at 65°C) and 3.4% (after 2

hours at 85°C) were obtained, after which copper concentrations decreased rapidly. The higher recovery rates observed for Cu at 25°C are due to the lower pH conditions found at this temperature range (pH 0.95-4.31), which implies that higher concentrations of protons were released at this temperature. Cu leaching from chalcopyrite, being an acid-consuming reaction, is favoured by these conditions, as solubility is also enhanced in acidic media (Acero et al., 2009). The mineralogical investigation conducted for the carbonatite mineral concluded that the hosting ore is mainly constituted of calcite-magnesium ($Mg_{0.06}\,Ca_{0.94}$) (CO_3) and dolomite ($CaMg\,(CO_3)_2$), and correlates with the results obtained from ICP analyses, in which high concentration of Ca and Mg were observed. The slower dissolution kinetics (45-85°C) are likely due to an increase in calcium ion (Ca^{2+}) released in solution as temperature increases, thereby effectively decreasing the concentration of hydrogen ions and, therefore, the acid levels essential for effective copper recovery to occur.

Copper recovery behaviour observed for the silicate host mineral is more stable, as the pH conditions are stabilised, and display an increasing trend in copper unit recovery for each of the measured temperature conditions. The low pH conditions are due to a high concentration of copper sulphide minerals (22.89% of the mineralogical composition), as well as the presence of pyrite, which, when dissolved, forms H_2SO_4; this will also explain the high sulphate concentration measured during experimentation, compared to the low concentration observed for the carbonate host mineral. Ca concentrations are also lower in the silicate mineral, as observed from the bulk elemental characterisation, therefore, Ca will have a smaller impact on acid formation and, by extension, proton concentration in solution. It is known that chemical reaction rates of the chalcopyrite mineral usually increase at higher temperatures in an acidic solution (Schaming, 2011), which was observed during leaching of the silicate mineral. Increase in temperature thermodynamically favours a rate increase in copper recovery from the chalcopyrite-containing host ore; 19.5% extraction was obtained at 85°C, whereas only 1% extraction was obtained at 25°C after 12 hours of leaching.

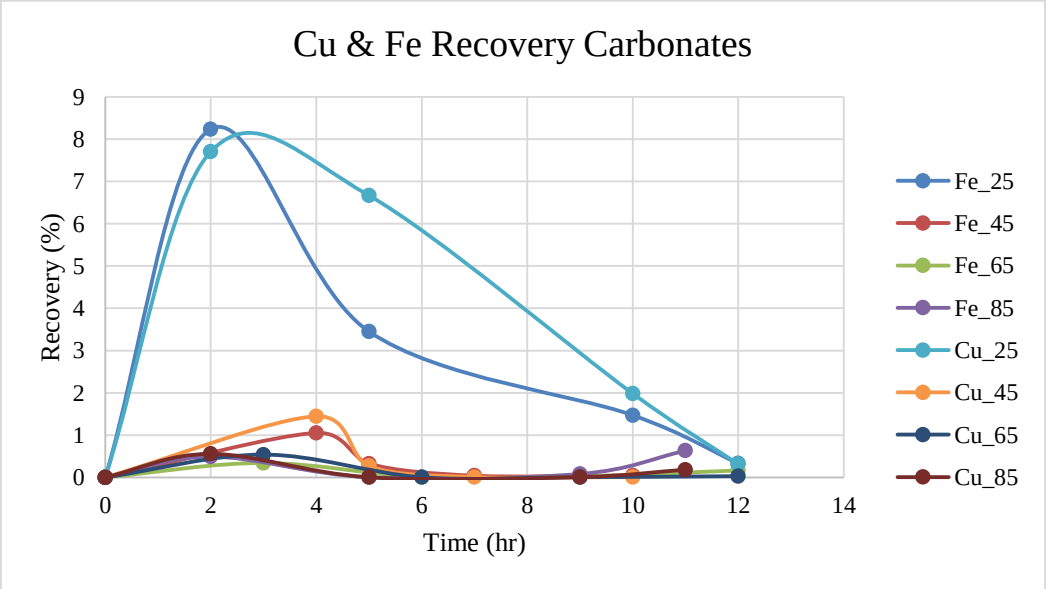

Figure 3-6: Dissolution of Cu and Fe for the carbonatite host ore

The data obtained during XRF analyses indicates that Fe acts as a major elemental component within the carbonatite mineral, and has a concentration of 26.31%, compared to 4.49% observed for Cu. As illustrated in Figure 3-5 and 3.6, retardation of the recovery rate of Cu occurs, which can be attributed to the increase in pH value and decrease in redox potential during dissolution of the carbonatite mineral; the same holds true for the extraction behaviour associated with Fe, for which an overall decrease in the recovery rate for each of the measured temperatures was observed. Although Fe displays the same behaviour as Cu over the temperature range when the dissolution behaviour yields better results under acidic conditions, the recovery rate of Fe is higher than for Cu for experiments conducted at 45°C, 65°C and 85°C. The iron in solution competes with Cu to form free hydrated ferrous ion (Fe^{2+}), rather than cupric ion (Cu^{2+}), where free hydrated species of metals are more soluble within an aqueous solution. Cu might favour the formation of the complex salt species $CuSO_4$ instead, which does not promote the dissolution of Cu, as it is insoluble in an aqueous medium. Although extraction of Cu is not favourable under these leaching conditions, passivation of the mineral was not yet reached, as a static plateau stage was not observed during the set leaching time (12 hours).

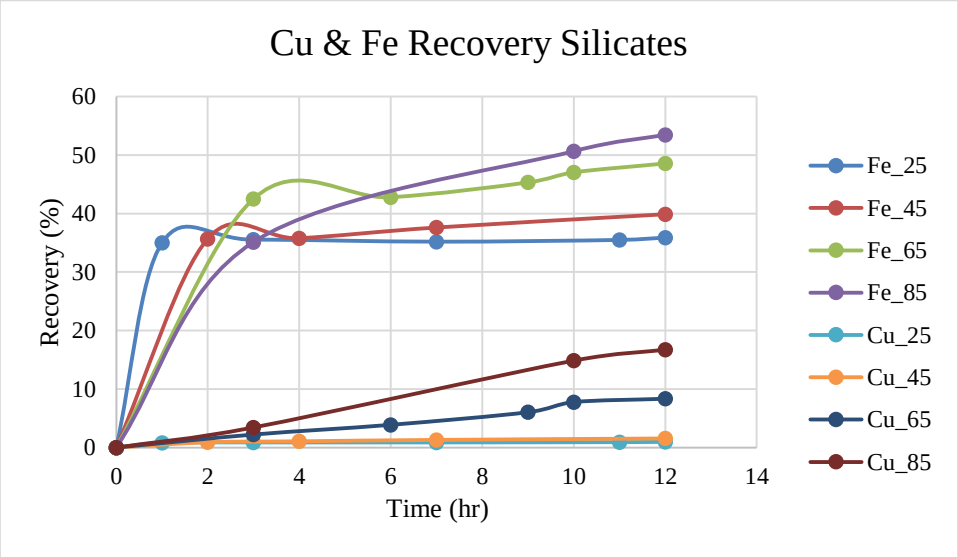

Figure 3-7: Dissolution of Cu and Fe for the silicate host ore

As with the carbonatite mineral, the Cu and Fe in solution display relatively similar dissolution behaviour. However, unlike the carbonatite mineral, the dissolution of the silicaclastic mineral increases with an increase in temperature under acidic conditions (pH stable at <2). Under the leaching conditions observed during dissolution of the silicaclastic mineral, the Fe curves for the measured temperature conditions, display parabolic behaviour, which indicates that a static plateau stage is reached during the set leaching time (12 hours); the retardation of iron recovery allows for

lower concentrations of competing ferrous ions (Fe^{2+}) in solution with soluble Cu^{2+} species. As a result, under these acidic condtions (pH 1-2), the extraction of Cu is promoted, as seen in Figure 3-7, where a linear recovery trend can be observed, which indicates that passivation was not reached for the silicaclastic mineral during the set leaching time for each of the measured temperature condtions (25-85℃). Furthermore, the formation of ferric salts at these pH conditions is reduced; ferric salt, such as jarosite, restricts the mass transfer of ions from the surface of the mineral and thereby slows the leaching kinetics (Khoshkhoo, 2014).

3.3.5 Speciation results

The species predicted to be present during leaching of the chalcopyrite-containing ores were obtained with the PHREEQC workbench software using input parameters obtained during experimentation. The species were predicted accurately, allowing for an error threshold of only 10%. Table 3-2 represents the species present for the major metal ions within the ROM solutions of both host minerals as a % range for each of the measured temperatures over the 12 hours dissolution period.

Table 3-2: Speciation results for Cu-containing chalcopyrite feed stream ores

Element	Species	Carbonates				Silicates			
		25℃	45℃	65℃	85℃	25℃	45℃	65℃	85℃
Ca	$CaSO_4$	48.12-51.59	40.40-45.38	41.86-42.69	35.55-43.45	44.95-52.31	50.14-52.12	61.2-65.91	59-93-62.77
	Ca^{2+}	48.41-50.01	54.62-56.05	54.35-55.21	53.24-60.43	48.49-55.04	47.88-49.87	34.11-38.78	36.45-40.08
	$CaOH^{+}$	<1	<1	<1	<1	<1	<1	<1	<1
	$CaHCO_3^{+}$	<1	0-4.21	2.94-3.37	3.71-4.17	<1	<1	<1	<1
Cu(2)	$CuSO_4$	43.03-51.69	31.81-46.94	27.64-37.93	20.25-31.13	45.11-51.7	50.28-52.26	61.22-65.71	59.72-63.39
	Cu^{2+}	48.14-49.69	43.34-54.34	35.70-50.08	34.94-53.33	48.33-54.89	47.85-49.75	34.27-38.77	37.37-40.27
	$CuOH^{+}$	<1	0-7.01	0-0.52	0.28-0.54	<1	<1	<1	<1
	$CuHCO_3^{+}$	<1	0-13.24	9.08-10.97	6.51-14.71	<1	<1	<1	<1
	CuCO3	<1	0-11.38	0.77-26.74	0.58-46.38	<1	<1	<1	<1
Fe(2)	Fe^{2+}	67.55-73.16	66.38-72.03	69.38-70.16	70.74-74.07	89.72-91.12	90.29-90.98	85.79-86.89	85.79-89.58

	$FeSO_4$	26.84-31.97	26.28-32.89	28.57-29.61	27.90-31.86	8.88-9.79	9.05-9.72	13.07-14.2	11.33-14.21
	$FeOH^+$	<1	<1	<1	<1	<1	<1	<1	<1
	$FeHCO_3^+$	<1	<1	1.27-1.47	1.35-1.77	<1	<1	<1	<1
Mg	$MgSO_4$	43.05-45.68	35.62-39.62	36.9-37.67	31.14-39.25	39.23-46.42	44.30-46.27	53.08-58.3	54.45-58.21
	Mg^{2+}	54.32-55.91	54.52-62.49	60.5-61.21	59.24-66.18	53.58-60.77	53.76-55.70	41.72-46.91	42.64-45.54
	$MgOH^+$	<1	<1	<1	<1	<1	<1	<1	<1

Speciation formation for the carbonatite mineral obtained at room temperature (25°C), differs from that obtained at the higher temperature conditions, as was expected. Calcium (Ca) favoured the formation of the complex hydroxide species $CaSO_4$, with concentrations of 48.12-51.59%; the free hydrated species Ca^{2+} was also present at slightly lower concentrations (50.01-48.41%). These ions are known to have an effect on pH levels, as they compete with the H^+ ions in solution to promote alkaline conditions (Balaria, 2011). Copper is primarily present as cupric copper (Cu(II)) at 99%, with cuprous copper (Cu(III)) also being observed in very low proportions (<1%). Cu favours the formation of the complex salt species $CuSO_4$ (50.08-51.69%), with a slightly lower concentration of free hydrated ionic species (Cu^{2+}). Iron is dominant as ferrous iron (Fe(II)), with ferric iron (Fe(III)) also present in solution in low proportions (<1%). Fe, in contrast to Cu, favours the formation of free hydrated ions (67.55-73.16%) in greater proportions to complex salt species (26.84-31.97%). From the prediction of species formation with PHREEQC simulation software, it is evident that acid attack occurs at lower temperature conditions within the carbonatite media; this occurrence is minimised as temperatures increase, as is evident from the parallel increase in Ca^{2+} ions as temperature rises, and from a decrease in the formation of calcium salt species.

It can, therefore, be said that calcium thermodynamically favours the formation of the free hydrated Ca^{2+} species, as at higher temperatures in the carbonatite-sulphate-based solution. The concentration of these species ranged from 48.36 to 60.43%, with the highest concentrations forming during experimentation conducted at 85°C. This would explain the difference in pH for the carbonate mineral over the temperature range, as observed in Figure 3-4, where the pH of the solution at 45-85°C tended to stabilise at pH levels above 7, and that of room temperature at just above 4; here $CaSO_4$ was identified as the dominant Ca species. Solubility of metals is increased within an acid medium (Hoffert, 1947; Fosso-Kankeu et al., 2017) and decreases in an alkaline media, which is evident from the higher recoveries of Cu at 25°C, as opposed to recoveries at higher temperature conditions, as observed from Figure 3-5. At higher temperature conditions (45-85°C), Cu^{2+} formation

was higher in concentration compared to $CuSO_4$, dominant at 25°C; however, the bulk of species present at these temperature conditions were complex hydroxide and carbonate species, $CuSO_4$, $CuHCO_3^+$ and $CuCO_3$ which are generally insoluble species, with $CuSO_4$ identified by previous studies as generally not promoting the leaching of copper in a sulphate system (Dutrizac, 1981; Barlow et al., 2018). The speciation data also displayed a direct correlation between an increase in temperature and the formation of complex carbonate species – a maximum of 11.38% at 45°C, to 46.38% at 85°C. Even with the decrease in concentration of Fe over the 12 hours leaching period for all temperatures, the dominant species formed to a great extent (70%), was the free hydrated ion Fe^{2+}. Iron is preferentially released in the solution over copper, explaining the low concentrations of free hydrated copper species observed in solution (Lu et al., 2016).

The speciation formation for the silicate mineral displays a better correlation than that of the carbonatite mineral, as Ca is dominant as the complex salt species, $CaSO_4$, at each of the measured temperature conditions. The free hydrates ionic species Ca^{2+} decreases with an increase in temperature and, consequently, an increase in $CaSO_4$ concentration was observed. It can, therefore, be said that an increase in temperature during sulphate leaching of the silicate mineral strengthened the effects of acid attack during mineral dissolution. The low concentration of the Ca^{2+} ions corresponds with the pH data obtained for the silicate host mineral (Figure 3-4). Just as with the carbonatite host mineral, Fe favours the formation of the free hydrate species Fe^{2+} over the whole temperature range, with average concentration of 90%, the remainder being $FeSO_4$. The formation of the free hydrates species in the acid media promotes the solubility of iron, as is visible from the increasing Fe concentration obtained during ICP analyses. Copper favours the formation of $CuSO_4$, as opposed to Cu^{2+}, over the whole temperature range, which could be due to the high Fe^{2+} concentration released in solution over Cu^{2+} ions; however, despite this occurrence, the dissolution of Cu in silicate mineral is much higher than that of the carbonates, and shows excellent recovery rates, as can be observed in Figure 3-5.

3.3.6 Mineralogical characterisation of leaching solid residue

3.3.6.1 Carbonatite

Figure 3-8 and 3.9 show the mineral content of the carbonatite solid residue samples, collected during experimentation, for each of the measured temperatures. Table 3-3 contains a list of all the major minerals present within the various residue samples as percentage values.

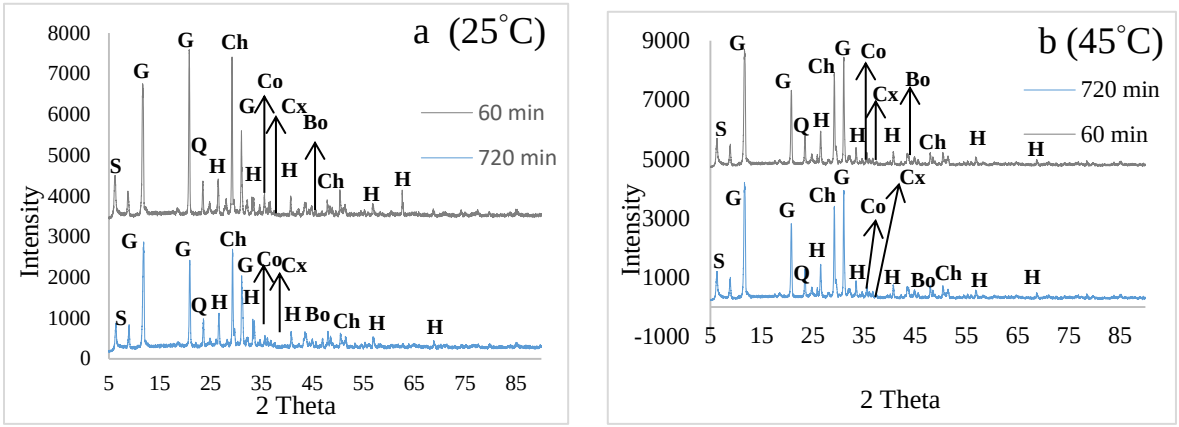

S: sulphur; G: gypsum; Q: quartz; H: hematite; Ch: chalcopyrite; Co: covellite; Cx: chalcocite; Bo: bornite

Figure 3-8: Diffraction spectrum of carbonatite residue samples at 25℃ and 45℃

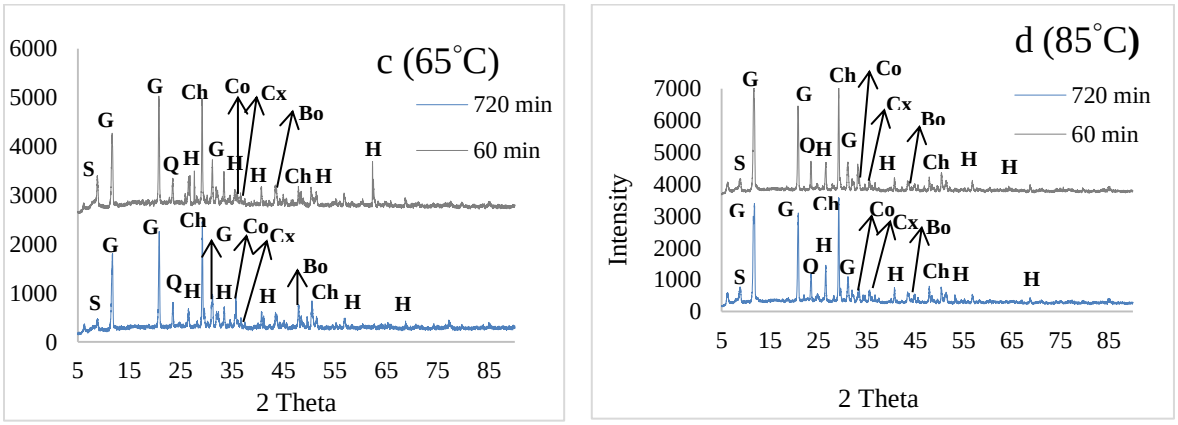

Figure 3-9: Diffraction spectrum of carbonatite residue samples at 65℃ & 85℃

Only during experimentation at 25℃ was a major decrease in peak intensity of chalcopyrite observed, which suggests that mineral dissolution from the carbonatite host mineral was effective (Santos et al., 2017) at these conditions; this also agrees with the recovery data obtained under these temperatures conditions, in which the recovery rates were observed to be the greatest (Figure 3-5). Over the whole temperature spectrum, new mineral phase formation was observed, as Cu dissolution was accompanied by new phases, such as bornite, covellite and digenite, which are regarded as intermediate steps before complete decompositions to the free ions, Cu^{2+} and Fe^{2+} (Cordoba et al., 2008b; Nyembwe et al., 2018). In addition to the intermediate phases formed, other precipitate minerals were also present and forming in the leaching media; the respective phases evolved were iron oxide mineral, hematite, and elemental sulphur, linked to the dissolution media as well as gypsum linked to carbonatite calcite-magnesium. Hematite formed during the leaching of the feed stream samples is believed to be the mutation phase of magnetite (Fe_3O_4), identified to be present within the carbonatite mineral from XRD (Nyembwe et al., 2019). The presence of hematite could be attributed to oxygen within the solution, diffusing through the magnetite mineral, as it is the most

stable phase of iron oxide (Gorbachev et al., 2007). Hematite formation was not influenced greatly by changes in temperature, as the peak that was analysed showed that the mineral concentration after 12 hours of dissolution was 19.72% (45℃) and minimum 16.86% (85℃), as seen in Table 3-3. As with hematite, gypsum accumulated during the course of the 12 hours dissolution period and was accompanied by increasing peak intensity. The formation of gypsum was more dependent on temperature, as the mineral phase cumulated from 37.75 to 47.13% at 25℃, whilst accumulation was observed from 57.84 to 67% at 85℃ during the course of mineral dissolution. The formation of gypsum is attributed to the relatively high levels (48.91%) of Ca in the carbonatite ore, as identified through bulk elemental characterisation in the presence of sulphuric acid (H_2SO_4), Ca is prone to form sulphate compounds (Antonijevic & Bogdanovic, 2004).

Table 3-3: Mineral composition of carbonatite residue samples (%)

Experimental temperature (℃)		25℃		45℃		65℃		85℃	
Sample time (hours)		1	12	1	12	1	12	1	12
Mineral	**Chemical composition**								
Bornite	Cu_5FeS_4	3.70	2,46	1,59	1,05	2,90	1,13	2,99	0,79
Calcium Iron Oxide	$CaFeO_2$	5.44	6,89	4,97	2,40	5,06	2,71	4,99	2,15
Chalcocite	Cu_2S	7.06	4,09	2,46	0,023	2,34	0,70	3,79	1,01
Chalcopyrite	$CuFeS_2$	20.00	11,6	9,90	6,25	12,85	8,09	6,46	5,12
Copper oxide	Cu_2O	2.88	9,85	5,79	7,13	7,89	9,85	5,42	7,90
Covellite	CuS	6.89	4,90	3,46	2,01	1,78	1,05	1,99	0,46
Cyclo-hexasulphur	S_6	4.23	3,46	2,16	0,05	1,77	0,91	2,02	0,50
Digenite	Cu_9S_5	1.98	0,59	1,03	0,47	1,97	0,23	0,71	0,12
Gypsum	$CaSO_4 \cdot 2H_2O$	37.75	47,13	51,79	60,91	50,50	56,97	57,84	67,00
Hematite	Fe_2O_3	15.67	18,9	16,76	19,72	11,92	18,43	14,24	16,86

3.3.6.2 Silicate

Figure 3-10 and 3.11 show the mineral content of the silicate solid residue samples collected during experimentation for each of the measured temperatures. The blue spectra represent the diffraction of minerals after 1 hour of leaching, and the grey that of the minerals after 12 hours of leaching. Table 3-4 contains a list of the major minerals present within the residue samples.

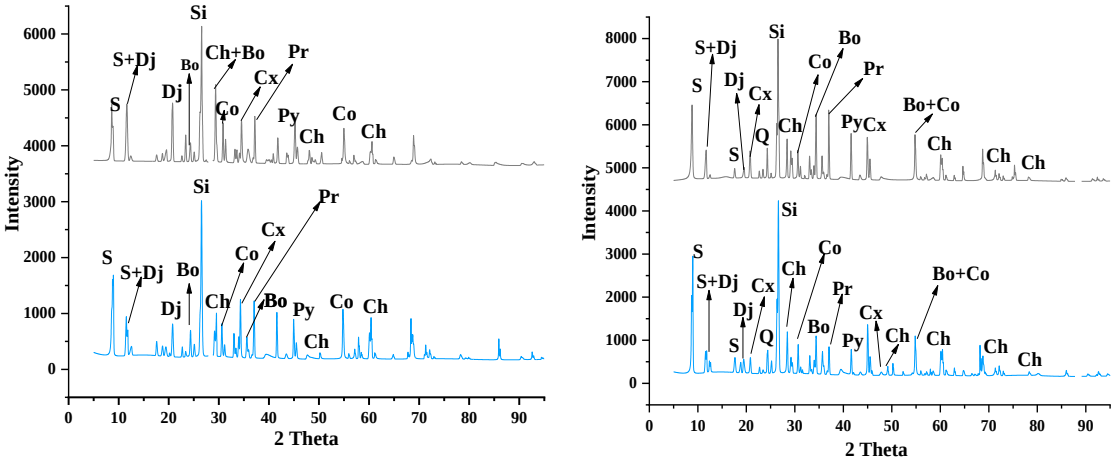

Bo: bornite; Ch: chalcopyrite; Co: covellite; Cx: chalcocite; Dj: digenite, djulerite; Pr: pyrhotite Py: pyrite; Q: quartz; S: sulphur.

Figure 3-10: Diffraction spectrum of silicate residue at 25°C (left) and 45°C (right)

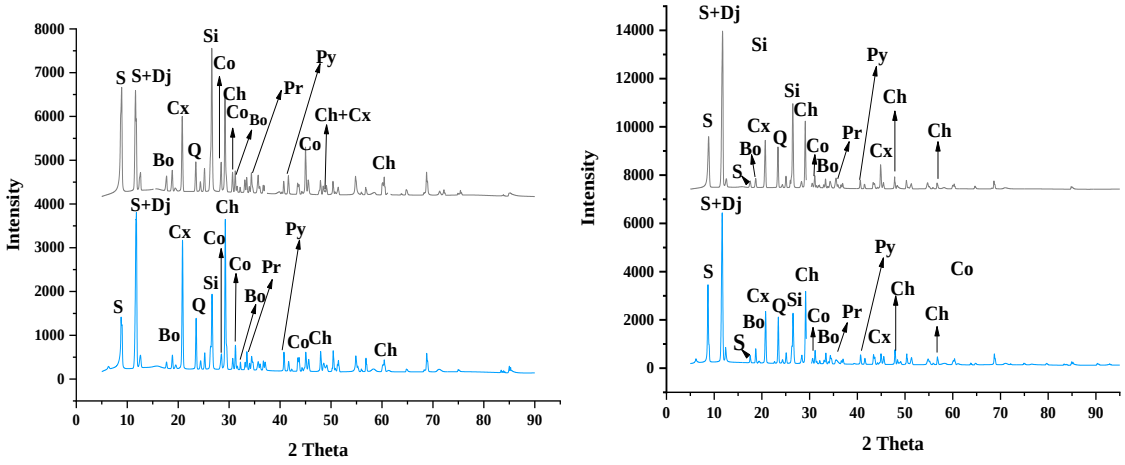

Figure 3-11: Diffraction spectrum of silicate residue at 65°C (left) and 85°C (right)

Unlike the carbonatite hosting ore, effective mineral dissolution of chalcopyrite was observed over the whole temperature range. Major decreases in peak intensities were observed over the whole spectrum. The greatest decreases in peak intensity of the mineral was observed during experimentation at higher temperatures (65-85°C), which corresponds with the recovery rates of copper during leaching at these temperature conditions, at which the recovery rates were the greatest.

As with the carbonatite host mineral, new phase formation occurred during leaching of the silicate hosting ore in the form of bornite, chalcocite, covellite and digenite. Other precipitate minerals present during leaching of the silicate host ore were elemental sulphur and pyrrhotite linked to the dissolution media, as well as quartz linked to the clastic nature of the host ore. The formation of elemental sulphur was influenced by the increase in temperature, as the peak of sulphur was 24% (45℃) and the minimum was 9.46% (25℃) after 12 hours of dissolution, as seen in Table 3-4 Although the peak at 85℃ was 15.79%, the formation of the natural monoclinic gamma form of sulphur, Rosickyite, being a high temperature polymorph (Meisser et al., 2015) displayed the highest formation under this temperature condition (12.20%), with peak concentration at 45℃ and 65℃ at 4.79% and 6.89% respectively. Pyrite present within the hosting ore also displayed a decrease in peak intensity during the 12 hours leaching period, indicating that dissolution of pyrite occurred; this behaviour was strengthened at higher temperatures (Table 3-4). The dissolution of pyrite is significant, as it will lead to galvanic interaction between pyrite and chalcopyrite, which has been identified to aid in the recovery of Cu (Berry, 1978).

Table 3-4: Mineral composition of silicate residue samples (%)

Experimental temperature (℃)		25℃		45℃		65℃		85℃	
Sample time (hours)		1	12	1	12	1	12	1	12
Mineral	**Chemical composition**								
Bornite	Cu_5FeS_4	2.08	0.70	2.90	1.26	2.00	1.45	1.46	1.00
Chalco-pyrite	$CuFeS_2$	2.80	1.43	1.62	1.56	3.79	1.79	2.90	1.79
Chalcocite	Cu_2S	0.92	1.08	4.46	1.48	3.89	1.00	2.90	1.79
Covellite	CuS	11.03	16.46	9.88	11.79	7.9	11.90	7.42	10.79
Djulerite	$Cu_{31}S_{16}$	3.81	0.40	6.99	3.90	8.48	2.79	7.79	3.90
Digenite	Cu_9S_5	18.4	7.79	2.90	1.41	11.90	6.90	4.46	1.19
Pyrite	FeS_2	3.67	4.06	4.9	1.26	4.87	1.45	1.46	1.00

Pyrrhotite	$Fe_{(1-x)}S$	4.01	5.73	3.45	3.48	4.54	1.28	1.79	2.02
Quartz	SiO_2	42.32	41.90	38.89	41.39	33.89	42.78	39.89	46.46
Rosickyite	S	8.98	11.39	4.00	4.79	7.46	6.89	11.79	12.20
Sulphur	S	5.79	9.46	18.05	24.00	11.24	19.99	13.89	15.79

3.3.7 Thermodynamic consideration (Pourbaix diagrams)

The dissolution of copper from chalcopyrite can be discussed on a theoretical premise when considering the Eh-pH diagrams for both Cu and Fe (Figure 3-12 & 3.14). The diagram shows all possible stability phases that could form relative to their equilibrium conditions as a function of the redox reactions (Huang, 2016).

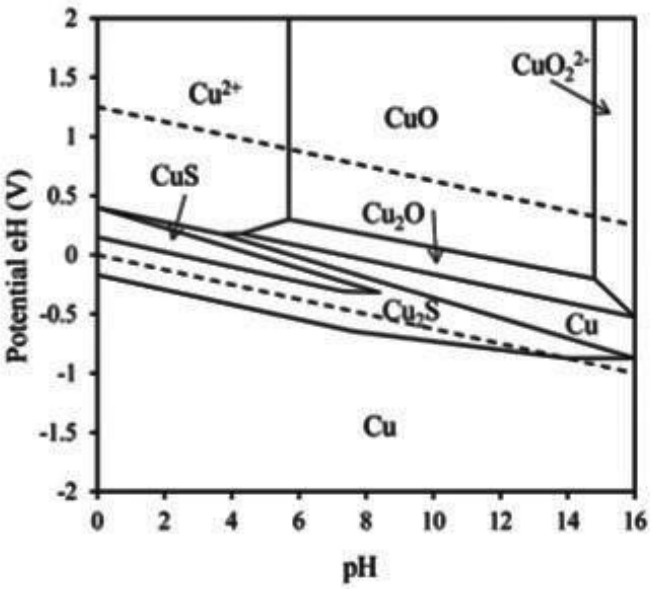

Source: (House, 1987; Khoshkhoo, 2014)

Figure 3-12: Potential-pH diagram Cu-S-O-H_2O at 25°C

Since both the ORP and pH values were allowed to evolve, the phase diagram in Figure 3-12 complements the recovery results that were obtained (Figure 3-5). With an increase in the pH value, various Cu phases are observed, depending on the Eh (redox potential). In the diagram it can be seen that Cu^{2+} could be maintained in solution at potential (Eh) value above 1 volts on a standard hydrogen within a pH region from 0 to 5. The experimental condition revealed that the recorded ORP range was low (0.6-0.2 V), to maintain Cu^{2+} in solution. In addition to that, the decreasing ORP value

corresponded with the XRD result, namely, that low-solution voltage favours the formation of covellite phase (CuS), as identified in the solid residue, and could, therefore, represent a dissolution barrier, as underlined in the study conducted by Nyembwe et al. (2018) since this phase was observed as refractory to dissolution. Figure 3-13 represents the change in Eh for the carbonatite and silicate hosting minerals, measured using an analytical Ag/AgCl electrode in 3 M KCl filling solution at each of the various temperature measurements.

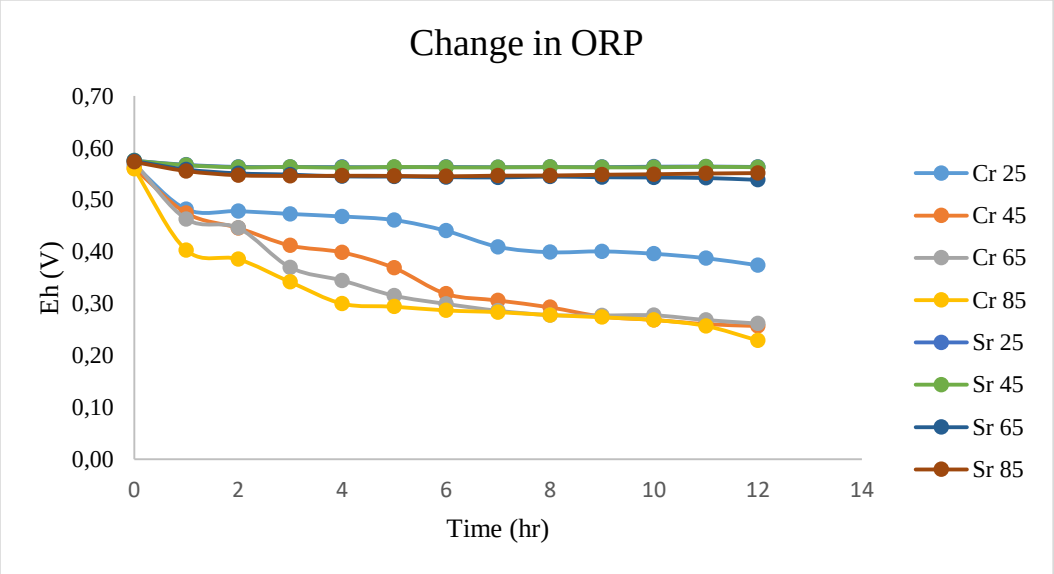

Figure 3-13: Change in oxidation reduction potential for chalcopyrite-containing ores

During leaching at 25°C, the potential and pH conditions were in the desired range during the first six hours of leaching using carbonatite hosting ores, thereafter, the Eh dropped and the phase formation shifted to that of insoluble copper oxide minerals; this is also visible in the steep decline in Cu recovery at this time. As the redox potential decreased as pH increased, when exposed to higher temperatures, the intermediate phases dissolved less frequently into solution, as is visible from the residue characterisation (Table 3-3), where the lowest bornite and covellite concentrations were observed as 0.46% and 0.79%, after 12 hours of leaching at temperature conditions of 85°C. The same could be seen for chalcopyrite, where 11.6% of the mineral was available after 12 hours of dissolution at 25°C, compared to 5.12% at 85°C.

Leaching of chalcopyrite-bearing silicate minerals displayed very different behaviour than leaching of the carbonate rich hosting ore. For each of the experimental runs at various temperature conditions for the silicate samples, the solution redox Eh was measured at values above 0.5 V (minimum of 0.54 V at 65°C after 12 hours of leaching; maximum of 0.58 after 1 hour of leaching for each of the measured temperature conditions). The pH of solution, regardless of change in solution temperature, was relatively stable and at the desired range (pH 1-2) for effective dissolution of the chalcopyrite mineral. At this pH range, the hydrolysis and precipitation of ferric salts, which are known to have a

retarding effect on Cu recovery, are minimised due to the acidity of the solution (Dew et al., 1997; Halinen et al., 2009a). The intermediate phases of bornite, chalcocite and digenite were observed to dissolve less frequently into solution, whereas the accumulation of covellite was, instead, observed over the whole temperature range (Table 3-4), regardless of the change in solution temperature. However, temperature had an effect on the amount of chalcopyrite available in the solution, as 1.43% of the mineral was available after 12 hours of dissolution at 25°C, compared to 1.79% at both 65°C and 85°C. The copper recoveries for silicate mineral correspond with the result obtained during residue characterisation, as well as predictions through applying the Pourbaix diagram, in which recovery rates tended to increase during the 12 hours of dissolution, with a further increase observed at higher solution temperatures.

At redox potentials between -0.6 V and 0.8 V, effective dissolution of Fe could occur over a wide pH range (pH 0-9). This finding agrees with the predicted species formations determined through PHREEQC software, at which the dominant species for iron in solution, over the whole temperature range for carbonatite, was Fe^{2+}, which is soluble as free hydrated ionic species. As temperature increases, however, the pH and ORP values gradually shift to favour the phase formation of the iron oxide mineral, hematite, instead. This is also seen in Figure 3-6, in which the recovery rate of Fe is observed to decrease as temperature increases.

Both the redox rates and pH conditions required for effective dissolution of Fe where achieved during leaching of the silicate host ores, regardless of the change in temperature and the leaching time. This finding agrees with the speciation of Fe, in which the highest concentrations of Fe species formed were those of ferrous ion (Fe^{2+}), however, during leaching at 25°C, the highest formation of pyrrhotite was observed at 5.76%. The dissolution mechanism of pyrrhotite is very similar to that of chalcopyrite, in the sense that both minerals passivate in acidic solutions by formation of a metal-deficient layer (Ghahremaninezhad, 2012).With this in mind, the concentration of free hydrate Fe species could be limited in cases where higher concentration of $Fe_{(1-x)}S$ are present. This corresponds with the lower recovery rates of Fe observed during leaching at 25°C.

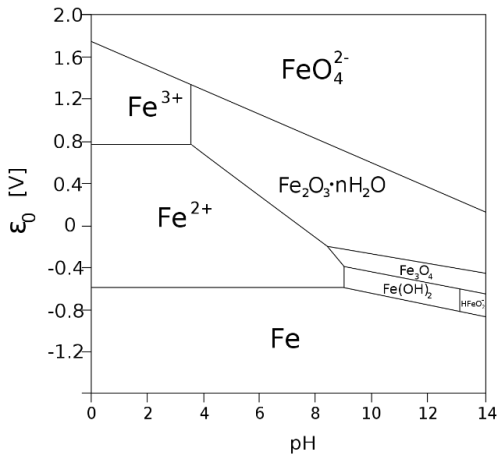

Sources: (Beverskog & Puigdomenech, 1996; Salgado et al., 2013)

Figure 3-14: Potential-pH diagram for Fe in aqueous media

The mineralogical characterisation of the residue samples, for each of the measured temperatures, showed that it was possible to obtain the Cu sulphate minerals, bornite, covellite and digenite, along with further chalcocite formation, as products of dissolution within the sulphate media (Nyembwe et al., 2018). The intermediate phases are believed to form according to the following Gibbs equations:

$$\mathbf{5CuFeS_2 + 4Fe_2(SO_4)_3 = Cu_5FeS_4 + 12FeSO_4 + 6S}$$ *(Bornite)* **Eq 6**

$$\mathbf{CuFeS_2 + Fe_2(SO_4)_3 = CuS + 3FeSO_4 + S}$$ *(Covellite)* **Eq 7**

$$\mathbf{2CuFeS_2 + 2Fe_2(SO_4)_3 = Cu_2S + 6FeSO_4 + 3S}$$ *(Chalcocite)* **Eq 8**

$$\mathbf{18CuFeS_2 + 9Fe_2(SO_4)_3 = 2Cu_9S_5 + 27FeSO_4 + 13S}$$ *(Digenite)* **Eq 9**

Equations for complete dissolution of copper from the intermediate phases:

$$\mathbf{Cu_5FeS_4 + 6Fe_2(SO_4)_3 = 13FeSO_4 + 4S + 5CuSO_4}$$ *(Bornite)* **Eq 10**

$$\mathbf{CuS + Fe_2(SO_4)_3 = 2FeSO_4 + S + CuSO_4}$$ *(Covellite)* **Eq 11**

$$\mathbf{Cu_2S + 2Fe_2(SO_4)_3 = 4FeSO_4 + S + 2CuSO_4}$$ *(Chalcocite)* **Eq 12**

$$\mathbf{5Cu_9S_5 + Fe_2(SO_4)_3 = FeSO_4 + S + CuSO_4}$$ **(***Digenite)* **Eq 13**

Copper dissolution can also occur directly from chalcopyrite:

$$\mathbf{CuFeS_2 + 2Fe_2(SO_4)_3 = CuSO_4 + 5FeSO_4 + 2S}$$ **Eq 14**

The Gibbs equations relating to the carbonate gangue mineral and that of the phase mutation of magnetite are given as follows:

$$\mathbf{CaCO_3 + H_2SO_4 = CaSO_4 + H_2O + CO_2}$$ **Eq 15**

$$\mathbf{4Fe_3O_4 + O_2 = 6Fe_2O_3}$$ **Eq 16**

Possible secondary copper sulphide reaction of covellite during leaching of silicate mineral:

$$\mathbf{CuS + 2H^+ = Cu^{2+} H_2S}$$ **Eq 17**

Although it is possible for direct mineral dissolution to occur from the surface of the chalcopyrite mineral, as is visible from the Gibbs equation (Eq 14), it is more likely that intermediate mineral phase formation will occur during the dissolution of the chalcopyrite-containing carbonatite mineral. As the dissolution of calcium is favoured at higher temperatures, the formation of gypsum increases, as seen from Table 3-3, and with pH increasing due to the carbonate calcium in solution, the phase mutation of magnetite to hematite and the formation of copper oxide is favoured at these higher temperature ranges (45-85°C). It can, therefore, be said that chalcopyrite is enclosed by a matrix

mixture of gypsum and hematite, which reduces the dissolution of Cu, as these conditions favour the formation of insoluble copper oxide. At room temperature, the pH conditions are favourable, but the formation of gypsum and the presence of spinal calcium iron oxide and the existence of elemental sulphur contribute to the passivation phenomenon.

Direct dissolution of Cu from chalcopyrite during leaching of the silicate host mineral was not observed, as intermediate phase formation and accumulation of covellite seems to occur for each of the measured temperatures (25-85°C) over the 12 hours dissolution period. From Table 3-5 it can be concluded that, from the positive Gibbs free energy obtained for Eq 11, that covellite is refectory in solution, which is also visible from the accumulation of covellite during each of the various experimental temperature runs (Doman & Alper, 1981). At these low pH conditions (pH 1-2), the concentration of H^+ ions is high, which increases the chance that the secondary reaction of CuS with hydrogen ions will occur, in which soluble Cu species (Cu^{2+}) and hydrogen sulphide (H_2S) are formed. Further oxidation of H_2S by ferric ion (Fe^{3+}) can lead to the formation of elemental sulphur, which is seen to increase during leaching of the silicate host mineral (Table 3-4) (Lu et al., 2016). The presence of pyrite within the host ore aids the kinetic dissolution of Cu, as it provides an alternative catalytic surface for ferric reduction, attenuating the passive behaviour of the chalcopyrite mineral in a ferric sulphate media (Schaming, 2011; Khoshkhoo, 2014).

Table 3-5: Gibbs free energy of associated reaction equations

Temperature	**25**	**45**	**65**	**85**	**Eq**
ΔG	-68.781	-69.512	-70.257	-71.017	Eq 6
ΔG	-18.652	-18.796	-18.943	-19.093	Eq 7
ΔG	-30.850	-31.226	-31.611	-32.003	Eq 8
ΔG	-13.969	-14.167	-14.384	-14.620	Eq 10
ΔG	2.102	2.060	2.015	1.966	Eq 11
ΔG	-2.250	-2.245	-2.248	-2.251	Eq 12
ΔG	-16.550	-16.736	-16.928	-17.127	Eq 14
ΔG	-33.890	-33.813	-34.485	-35.154	Eq 15

3.4 Conclusion and recommendations

The purpose of this study was to perform a comparative observation of the leaching kinetic of copper from carbonate-rich and sediment-siliciclastic chalcopyrite hosting ores in a sulphate medium using ferric sulphate as oxidant, with particular focus on the effects of mineralogical compositions and species formation from the hosting ores on the leaching rates, as well as the role temperature plays in the formation of gangue and other species that affect the dissolution kinetics.

The major constituents of Ca and Mg minerals (calcite magnesium at 49.6% and dolomite at 32.34%) within the carbonatite host rock, observed during characterisation of the host rock, played an important role in the dissolution of copper, as these mineral species are known to have a neutralising effect on soil pH levels. Speciation predication also concluded that, at elevated temperature, the likelihood of higher concentration of Ca^{2+} and Mg^{2+} ion forming is greater, raising pH conditions as temperature increases due to competition with the hydrogen ion, thereby reducing the pH of the solution. The formation of gypsum is also preferred at higher temperature conditions, which increase the likelihood that chalcopyrite will be enclosed by a matrix mixture of gypsum; furthermore, an increase in pH favours the formation of ferric salts (jarosite) and contributes to the formation of a passivation layer on the surface of the mineral. Solubility of metals is reduced under these conditions, particularly for copper, as the formation of the insoluble copper oxide species is promoted at higher pH and temperatures.

The major constituent of the silicate mineral was quartz (19.66%), with other quartz species also present being coesite quartz (11.47%) and rose quartz (3.47%). Copper sulphide minerals were the second-biggest constituent within the silicate mineral, with a combined concentration of 22.89%. Pyrite was also present within the silicate mineral (6.89%), but generally absent within the carbonatite host rock. The large concentration of sulphide minerals as well as the presence of pyrite, which oxidises to form H_2SO_4, and low Ca concentration (7%), as observed by XRF analyses, promoted low pH conditions of solutions. Under these conditions, Cu recovery was enhanced, as ferric salt formation was minimised at pH 1-2. The presence of pyrite also increased recovery through galvanic interaction with the chalcopyrite mineral. The tendency of the intermediate phase of covellite to form also enhanced leaching as a secondary reaction of covellite, with hydrogen ions promoting further formation of soluble free hydrate copper ions.

It is recommended that static (controlled) pH test at pH 1-2 is conducted on the different mineralogical hosting ores, as it is known that copper recovery tends to increase at these levels. It is presumed that, under these conditions, the formation of gypsum and the release of alkaline earth metals will be reduced, which could favour recovery of copper from the carbonatite hosting ore. These conditions might also provide the high Eh values required for effective copper extraction from the carbonatite mineral. Recovery from the silicate mineral might remain unaffected by controlling

pH, though a constant injection of acid in solution to control pH levels might lead to increased formation of elemental sulphur, which is detrimental for leaching copper from the surface of chalcopyrite. The same temperature conditions should be studied as it might have different effects under controlled pH conditions.

References

Acero, P., Cama, J., Ayora, C. & Asta, M., 2009. Chalcopyrite dissolution rate law from pH 1 to 3. *Geologica Acta,* 7(3), pp. 389-397.

Antonijevic, M. & Bogdanovic, G., 2004. Investigation of the leaching of chalcopyrite ore in acidic solutions. *Hydrometallurgy,* 73(2), pp. 245-56.

Balaria, A., 2011. *Effects of calcium addition on structure and bioavailability of soil organicmatter,* New York: Syracuse University.

Barlow, B., Nyembwe, K., Wanders, F. & Fosso-Kankeu, E., 2018. *Prediction of dissolution of copper from a chalcopyrite carbonatite ore of South Africa.* CapeTown, South Africa, s.n., pp. 99-103.

Beale, C., 1985a. Copper in South Africa-Part I. *Journal of the South African Institute of Mining and Metallurgy,* 85(3), pp. 73-80.

Berry, V., 1978. Galvanic interaction between chalcopyrite and pyrite during bacterial leaching of low grade waste. *Hydrometallurgy,* 3(4), pp. 309-326.

Beverskog, B. & Puigdomenech, I., 1996. Revised pourbaix diagrams for iron at 25-300 C. *Corrosion Science* , 38(12), pp. 2121-2135.

Chakhmouradian, R., Reguir, E. & Zaitsev, A., 2016. Calcite and dolomite in intrusive carbonatites: I. Textural variations. *Mineralogy Petrology,* 110(2-3), pp. 333-360.

Cordoba, E., Munoz, J., Blazquez, M. & Ballester, A., 2008a. Leaching of chalcopyrite with ferric ion Part I: General aspects. *Hydrometallurgy,* 93(3-4), pp. 81-87.

Cordoba, E. et al., 2008b. Leaching of chalcopyirte with ferric ion Part II: Effect of redox potential. *Hydrometallurgy,* 93(3-4), pp. 88-96.

Dew, D., Lawson, E. & Broadhurst, J., 1997. The BIOX process for biooxidation of gold-bearing ores or concentrates. In: *Biomining.* Berlin: Springer, pp. 45-80.

Doman, R. & Alper, A., 1981. Refractory minerals. In: *Mineralogy: Encyclopedia of earth science.* Boston: Springer.

Dutrizac, J., 1981. The dissolution of chalcopyrite in ferric sulphate and ferric chloride media. *Metallurgy and Materials Transaction,* 12(2), pp. 371-378.

Dutrizac, J., MacDonald, R. & Ingraham, T., 1969. The kinetics of dissolution of synthetic chalcopyrite in aqueous acidic ferric sulfate solutions. *Transactions of the Metallurgical Society,* pp. 955-959.

Fosso-Kankeu, E., Barlow, B., Lemmer, N. & Waanders, F., 2017. *Geochemical Speciation of Metal Ions in the Leachate of Tailings Treated with Synthetic Rain Water.* Parys, South Africa, s.n., pp. 19-23.

Ghahremaninezhad, A., 2012. *The surface chemistry of chalcopyrite during electrochemical dissolution,* Vancouver: University of British Columbia.

Gorbachev, V., Abzalov, V. & Yur'ev, B., 2007. Conversion of magnetite to hematite in iron-ore pellets. *Steel in Translation,* 37(4), pp. 336-338.

Hackl, R., Dreisinger, D., Peters, E. & King, J., 1995. Passivation of chalcopyrite during oxidative leaching in sulfate media. *Hydrometallurgy,* 39(1-3), pp. 25-48.

Halinen, A., Rahunen, N., Kaksonen, A. & Puhakka, J., 2009a. Heap bioleaching of a complex sulfide ore: Part I: Effect of pH on metal extraction and microbial composition in pH controlled columns. *Hydrometallurgy,* 98(1-2), pp. 92-100.

Heinrich, E., 1970. *The Palabora Carbonatitic Complex: A Unique Copper Deposit,* s.l.: s.n.

Hoffert, J., 1947. Industrial Wastes: Acid Mine Drainage. *Industrial and Engineering Chemestry,* 39(5), pp. 642-646.

House, C., 1987. Potential-pH diagram and their application to hydrometallurgical systems. In: *Separation Processes in Hydrometallurgy.* Chichester: Ellis Horwood, pp. 3-19.

Huang, H., 2016. The Eh-pH Diagram and Its Advances. *Metallurgical and Materials Engineering,* 6(1), p. 23.

Joe, S. et al., 2009. Effects of pH and temperatrue on the leaching reaction of primary copper sulfide fine ore in sulfuric acid aqueous solution. *Journal of MMIJ,* 125(3), pp. 115-120.

Khoshkhoo, M., 2014. *Chalcopyrite Disolution in Sulphate-Based Leaching and Bioleaching Systems,* s.l.: s.n.

Lamar, J. E., 1961. *Uses of Limestone and Dolomite,* Urbana: s.n.

Li, Y. et al., 2013. A Review of the Structure, Fundamental Mechanisms and Kinetics of the Leaching of Chalcopyrite. *Advances in Colloid and Interface Science,* 197-198(September), pp. 1-32.

Lu, D. et al., 2016. Thermodynamic Analysis of Possible Chalcopyrite Dissolution Mechanism in Sulphuric Acid Aqueous Solution. *Metals,* 6(12), p. 303.

Lydall, M. & Auchterlonie, A., 2011. *The Democratic Republic of the Congo and Zambia: A Growing Global Hotspot for Copper-Cobalt Mineral Investment and Exploitations,* s.l.: s.n.

Meisser, N., Schenk, K. & Spangberg, J., 2015. Rosickyite (monoclinic y-sulphur) from La Presta Asphalt Mine, Neuchatel, Switzerland: New X-ray powder diffraction data. *Swiss Journal of Geoscience Supplement*, 80(3), pp. 299-303.

Nyembwe, K., Fosso-Kankeu, E. & Waanders, F., 2019. Structural, composition and mineralogical characterization of carbonatitic copper sulfide: Run of mine, concentrate and tailings. *International Journal of Minerals, Metallurgy and Materials*, 26(2), pp. 143-151.

Nyembwe, K., Fosso-Kankeu, E., Wanders, F. & Malenga, E., 2018. *Mineralogical observation made during the kinetic dissolution study of chalcopyrite mineral in sulphate media under free pH at room temperature.* Cape Town, s.n.

Salgado, P. et al., 2013. Fenton reaction driven by iron ligands. *Journal of Chilean Chemical Society,* 58(4), pp. 2096-2100.

Santos, A., Arena, F., Benedetti, A. & Bevilaqua, D., 2017. Effect of redox potential on chalcopyrite dissolution imposed by addition of ferrous ions. *Eclética Química Journal*, 42(1), pp. 40-50.

Schaming, J., 2011. *An investigation of leaching chalcopyrite ores.* Kingston, Ontario: Queen's University.

Scrivener, K., 1998. Calcium aluminate cements. In: *Lea's chemistry of cement and concrete.* s.l.:Butterworth-Heinemann, pp. 713-782.

Sokic, M., Markovic, B. & Zivkovic, D., 2009. Kinetics of chalcopyirte leaching by sodium nitrate in sulphuric acid. *Hydrometallurgy,* 95(3-4), pp. 273-279.

Stiggov, B., 2013. *Field measurements of oxidation-reduction potentail (ORP),* Athens, GA: US Environmental Protection Agency.

Stott, M., Wattling, H. & Franzmann, P., 2000. The role of iron-hydroxy precipitates in the passivation of chalcopyrite during bioleaching. *Minerals Engineering,* 13(10), pp. 1117-1127.

Tshilombo, A., 2004. *Mechanism and kinetics of chalcopyrite passivation and depassivation during ferric and microbial leaching,* s.l.: Vancouver: University of British Columbia.

Vilca, A., 2013. *Studies on the curing and leaching kinetics of mixed copper ores.* Vancouver: The University of British Columbia.

Chapter 4: Leaching kinetics of copper from different chalcopyrite ores: Effects of additive addition under fixed temperature conditions

Abstract: The aim of this study was to observe the dissolution rate of copper from different chalcopyrite-bearing ores and different stream samples (ROM and tails for carbonatite samples) at fixed temperature conditions, in the presence of an additive, where pH evolution was allowed to occur. The objectives were to observe the effects of mineralogical background, especially a comparison between the tailings and ROM samples of the carbonatite host ore, under fixed temperature conditions (85°C), as well as the effects of magnetite addition. To determine the elemental and mineralogical characterisation of the host rock samples and magnetite, XRF (X-ray fluorescence) and XRD (X-ray diffraction) were used respectively. The geochemical workbench software, PHREEQC, was used to predict species, with input parameters such as pH, ORP, acidity, alkalinity, Cl^- and SO_4^{2-} required. Untreated carbonate minerals (ROM and tails) displayed acid-consuming behaviour, which lead to a rise in pH levels, thereby promoting alkaline conditions. Hindered Cu recovery was observed under these conditions, as the mineral surface was covered by a matrix mixture of gypsum and hematite; ferric salt formation in the tailings was also a contributing factor, as it reduces the transport of electrons. The addition of magnetite aided in Cu recovery, as Ca concentrations were lowered and general acidic conditions, favourable for Cu recovery, were achieved while, ferric salt was also minimised at these conditions. The siliciclastic mineral displayed characteristics of enhanced acid attack, above that of the carbonatite ore as pH remained at low levels. Favourable Cu recovery was achieved under these conditions, as ferric salt formation was reduced. Thus, additional pyrite formation improved leaching conditions through galvanic interactions. The formation of gypsum and ferric salts (formed at pH <1) during dissolution in the presence of magnetite hindered Cu dissolution slightly, as lower recovery was observed, compared to clean silicate samples.

Keywords: chalcopyrite, carbonatite, silicate, tails, magnetite, species

4.1 Introduction

The mechanism for the formation of a passivation film on the surface of the low-grade copper mineral, chalcopyrite, has been the focus of many studies and to date the exact cause of its formation has not been effectively identified (Cordoba et al., 2008a; Li et al., 2010). Due to the difficulty in identifying the exact contributing factor to the formation of the film, recent studies have rather invested time in identifying optimal conditions to improve the dissolution rate of Cu before passivation can occur. Parameters, such as acidity of solution, reaction temperature, particle size distribution, mineralogical composition, redox potential, oxidant concentration and addition of additives, play key roles in achieving these optimal leaching conditions (Hackl et al., 1995; Antonijevic & Bogdanovic, 2004; Acero et al., 2009). In this chapter, mineralogical composition and the effects of additives on the leaching rate from the chalcopyrite hosting ores were observed along with a comparative observation between the different samples streams of the carbonatite host ore.

Pyrite, as an additive, has been researched by numerous studies and has been observed to aid the dissolution rate of Cu from chalcopyrite during the galvanic reaction between the two minerals (Berry, 1978). Using ground pyrite has proven to be effective in this endeavour, as pyrite creates an alternative catalytic surface for ferric reduction, and attenuates the passive behaviour of the chalcopyrite mineral in a ferric sulphate media (Schaming, 2011). This behaviour has been identified in a concentration ratio of 4-2:1 pyrite to chalcopyrite; higher mass concentrations of pyrite to chalcopyrite aids in providing a bigger alternative surface for ferric reduction and increasing the dissolution rate – this method has been patented as the Galvanox process (Dixon, 2008). The addition of silver (Ag^{+}) during leaching has also proven to enhance the ferric leaching of chalcopyrite (Pawlek, 1976; Banerjee et al., 1990). As elemental sulphur is one of the contributors to lower rate of chalcopyrite leaching, the addition of silver improves the leaching rate of copper, because a product layer of Ag_2S is formed, instead of a layer solely composed of sulphur. The porous silver-sulphate layer does not exert the same barrier effect found in the presence of the elemental sulphur layer, and provides higher electrical conductivity and improves the transport of electrons through the surface of the chalcopyrite mineral (Burkin, 1982; Prince & Warren, 1986).

Magnetite is an iron oxide (Fe_3O_4) and is generally magnetic. Its chemical composition can also be written as $Fe^{2+}Fe^{3+}{}_2O_4$ which implies that magnetite contains both ferrous (Fe^{2+}) and ferric ions (Fe^{3+}), making the mineral stable in environments where iron is present in reduced and oxidised states (Skinner & Jahren, 2003). The formation of magnetite can occur under a wide variety of conditions, from magmatic systems where it crystallises in either silicate or sulphide melts at high temperatures, to hydrothermal systems, where it precipitates from hydrothermal fluids at lower temperatures (Dare et al., 2014). Magnetite from silicate melts are typically found in Fe-Ti-V-P deposits, whereas magnetite from sulphide melts are found in Ni-Cu-platinum group metals deposits (Dare et al., 2012;

Boutroy et al., 2014). Magnetite used in this study is from a magmatic system of silicates melts in the Bushveld Complex, the largest layered ingenious intrusion in the Earth's crust, situated in the northern part of South Africa. Magnetite reacts with sulphuric acid to form ferrous sulphate, ferric sulphate and water, making magnetite addition significant, as it is known that chalcopyrite dissolution is strongly affected by ferric ion concentration (Cordoba et al., 2008a) and an increase in ferric sulphate concentration coincides with an increase in Fe^{3+} concentration, leading to increased dissolution.

This study's focus was primarily on the kinetics and chemistry of Cu dissolution from the carbonatitic and siliciclastic chalcopyrite-bearing ores in the presence of magnetite. In addition, tailings from the carbonatite mineral was also investigated to determine the effects of different gangue species and mineral phases within the same carbonatite ore complex. The effects of additives during dissolution were examined, with the intention to outline the effect of the added mineral phases on the behaviour of the gangue-related species in the sulphate media.

4.2 Experimental setup and methodology

4.2.1 Materials

Solutions of the desired pH values were prepared using analytical reagent-grade sulphuric acid (H_2SO_4 98% ACE), ferric sulphate ($Fe_3(SO_4)$ X H_2O ACE), sodium hydroxide (NaOH pellets ACE) and distilled, deionised water (7.0 µs/cm). A pH meter and temperature probe (Hanna pH HI 8424) were used to measure pH; the probe was regularly calibrated with 4 and 7 standard buffer solutions, and the measured Eh (Ag/AgCl) values were referenced to the Standard Hydrogen Electrode.

4.2.2 Chalcopyrite samples

The carbonatite samples (ROM and tails) that were used in the study were provided by PMC and received from their mine in Phalaborwa, South Africa. Prior to use, the ROM samples required for experimentation were, first, crushed, then sieved to -150 micron, after which the sieved samples were stored in tightly sealed plastic containers until use. The tailings samples were subjected to a heating oven, for 3 hours at 110°C, to get rid of any excess moisture obtained from the tailings dam. As with the ROM, the tailings were stored in tight sealed plastic containers, at room temperature conditions, until further use. The silicate samples were provided by Ruashi Mine, in the Katanga province of the DRC. As with the carbonatites, the silicates were crushed, then sieved to -150 micron and stored until further use. Both chalcopyrite-containing minerals were also subjected to chemical/elemental- and mineralogical characterization using X-ray Diffraction (XRD) and X-ray Fluorescence (XRF), respectively.

4.2.3 Chemical leaching

For the purpose of leaching chalcopyrite-containing silicate and carbonatite minerals, an incubator with a built-in orbital shaker was used (Labcon Laboratory Equipment (PTY) LTD, South Africa) The incubator acted as a containment chamber prevented contamination of the solutions during experimentation, it also maintained both the temperature (85°C) and rotational speed (200 rpm) stable set values. A 500 ml volumetric flask was used to prepare a 10% mass by volume solution; the liquid solution was prepared using distilled water, sulphuric acid and ferric sulphate to produce a ferric sulphate solution of 0.1 M (Cordoba et al., 2008a). The experiments were carried out in triplicate for each of the chalcopyrite-bearing ores. The additive shake flask solution was prepared by adding magnetite in a 1:1 ratio with the chalcopyrite minerals to produce the 10% mass by volume solution. The solutions in shake flask tests, incubated at 85°C, were prepared at pH values of 0.5-1, after which pH evolution was allowed to occur over the course of a leaching period of 12 hours. The dissolution kinetic information was obtained from a 30 mL sample that was withdrawn from the leaching vessel hourly, and analysed for its dissolved metal content using ICP-OES analysis. Prior to that, the withdrawn slurry was filtered using 150 mm filtration paper. Lastly, the filtered residue was dried, stored in a desiccator and subjected to mineralogical and chemical characterisation using XRD and XRF.

4.2.4 Equipment

The extracted slurry was filtered to obtain a clean leachate solution, of which a 1 ml sample was extracted and diluted by a factor of 10 using a 1% HNO_3 solution for standardisation. The samples were stored in a laboratory fridge at 4°C until use. The standardised solutions were analysed for dissolved metal concentration (specifically Ca, Cu, Fe and Mg totals) using the ICP-OES (Agilent Technologies, USA). The iron content was determined by chromatometric titration using potassium dichromate ($K_2Cr_2O_7$). The solid residues were assessed for mineral content by means of XRD analysis using a Rigaku Ultima IV (operated at 40 kV and 30 mA) and PDXL analysis software; the instrument's detection limit was 2%. This technique enabled the identification of the various mineral phases and their quantification. The operating conditions of the diffractometer's copper radiation source were 30 kV and 25 mA. Data was recorded over the range $5° \leq 2\theta \leq 95°$. The samples were milled further, to 53 microns, and were scanned at 0.5°/min, with a step width of 0.01°.

4.2.5 Leachate analyses

Leachate samples obtained after leaching chalcopyrite solutions were characterised by measuring electrical conductivity (EC), pH, ORP and temperature. For the measurements of pH, temperature and ORP (for each leachate solution), a portable pH meter with an analytical electrode HI8424 (Hanna Instruments Inc.) was used. Samples were also measured for sulphate ion concentration,

chloride ion concentration, iron ion concentration, acidity and alkalinity. A Multiparameter Photometer HI 83099 was used to measure sulphate ion concentration of the selected carbonate and silicate samples.

4.2.6 Titration tests

The alkalinity was measured through titration method with 0.1 N sulphuric acid (H_2SO_4), where the solution was titrated from pH values lower than 8.3 to 4.5 using an indicator for clear endpoint visibility. The acidity was measured through titration method with 0.02 N sodium hydroxide (NaOH), where 0.02 N sodium carbonate (Na_2CO_3) was used as standardisation procedure. Silver nitrate ($AgNO_3$), as titrant, along with potassium dichromate (K_2CrO_4) as indicators were used to measure chloride ion concentration. (Fosso-Kankeu et al., 2017).

4.2.7 Speciation modelling

To determine the aqueous speciation of the major metal ions in the leachate of the ROM feed stream sample, AQUACHEM software was used, interfaced with PHREEQC (program version 3.3.12-12704) modelling software (Barlow et al., 2018). The PHREEQC database, Minteq.v4.dat, was used for the purpose of this report. The ORP had to be adjusted with a correction factor before it could be used as input data. The correction factor was obtained from Field Measurements of Oxidation-Reduction Potential (Stiggov, 2013) . The corrected ORP value was then used to calculate the pe value using the following equation:

$$pe = E\_h/(0.059)$$

pe donates the negative logarithm of the electron activity

Eh donates the ORP of the sample

To predict the speciation of the major metals present within the leachate of the chalcopyrite-bearing minerals, the following input data were used within the PHREEQC workbench interface: acidity, alkalinity, pH, pe, temperature (°C), ICP data (metal ion concentrations), Cl^- and SO_4^{2-}.

4.3 Results and discussion

4.3.1 Mineralogical composition

The mineralogical composition and diffraction spectrum of the mineral phases present within the carbonatite tailings sample will be discussed in this section, as will the phases present within the magnetite sample. The diffraction spectrum of the tailings samples is summarised in Figure 4-1; the diffraction spectrum of the carbonatite- and silicate rom is available in 3.3.1.

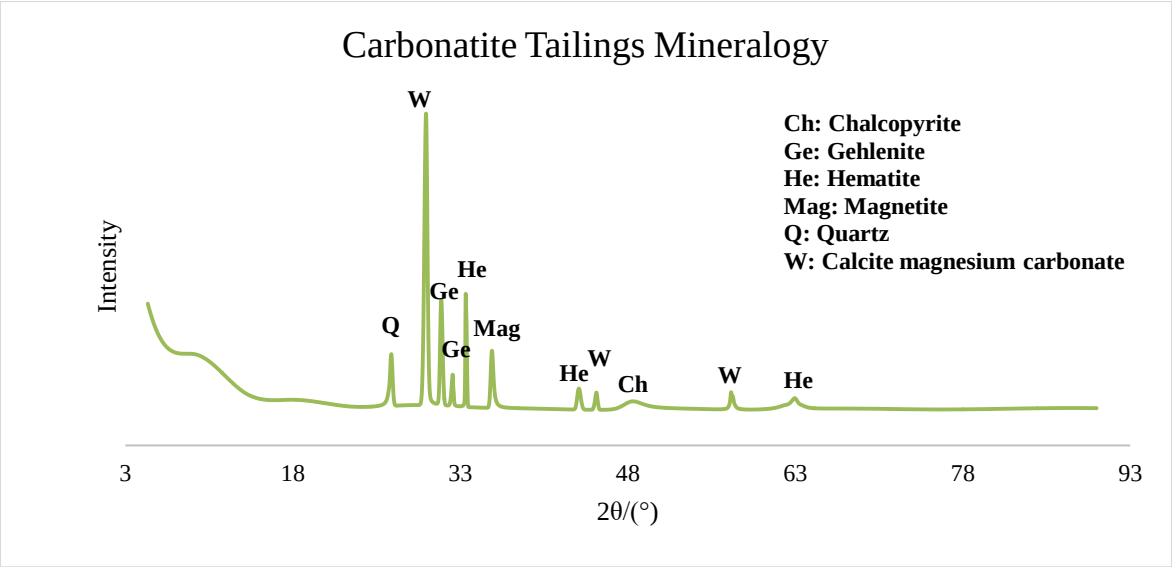

Figure 4-1: Diffraction spectrum of chalcopyrite-containing host ores (carbonatite tailings)

The tailings from the alkaline-carbonatitic complex were principally constituted of carbonate minerals, with calcite magnesium (W) as the dominant carbonate phase found, at 73% (Nyembwe et al., 2019). The other dominant phases observed within the mineral were those of hematite (He) and quarts (Q), at 10 wt% and 12 wt% respectively. The new phase formed and deposited in the tailings samples after concentrating the ROM samples was that of Gehlenite (Ge), at 6 wt%. The hematite, as the most stable phase of iron oxide present in the tails, is the result of phase mutation of magnetite from the feed stream samples because of oxygen diffusion during bubble creation in the flotation process conducted at the Phalaborwa Mining Company's Rio Tinto mining site (Gorbachev et al., 2007). The new phase, Gehlenite, is also thought to be as a result of the concentration process (Nyembwe et al., 2019). The presence of chalcopyrites (Ch) within the tailings was low (0.47 wt%), as the mineral accumulated in the concentrate of the ROM material during the flotation process, which only allowed for low accumulation of the mineral in the tailings. This indicates that extraction through flotation of chalcopyrite was effective.

The distribution of identified minerals phases present within the studied samples are summarised as weight percentages in Table 4-1, where Cr, Ct and Sr represent the carbonatite ROM, carbonatite tailings and silicate ROM samples respectively.

Table 4-1: Mineral composition of host rock and additive samples

XRD RIR: observed phase quantification					
Observed phases		**Weight % in sample ores**			
Phase name	**Phase chemistry**	**Cr**	**Ct**	**Magnetite**	**Sr**
Analite	Cu_7S_4	****	****	****	6.76
Barium silicate	Ba_2SiO_4	****	****	****	13.31
Calcite magnesium	$(Mg_{0.06}Ca_{0.94})$ (CO_3)	48.20	73	****	****
Chalcopyrite	$CuFeS_2$	1.54	0.47	****	6.20
Coesite	SiO_2	****	****	****	11.47
Copper sulphide	Cu_2S	****	****	****	3.70
Digenite	Cu_9S_5	1.48	****	****	6.23
Dolomite	$CaMg(CO_3)_2$	32.34	****	****	****
Gehlenite	$Ca_2Al_2O_7$	****	5.78	****	****
Hematite	Fe_2O_3	****	10.07	****	9.50
Lime	CaO	****	****	****	0.09
Magnetite	Fe_3O_4	7.02	****	100	****
Moganite	SiO_2	****	****	****	3.47
Periclase	MgO	5.64	****	****	9.10
Pyrite	FeS_2	****	****	****	6.89
Potassium oxide	K_2O	****	****	****	3.61
Quartz	SiO_2	3.86	12	<1	19.66

4.3.2 Elemental composition

The bulk elemental chemistry of the chalcopyrite-containing carbonatite samples (ROM and tails), and that of the additive (magnetite), will be discussed in this section. The elemental composition of the main elements identified within the analysed samples are presented by Figure 4-2 and that of the trace elements by Figure 4-3. The chemical composition related to the siliciclastic hosting ore can be obtained from 3.3.2.

As with the feed stream samples from the carbonatite complex, the tailings samples of the carbonate host mineral contained calcium as its main component (47.5 wt%), with elemental compositional magnitude of Si and Mg increasing in the tailings streams samples by 0.5 and 1 wt%, respectively. The operations at the Phalaborwa Mining Company's Rio Tinto mine extracts copper through concentrating the carbonatite feed stream samples through flotation techniques; it can be said that the flotation process that is used is effective, as the Cu in the tailings stream is almost 10 times lower than that reported from the feed stream samples (0.47 wt% and 4.49 wt%, respectively). Although

0.47 wt% is low compared to the feed stream samples, the tailings are of significance, as global average copper ore grades hold nearly the same compositional magnitude, at 0.62 wt% (Mudd & Weng, 2012; Calvo et al., 2016).

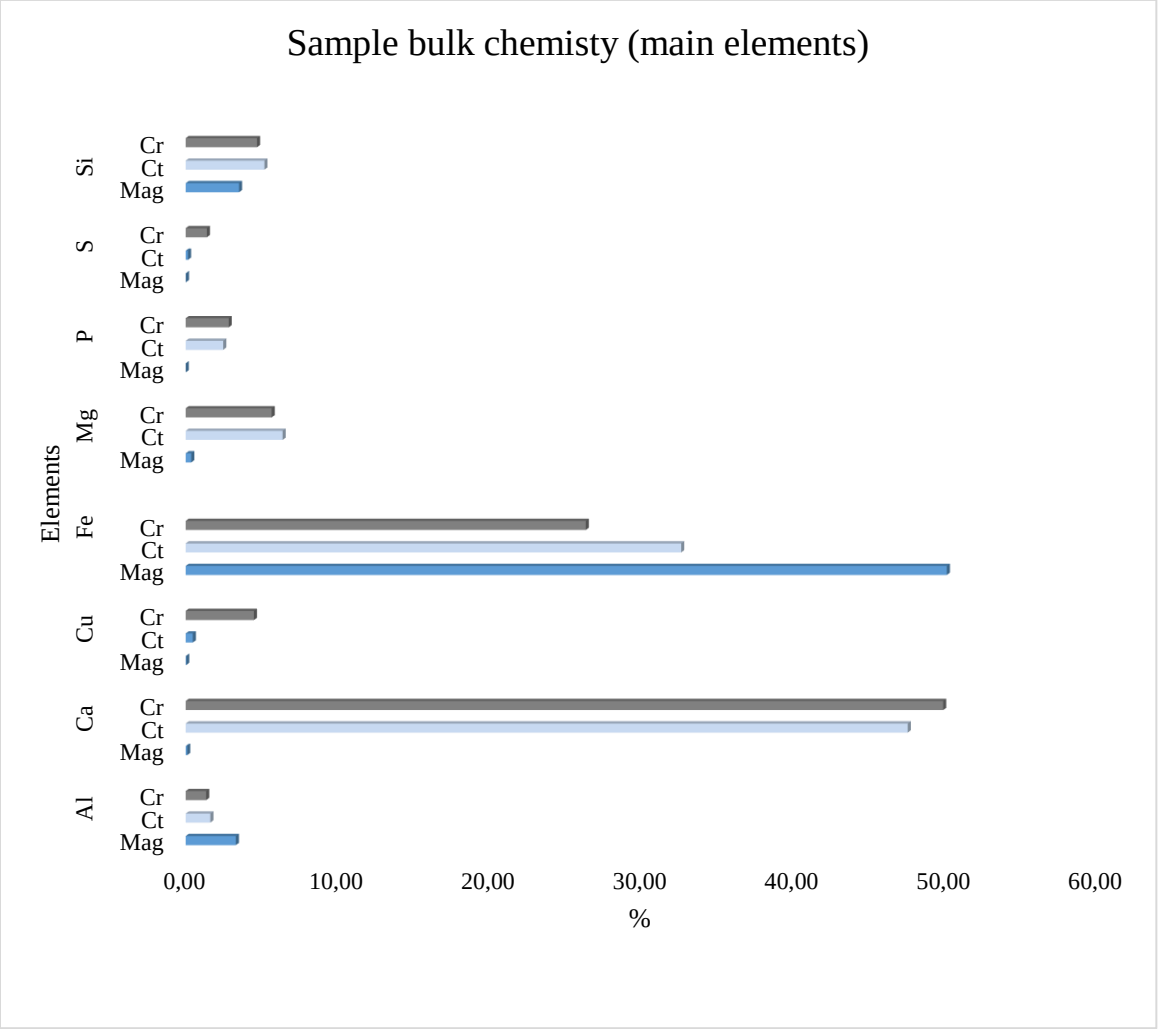

Cr: Carbonatite rom; Ct: Carbonatite tailings; Mag: magnetite

Figure 4-2: Bulk elemental chemistry: Main elements

The magnetite samples originating from the Bushveld Complex was dominated by Fe (50.05 wt %), with the second-highest bulk elemental constituent being Ti (titanium), at 6.78 wt%. The magnetite ore from the Bushveld Complex in South Africa are from a magmatic system crystallised in silicate melts (Dare et al., 2014) – magnetite from these melts are generally found in Fe-Ti-V-P deposits (Dare et al., 2012; Boutroy et al., 2014). The magnetite in the Bushveld Complex is typically identified as titanium rich, with grades of 6-12 wt% (Toplis & Carrol, 1995; Namur et al., 2010) and that of vanadium (V) at 0.14-0.8 wt% (Barnes et al., 2004; Dare et al., 2014). These figures correspond with the data that was captured during elemental investigation into the additive samples, which identified the concentration of Ti and V as 6.78 wt% and 0.86 wt% respectively.

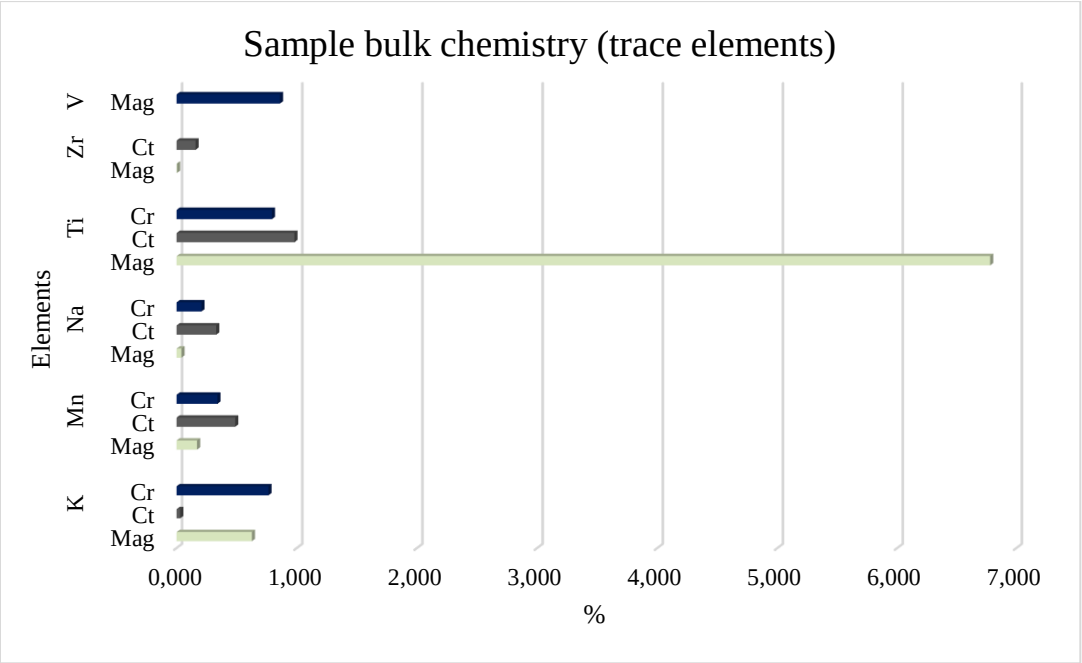

Cr: Carbonatite rom; Ct: Carbonatite tailings; Mag: magnetite

Figure 4-3: Bulk elemental chemistry: Trace elements

4.3.3 pH variation in the presence of magnetite

The sulphide sample solution pH was adjusted (pH 0.5-1) for all samples, after which pH evolution was allowed to occur. The pH behaviour of both tailings (Ct) and carbonatite ROM (Cr), the silicate ROM (Sr), as well as the samples treated with magnetite, all at fixed temperature conditions (85°C), are displayed in Figure 4-4.

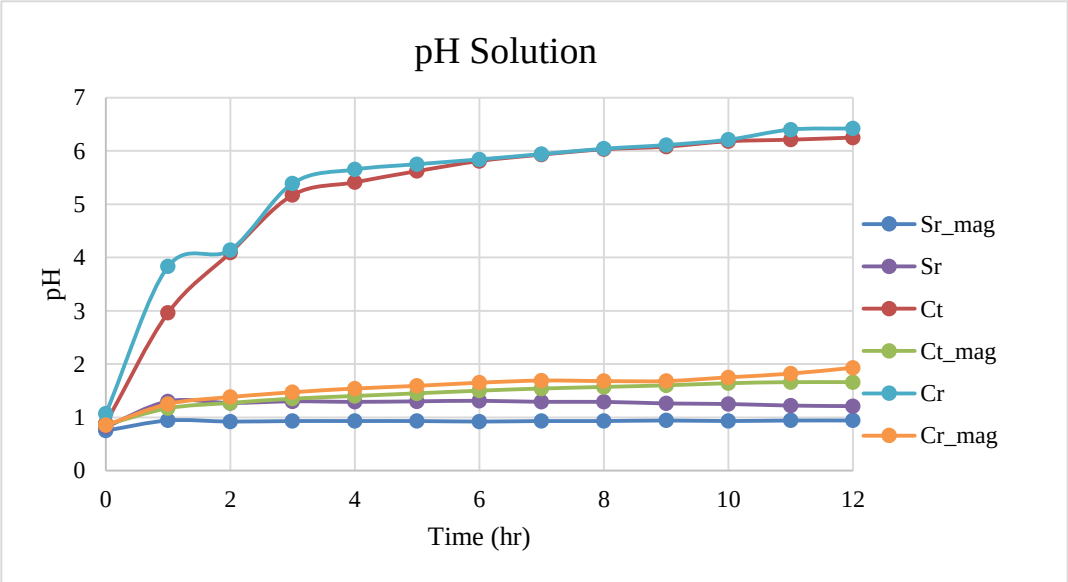

Cr: Carbonatite rom; Cr_mag: Carbonatite rom treated with magnetite; Ct: Carbonatite tailings; Ct_mag: Carbonatite tails treated with magnetite; Sr: Silicate rom; Sr_mag: Silicate rom treated with magnetite

Figure 4-4: pH behaviour of treated and untreated samples at 85°C

The pH behaviour of the untreated Cr samples at 85°C can be attributed to higher concentrations of alkaline earth metals (Ca and Mg) which were released under these conditions; the dominant species formation for these metals was likely that of free hydrated ionic species of Ca^{2+} and Mg^{2+}. Ca^{2+} is known to compete with hydrogen ions in solution, causing neutralisation of the solution acidity (Lamar, 1961). For the Cr samples treated with magnetite, the pH evolution was very different, as acidic conditions (pH of 1.93) were observed after the set leaching period (12 hours). By adding magnetite in a 1:1 ratio to the carbonatite samples, the effects of the free hydrated ionic species Ca^{2+} were minimised, as the wt% of calcium in solution was reduced and, by extension, the formation of Ca^{2+}. Under these conditions the effects of acid attack were enhanced, and was visible from the solution pH.

The pH evolution of the untreated Ct samples was similar to that of the ROM. Increased pH conditions (pH 0.89-6.25) were observed over the course of the set leaching period. The elemental investigation indicated that the wt% of calcium in the Ct samples was slightly lower than that of the Cr samples (47.5wt% and 49.81wt%, respectively). As calcite-magnesium was identified as the main mineral present within the tailings sample, the higher pH conditions are thought to be a result of acid neutralisation through calcium ions. The slightly higher pH levels observed for the Cr samples after the set leaching period (pH of 6.42) could be the result of higher concentrations of Ca^{2+} ions releasing under these conditions. The total wt% of calcium containing minerals, as seen from Table 4-1, amounts to 80.54% (calcite-magnesium and dolomite) compared to 78.78% for the Ct samples (calcite-magnesium and Gehlenite). Similar to the behaviour observed for the Cr samples treated with magnetite, the treated Ct samples also displayed acidic behaviour (pH of 1.66) after the set leaching period. As seen with the untreated Cr and Ct samples, the pH of the tailings solution, in the presence of magnetite, was lower than that of the feed stream samples (pH of 1.93), indicating that acid consumption was lower in the carbonatite tailing samples, because lower concentrations of Ca were present.

Chalcopyrite-containing silicate host ore, treated with sulphuric acid and ferrous sulphate, displayed stable pH behaviour as a 0.4 value change, was observed over the course of the set leaching period (pH 0.82-1.21). This was the result of lower acid consumption during mineral dissolution, as sulphide species contained within the host ore, such as pyrite, undergo oxidation during leaching to form secondary $H_2SO_4^-$ which aided in replenishing the acid consumed during mineral dissolution (Fosso-Kankeu et al., 2017). The silicate host ore, in the presence of magnetite, behaved similarly to the untreated samples. Stable pH evolution was observed, with a 0.2 value change (pH 0.75-0.94) over the set leaching period, indicating that acid consumption during mineral dissolution of the Sr_mag sample was lower than that of the untreated sample.

4.3.4 Effects of additives

The dissolution behaviour of the feed stream samples (Cr and Sr) and Ct samples treated with magnetite, as well as the dissolution behaviour of the untreated samples, will be discussed in this section. The dissolution curve of Cu for the treated and untreated samples are displayed in Figure 4-5.

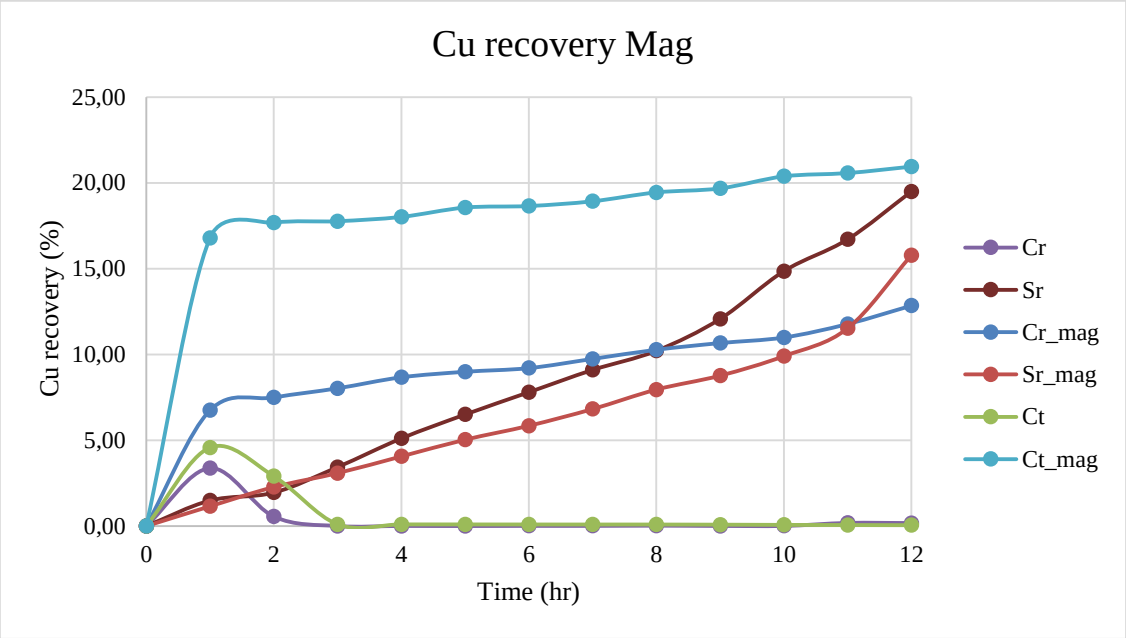

Cr: Carbonatite rom; Cr_mag: Carbonatite rom treated with magnetite; Ct: Carbonatite tailings; Ct_mag: Carbonatite tails treated with magnetite; Sr: Silicate rom; Sr_mag: Silicate rom treated with magnetite

Figure 4-5: Comparative dissolution behaviour of treated and untreated ore samples

The recovery of Cu from the carbonatite-rich ore, was reduced during sulphuric-acid-based leaching using ferric sulphate as oxidising agent at elevated temperature conditions (85°C). At these temperature conditions, high concentrations of Ca was released in solution and, with it, the formation of Ca species such as Ca^{2+}, which neutralised the solution pH (Figure 4-4) and gypsum ($CaSO_4.2H_2O$), forming a matrix mixture on the mineral surface, encapsulating the undissolved mineral and thus hindering further dissolution. Recovery was also reduced as the increase in pH and reduction in redox potential promoted the formation of insoluble CuO species. The addition of magnetite during leaching of the Cr mineral proved to be beneficial for the leaching process, as Cu recoveries increased significantly, with 12.8 wt% of Cu recovered over the set leaching period, compared to the 0.18 wt% obtained from the untreated Cr solution. As mentioned in 4.3.3, by adding magnetite in a 1:1 ratio, the total concentration of Ca in solution was reduced, which aided in keeping the solution pH at acidic conditions and improved Cu recovery, as higher concentrations of protons are released under these conditions (Acero et al., 2009; Koleini et al., 2011).

The untreated Ct samples displayed similar dissolution behaviour as that observed for the Cr samples; however, early Cu mobilization was more rapid in the tails: 4.6 wt% Cu was recovered after 1 hour dissolution, compared to 3.4 wt% recovered for the feed stream samples. The recovery at this stage is believed to be higher in the tailings stream samples because the conditions were more acidic than those observed for the feed stream samples (pH 2.96, compared to pH 3.83). As leaching progressed, the recovery of Cu from the carbonatite tails mineral reduced similarly to the feed stream samples. pH levels increased, which is unfavourable for Cu dissolution; this was visible from the 0.05 wt% recovery after the 12 hours leaching period. Similarly, by treating the tailings in a 1:1 ratio with magnetite, the recovery of Cu improved (20.94 wt% Cu recovered after 12 hours leaching period, as opposed to the 0.05 wt% for the untreated sample).

It was observed that, under these temperature- and acidic pH conditions, the dissolution rate of Cu increased from the surface of the chalcopyrite-containing siliciclastic sample. After 12 hours of dissolution, 19.5 wt% Cu was recovered and continued to increase. The pyrite (FeS_2), along with other Cu sulphides, aided in the formation of acidic conditions during shake flask leaching within the solution sample. Pyrite also dissolves in water to form H_2SO_4, which increases the sulphuric acid concentration in solution. Studies have reported that the Cu dissolution rate increased as H_2SO_4 concentration increased which holds true for the untreated silicate samples (Aydogan et al., 2006). Unlike the carbonate samples treated with magnetite, the silicate samples displayed better recovery rates for the untreated samples; the treated sample Cu recovery, after 12 hours of dissolution, was 15.8 wt%.

Figure 4-6 displays the comparative dissolution behaviour of Cu and Fe (at 85°C) for the carbonate and silicate rom samples treated with magnetite (Cu_Mag_C and Fe_Mag_C for Cr and Cu_Mag_S and Fe_Mag_S for Sr, respectively). Both treated and untreated behaviour of the carbonatite tailings samples are also present in the graph; Cu_85_T and Fe_85_T for the untreated tails and Cu_Mag_T and Fe_Mag_T for the treated tails mineral.

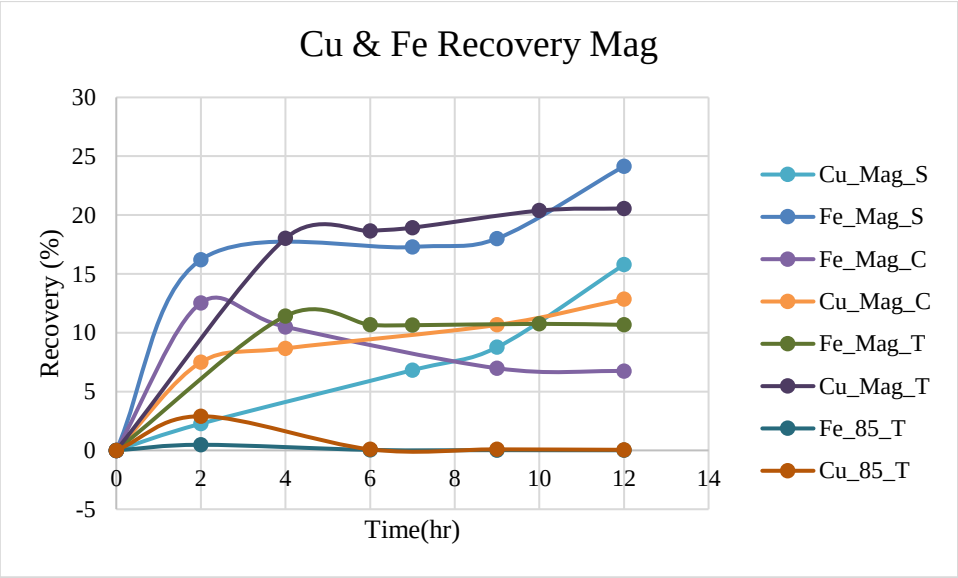

Figure 4-6: Dissolution behaviour of Cu and Fe for treated and untreated samples

As with the run of mine samples, the carbonatitic tails were also observed to contain Fe as a major elemental component within the mineral. A concentration of 32.58% was obtained from the bulk elemental investigation. As seen in Figure 4-5 and 4.6, Cu and Fe recovery is reduced under these conditions (85°C); alkaline pH conditions and a general decrease in redox potential were observed in untreated Ct samples over the course of the leaching period; and the recovery rates of the two metals after the set leaching time was 0.05 wt% for Cu and 0.012 wt% for Fe, respectively. As with the Cr samples, these conditions for the untreated tailings samples were unfavourable for leaching Cu from the surface of the mineral; however, a static plateau stage was not present, indicating that passivation had not been achieved after 12 hours of dissolution. In the presence of magnetite, the samples streams of the carbonatitic host ore (Ct and Cr) behave very differently, as recovery of Cu is favoured at this temperature (85°C) and pH condition (pH stable at <2). Under these conditions for both mineral stream samples, a static plateau stage is visible for Fe, where parabolic behaviour is observed, along with reduction in the recovery rate over the set leaching period. With less Fe being released in solution from the surface of the host minerals, lower concentrations of ferrous ions are available to compete with Cu^{2+} ions, thereby effectively increasing the solubility of Cu and promoting increased dissolution rates. Additionally, the formation of ferric salts, such as jarosite, is reduced at these low pH conditions for both Cr and Ct samples. This is advantageous for Cu recovery, as retardation of the leaching kinetics occurs in the presence of jarosite, when mass transfer of Cu ions is restricted from the surface of the mineral (Khoshkhoo, 2014).

The silicate samples treated with magnetite displayed the same behaviour as that of the untreated samples: kinetic leaching of Cu was favourable at 85°C and stable acidic conditions (pH at 0.94). In Figure 4-6 it can be seen that chalcopyrite dissolves incongruently in solution. Fe is preferentially released over Cu, as seen from the higher recoveries (Acero et al., 2009). The bulk elemental

investigation found that the magnetite samples consist of 50.05% Fe, thus, indicating that a higher concentration of Fe:Cu is present in the treated samples than in the untreated samples, and a higher concentration of ferrous ion is available in the treated sample, which competes with the cupric ion (Cu^{2+}). The sligtly lower recoveries observed for the treated samples (15.78 wt% compared to 19.49%) are believed to be as a result of this behaviour.

4.3.5 Speciation results

The speciation results predicted using PHREEQC workbench software and input parameters obtained during experimentation, will be discussed in this section. As with the untreated samples, the magnetite pre-treated samples were predicted accurately using the geochemical workbench software, only allowing for a 10% error margin. Table 4-2 presents the species for the major metal ion within the ROM solution of both host minerals, treated and untreated, as well as that of the tailings mineral, as a percentage range obtained under temperature conditions of 85℃ for the duration of 12 hours leaching test.

Table 4-2: Predicted species formation of treated and untreated host ores samples

Element	Species	Untreated			Treated		
		Cr	Sr	Ct	Cr	Sr	Ct
Ca	$CaSO_4$	35.55-43.45	59.93-62.77	48.37-41.26	56.98-60.13	55.31-64.95	61.33-65.11
	Ca^{+2}	53.24-60.43	36.45-40.08	51.63-54.58	39.88-43.00	42.32-43.32	34.91-38.71
	$CaOH^{+}$	<1	<1	<1	<1	<1	<1
	$CaHCO_3^{+}$	<1	<1	3.71-4.17	<1	<1	<1
Cu(2)	$CuSO_4$	20.25-31.13	59.72-63.39	20.33-48.21	57.06-60.22	57.84-65.06	61.47-65.26
	Cu^{+2}	24.94-53.33	37.37-40.27	27.02-51.79	39.65-42.79	34.94-42.16	34.74-38.53
	$CuOH^{+}$	0.28-0.54	<1	0.32-0.63	<1	<1	<1
	$CuHCO_3^{+}$	6.51-14.71	<1	8.56-10.94	<1	<1	<1
	CuCO3	0.58-46.38	<1	20.07-42.94	<1	<1	<1
Fe(2)	Fe^{+2}	70.74-74.07	85.79-89.58	66.39-69.55	76.69-83.94	90.29-92.25	80.04-83.05
	$FeSO_4$	27.90-31.86	11.33-14.21	28.58-33.61	16.06-23.31	7.70-9.72	16.95-19.96
	$FeOH^{+}$	<1	<1	<1	<1	<1	<1
	$FeHCO_3^{+}$	1.35-1.77	<1	1.68-1.85	<1	<1	<1

Mg	$MgSO_4$	31.14-39.25	54.45-58.21	36.56-42.78	51.16-54.35	49.45-59.44	55.56-59.56
	Mg^{+2}	59.24-66.18	42.64-45.54	57.22-60.65	45.65-48.84	40.56-48.15	40.44–44.44
	$MgHCO_3^+$	2.2-2.71	<1	2.48-2.78	<1	<1	<1

The concentrations of the formed species of calcium differ for the untreated carbonate ROM samples and those treated with magnetite. Although the concentration of the free hydrated Ca^{2+} species appears to decline during the 12 hours dissolution period, it still formed the bulk of the Ca species in solution (53.24% at 12 hours dissolution). The assumption that the pH behaviour conditions of pH evolution for the untreated carbonate feed stream samples are effected by the formation of free hydrated species of alkaline earth metals holds true, as the bulk concentrations of Ca^{2+} species indicates. The treated samples were dominated by the insoluble salt species, calcium sulphate ($CaSO_4$), and displayed an increase in concentration during the 12 hours dissolution, whereas the formation of Ca^{2+} ions in solution declined. This finding is represented by the low pH levels observed during dissolution of this mineral, as more hydrogen ions were released in solution, with a lower concertation of competing Ca^{2+} ions. The preparation of a 1:1 solution aided in reducing the initial amount of Ca ions in solution and, in so doing, lead to the formation of a generally acidic environment favourable for the dissolution of Cu from the chalcopyrite host ore. The bulk concentration of Fe in solution was identified as ferrous iron (Fe(II)); a trace amount (<1%) of ferric iron (Fe(III)) was also identified. Fe was dominant as the free hydrates ionic species Fe^{2+} in both treated and untreated samples, whereas Cu was dominant as the insoluble salt species, $CuSO_4$, once again indicating that chalcopyrite preferentially releases Fe over Cu in solution (Lu et al., 2016). However unlike the treated samples, an increase in the formation of the insoluble species $FeSO_4$ was observed, along with a decline in Fe^{2+} concentration. This behaviour agrees with the Fe recovery curve in Figure 4-6, where parabolic behaviour is observed for the Fe curve, indicating that the plateau stage, and therefore passivation of Fe, occurred.

The untreated tailing samples showed the same behaviour as the ROM samples: Ca was dominant as a free hydrates ion species Ca^{2+}, however, unlike the ROM samples, the concentration of $CaSO_4$ declined in concentration. Fe was dominant as Fe^{2+}, and an overall increase in concentration of this Fe species was observed, unlike in the ROM samples. As with the Cr samples, both these factors caused reduced recovery of Cu from the host ore in solution. The treated tailings sample results are similar to those of the treated feed stream samples: Ca favoured the formation of $CaSO_4$ ions, however, the formation of the complex salt species was higher in the tailings samples. This is also visible from the lower pH levels observed for these samples (Figure 4-4). The behaviour of Fe was similar to that of the ROM samples, as the Fe^{2+} ion concentration declined (although it was still the dominant ion species) as $FeSO_4$ concentration increased.

For the treated and untreated silicate feed stream samples, the Ca species that formed during experimentation correspond with the low pH values associated with both these samples during the 12 hours dissolution, as the bulk concentration of the Ca ions was in the form of the complex salt species $CaSO_4$, as shown in Table 4-2. The concentration of Cu^{2+} was slightly higher in the untreated samples (37.37% and 34.94% for untreated and treated samples, respectively) which corresponds with the recovery rates of Cu observed for these samples. Higher concentrations of the dominant Fe species of ferrous ion were also present in the silicate samples that had been treated with magnetite, further strengthening the Cu recovery behaviour, as more Fe^{2+} ions compete with Cu^{2+} in solution, as opposed to the behaviour observed for the untreated silicate mineral.

4.3.6 Mineralogical composition of residue samples

4.3.6.1 Carbonatite (ROM and tails)

Figure 4-7 shows the diffraction spectra of the mineral content present within the residue of the Cr and Ct samples treated with magnetite. The black spectrum represents the diffraction of the mineral after 60 minutes of leaching, and the red spectrum that of the mineral after 720 minutes of leaching.

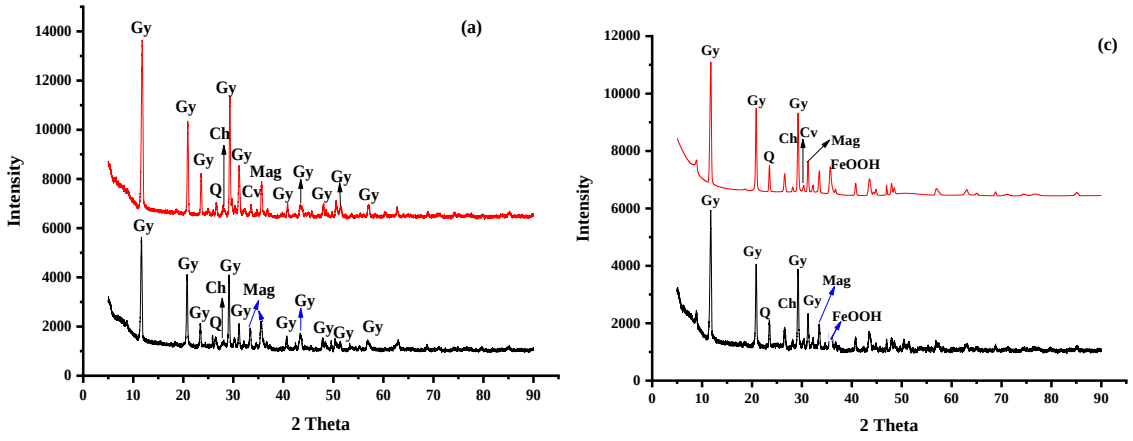

Ch: chalcopyrite; Cv: covellite; FeOOH: goethite; Gy: gypsum; Mag: magnetite; Q: quartz

Figure 4-7: Diffraction spectrum of ROM (left) and tailings (right) of carbonatites treated with magnetite

In both the Cr and Ct samples, a decrease in peak intensity of chalcopyrite was observed from 60 minutes to 720 minutes, which indicates effective mineral dissolution from the carbonate host rock in the presence magnetite (Santos et al., 2017). During leaching with sulphuric acid using ferric sulphate as an oxidant, new mineral phases were formed; bornite and covellite were identified as the intermediate Cu phases formed for both carbonatite samples. Besides the intermediate phase formation of Cu minerals, other precipitate minerals also formed during dissolution of the host samples; these precipitate minerals being hydronium iron oxide (goethite), hydronium jarosite ($(H_3O)\ Fe_3^{3+}(SO_4)_2(O_6H)$) and further formation of magnetite (Fe_3O_4) as well as elemental sulphur

linked to the dissolution media. Additional intermediate Cu phases were present within the untreated Cr & Ct samples, these being digenite and djulerite along with bornite and covellite before complete decompositions to the free ions, Cu^{2+} and Fe^{2+}, could occur (Cordoba et al., 2008b; Nyembwe et al., 2018). Precipitates of hematite were also formed during mineral dissolution of the untreated Cr sample, through oxygen diffusion of the initial magnetite concentration within the mineral (Gorbachev et al., 2007). Iron mineral phases of hematite, magnetite and jarosite were also formed during mineral dissolution of the Ct mineral, where progressive accumulation of Mg and Ja was observed. Gypsum associated with the carbonate dissolution of the clean Cr and Ct samples was also present during additive addition, and can be linked to the main mineral composition of calcite-magnesium for both carbonate minerals (Table 4-1). For both samples, an increase in gypsum concentration was observed, though the formation of gypsum was greater for the Cr samples (75.93%) than for that of the Ct samples (70.01%). The same behaviour was observed in the untreated samples, where gypsum accumulation after the dissolution period was 67.00% for the Cr sample, compared to 65.96% for the Ct sample (Table 4-4). This behaviour can be attributed to higher concentrations of Ca in the Cr samples (49.81%) than in the Ct samples (47.48%) obtained from the elemental characterisation of both samples; this is also evident in the enhanced reduction of sulphur (S) in the Cr_Mag samples (2.46-1.02%) compared to the Ct_Mag samples (2.46-2.08%) and the higher pH (pH 1.93 compared to pH 1.66).

4.3.6.2 Silicate

The diffraction spectrum for the mineral residue of the siliciclastic host ore (Sr) in the presence of magnetite can be seen in Figure 4-8.

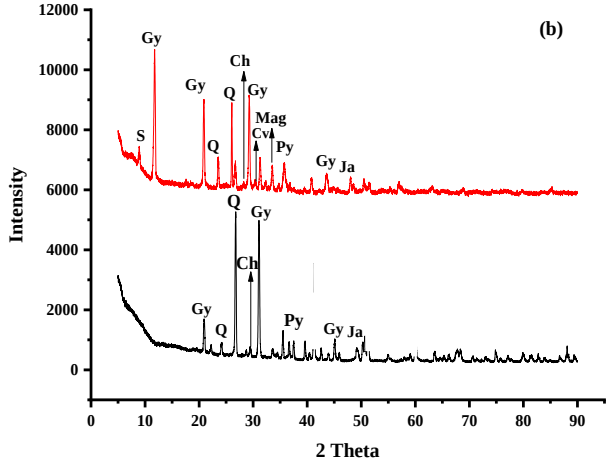

Ch: chalcopyrite; Cv: covellite; Gy: gypsum; Mag: magnetite; Py: pyrite; Q: quartz; S: Sulphur

Figure 4-8: Diffraction spectrum of silicate ROM treated with magnetite

From the diffraction spectrum and the mineral composition table for the treated minerals (Table 4-3), a major decrease in peak intensity for chalcopyrite is observed in the presence of magnetite, which indicates effective mineral dissolution. Just as with the carbonate minerals (Cr and Ct), new phase formation was observed during leaching of the silicate mineral (Sr), where intermediates of bornite and covellite were present. The formation of coesite quartz and other quartz can be attributed to the clastic nature of the hosting ore, whereas precipitates of elemental sulphur, goethite and hydronium jarosite can be linked to the dissolution media. The presence of sulphur in the silicate solution varies for the treated and untreated samples. High temperature polymorphs of sulphur (Rosickyite), along with elemental sulphur, were present in the untreated sample, compared to the treated sample, where only elemental sulphur was present. Just as in the untreated samples, a decrease in peak intensity of pyrite was observed, indicating effective pyrite dissolution; the presence of pyrite is beneficial, because galvanic interaction with chalcopyrite increases Cu recoveries (Berry, 1978; Dixon, 2008) . A major change from the untreated Sr samples to the Sr_mag samples is the presence of gypsum, which accumulated over the course of the dissolution period (21.12-32.10%). Other intermediates were also available in the untreated Sr samples, and did not form during mineral dissolutions of the Sr_mag samples, these being chalcocite and digenite. Additionally, pyrrhotite ($Fe_{(1-x)}S$) was formed during mineral dissolution of the untreated silicate samples.

Table 4-3 shows the mineral composition of the major minerals present within the residue samples of each of the study's chalcopyrite hosting ores treated with magnetite, while Table 4-4 shows that of the untreated samples at 85℃.

Table 4-3: Mineral composition of chalcopyrite-containing mineral residue (magnetite addition)

		Silicate (Sr)		**Tail (Ct)**		**Carbonate (Cr)**	
Phase name	**Chemical composition**	**After 20**	**After 720**	**After 20**	**After 720**	**After 20**	**After 720**
Bornite	Cu_5FeS_4	0,09	0,20	0,05	0,31	0,05	0,02
Chalcopyrite	$CuFeS_2$	3,12	1,51	0,90	0,65	2,59	1,81
Coesite	SiO_2	46,89	55,27	20,19	13,97	14,57	10,11
Covellite	CuS	0,25	0,64	0,02	0,02	0,04	0,04
Goethite	FeO(OH)	0,01	0,03	2.317	5,08	1,70	3,39
Gypsum	$CaSO_4$ $2H_2O$	21,12	32,10	68,12	70,01	69,90	75,93
Hydronium-jarosite	(H_3O) $Fe_3^{3+}(SO_4)_2(O$	11,24	2,40	2,46	3,90	1,79	4,46
Magnetite	Fe_3O_4	1,05	3,65	3,79	3,97	1,79	3,21
Sulphur	S	1,89	4,20	2,46	2,08	2,46	1,02
Quartz	SiO_2	14,33	***	2,02	***	5,12	***

Table 4-4: Mineral composition of chalcopyrite-containing mineral residue (clean)

		Silicate (Sr)		Carbonate (Cr)		Tails (Ct)
Phase name	**Chemical composition**	**After 20**	**After 720**	**After 20**	**After 720**	**After 720**
Bornite	Cu_5FeS_4	1.46	1.00	2,99	0,79	0,49
Calcium iron oxide	$CaFeO_2$	***	***	4,99	2,15	***
Chalcopyrite	$CuFeS_2$	2.90	1.79	6,46	5,12	0,10
Chalcocite	Cu_2S	2.90	1.79	3,79	1,01	0,02
Copper oxide	CuO	***	***	5,42	7,90	4.30
Covellite	CuS	7.42	10.79	1,99	0,46	0,78
Cyclo-hexasulphur	S_6	***	***	2,02	0,50	***
Djulerite	$Cu_{31}S_{16}$	7.79	3.90	***	***	***
Digenite	Cu_9S_5	4.46	1.19	0,71	0,12	***
Gypsum	$CaSO_4 \cdot 2H_2O$	***	***	57,84	67,00	65,96
Hematite	Fe_2O_3	***	***	14,24	16,86	5,86
Jarosite	$XFe^{3+}{}_3(OH)_6($	***	***	***	***	6,48
Magnetite	Fe_3O_4	***	***	***	***	7,46
Pyrite	FeS_2	1.46	1.00	***	***	***
Pyrrhotite	$Fe_{(1-x)}S$	1.79	2.02	***	***	***
Quartz	SiO_2	39.89	46.46	***	***	8,56
Rosickyite	S	11.79	12.20	***	***	***
Sulphur	S	13.89	15.79	***	***	***

4.3.7 Eh-pH diagrams of associated minerals (thermodynamic consideration)

The Eh-pH diagram for both Cu and Fe, along with all possible stability zones relative to their equilibrium conditions, are available from Figure 4-9 and 4.11. The change in redox potential (Eh) for both ROM and tails carbonatite minerals, as well as that of the silicate hosting ore is available form Figure 4-10. The ORP was measured using an analytical Ag/AgCl electrode in a 3M KCl filling solution.

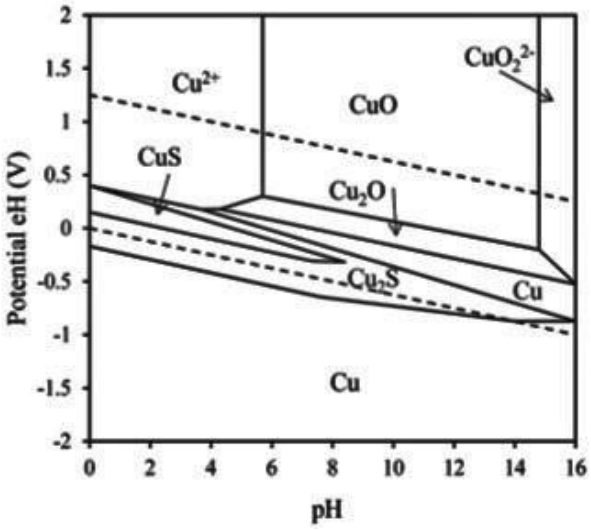

Sources: (House, 1987; Khoshkhoo et al., 2014)

Figure 4-9: Pourbaix diagram for Cu-S-O-H_2O

In the Pourbaix diagram, it can be seen that free hydrated cupric ions (Cu^{2+}) could be maintained where solution pH was maintained between 0-5, and potential value above 1 V. The experimental conditions for the chalcopyrite-containing samples in the presence of Fe_3O_4 were similar to that of the untreated samples, where the potential range was low (0.6-0.2 V). The inclusion of magnetite during minerals dissolution of the calcite-rich carbonate minerals (both Cr and Ct) aided in stabilising the solution potential above 0.5 V, which reduced the formation of the covellite phase (CuS). The concentration of the mineral was stable at 0.04% and 0.02% for Cr and Ct respectively – it did not increase over the course of the leaching period; furthermore, the stability zones for the carbonate minerals did not allow for the formation of chalcocite (Cu_2S). During mineral dissolution of both untreated carbonatite samples streams, solution pH increased, and redox potential decreased, which correspond with the XRD results, where the formation of the covellite phase is favoured. However, during the course of the dissolution period, the formation of covellite was reduced with an increase in pH and a decrease in ORP value, which favoured the formation of insoluble copper oxides (CuO) instead.

The mineral dissolution of the chalcopyrite-containing silicate run of mine samples treated with magnetite was similar to that of the untreated silicate host ore. The solution redox potential was stable between 0.56 and 0.57 V for the course of the leaching period (12 hours); that of the untreated samples was at 0.58 V after 60 minutes and 0.55 V after 720 minutes. Similarly, the pH of solution was stable at acidic conditions (pH of 0.94 after 720 minutes). As with the carbonatite minerals, the formation of intermediate phases of chalcocite and digenite was not present during mineral dissolution with magnetite. As with the untreated samples, the accumulation of covellite was observed during the course of the leaching period, although at much lower concentrations than those

seen in the untreated mineral residue (0.64% compared to 10.79%). The results obtained during mineral residue characterisation, along with phase predictions through the using the Pourbaix diagram, complements the Cu recovery results (Figure 4-5) observed for the silicate host ore, where an increase in the dissolution rate was observed over the leaching period for both treated and untreated samples.

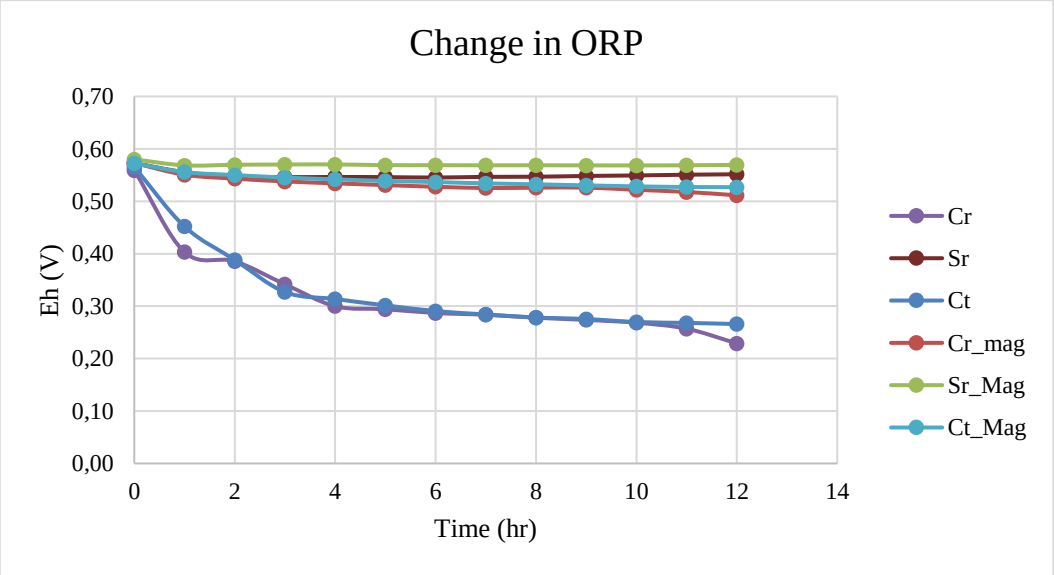

Cr: Carbonatite rom; Cr_mag: Carbonatite rom treated with magnetite; Ct: Carbonatite tailings; Ct_mag: Carbonatite tails treated with magnetite; Sr: Silicate rom; Sr_mag: Silicate rom treated with magnetite

Figure 4-10: Change in ORP for treated and untreated chalcopyrite-containing minerals at 85°C

From the given Pourbaix diagram of iron in an aqueous solution at 85°C, it is evident that effective dissolution could occur over a wide pH range, where redox potential is stable between -0.6 V and 0.8 V. During dissolution of the carbonate minerals (Cr and Ct) in the presence of magnetite, these conditions were met, as shown by the predicted species formation, where the dominant iron species was Fe^{2+}. However, during the course of the leaching process, Fe recovery decreased as the concentration of ferrous ion reduced, and the formation of insoluble Fe salt species, $FeSO_4$ was favoured instead. The phase formation of the iron oxide minerals, goethite and magnetite, was also favoured during the leaching process, thereby further strengthening the observed reduction behaviour. Iron dissolution was favoured during leaching of the untreated carbonate minerals, where Fe^{2+} formation was favoured during the first 7 hours of leaching, after which the redox potential and pH values gradually shifted to favour the formation of the iron oxide mineral hematite during dissolution of the Cr mineral. Further formation of hematite and of magnetite was favoured during leaching of the Ct mineral (Table 4-4). The redox potential and pH conditions were met during leaching of the siliciclastic host ore (treated and untreated), as effective dissolution of Fe was observed. Fe^{2+} was predicted as the dominant iron species formed, and it increased over the course of the leaching period (90.29-92.25% for the treated Sr and 85.79-89.58% for untreated Sr).

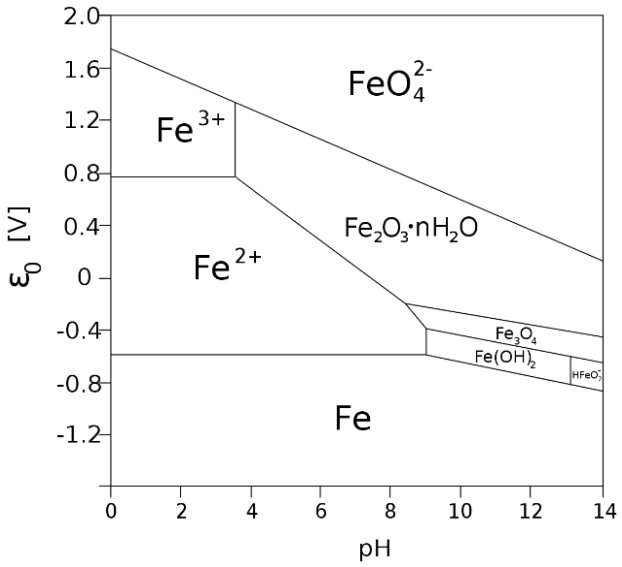

Sources: (Townsend, 1970; Beverskog & Puigdomenech, 1996; Salgado et al., 2013)

Figure 4-11: Pourbaix diagram of Fe in an aqueous media

During dissolution of the chalcopyrite-containing minerals in a sulphate medium, the results of the mineralogical characterisation of the residue samples showed that formation of the Cu minerals, bornite, chalcocite, covellite and digenite, was possible (Nyembwe et al., 2018). Furthermore, the results revealed the possible formation of the Fe species, magnetite and hematite. The intermediate phases formed during mineral dissolution of the treated and untreated chalcopyrite-containing minerals can be shown through the following Gibbs equations:

Copper dissolution of intermediate phases present during mineral dissolution of untreated samples:

$$\mathbf{2CuFeS_2 + 2Fe_2(SO_4)_3 = Cu_2S + 6FeSO_4 + 3S}\ \textit{(Chalcocite)} \qquad \textbf{Eq 18}$$

$$\mathbf{18CuFeS_2 + 9Fe_2(SO_4)_3 = 2Cu_9S_5 + 27FeSO_4 + 13S}\ \textit{(Digenite)} \qquad \textbf{Eq 19}$$

Equation for intermediate phases present in treated and untreated samples:

$$\mathbf{5CuFeS_2 + 4Fe_2(SO_4)_3 = Cu_5FeS_4 + 12FeSO_4 + 6S}\ \textit{(Bornite)} \qquad \textbf{Eq 20}$$

$$\mathbf{CuFeS_2 + Fe_2(SO_4)_3 = CuS + 3FeSO_4 + S}\ \textit{(Covellite)} \qquad \textbf{Eq 21}$$

Equations for complete dissolution of copper from the intermediate phases:

$$\mathbf{Cu_5FeS_4 + 6Fe_2(SO_4)_3 = 13FeSO_4 + 4S + 5CuSO_4}\ \textit{(Bornite)} \qquad \textbf{Eq 22}$$

$$\mathbf{Cu_2S + 2Fe_2(SO_4)_3 = 4FeSO_4 + S + 2CuSO_4}\ \textit{(Chalcocite)} \qquad \textbf{Eq 23}$$

$$\mathbf{CuS + Fe_2(SO_4)_3 = 2FeSO_4 + S + CuSO_4}\ \textit{(Covellite)} \qquad \textbf{Eq 24}$$

$$\mathbf{5Cu_9S_5 + Fe_2(SO_4)_3 = FeSO_4 + S + CuSO_4}\ \textit{(Digenite)} \qquad \textbf{Eq 25}$$

Direct copper dissolution for chalcopyrite:

$$CuFeS_2 + 2Fe_2(SO_4)_3 = CuSO_4 + 5FeSO_4 + 2S \quad \textbf{Eq 26}$$

Equations related to gypsum formation, phase mutation of magnetite and reduction of hematite:

$$CaCO_3 + H_2SO_4 = CaSO_4 + H_2O + CO_2 \quad \textbf{Eq 27}$$

$$4Fe_3O_4 + O_2 = 6Fe_2O_3 \quad \textbf{Eq 28}$$

$$3Fe_2O_3 + H_2 = 2\,Fe_3O_4 + H_2O \quad \textbf{Eq 29}$$

From the chemical reactions presented for the dissolution of copper, it is visible that during chemical leaching of the clean carbonatite mineral, direct mineral dissolution of chalcopyrite can occur. However, the formation of intermediate phases is more likely to occur where the redox potential and alkaline pH conditions are favourable for the formation of bornite, chalcocite, covellite and digenite. In turn, acidic pH conditions, observed for the carbonatite minerals in the presence of added magnetite, were only favourable for phase formation of bornite and covellite. It was also observed that the dissolution of calcium was favoured at 85℃, in carbonatite samples where magnetite was not added, which is shown by the increase in pH as higher concentration of Ca^{2+} ions are released into solution. The formation of insoluble Cu oxide species was also promoted under these alkaline pH and redox conditions. Dissolution of Cu for clean Cr samples at 85℃ was hindered due to the formation of gypsum, which formed a matrix mixture on the surface of the mineral, along with hematite formation; the presence of spinal calcium iron oxide and the existence of elemental sulphur also contributed to the low recovery rates. Additionally, the pH conditions favouring the formation of insoluble copper oxides aided in reducing recovery of Cu in solution (Figure 4-5). During mineral dissolution of the clean Ct samples, the same effects of gypsum were observed, along with solution pH favouring the formation of copper oxides. Furthermore, the formation of the ferric salt, jarosite, also lead to the observed Cu recovery, as jarosite slows the leaching kinetics by restricting mass transfer of ions from the surface of the mineral. During mineral dissolution of the carbonatite minerals (Cr and Ct) in the presence of magnetite, formation of gypsum occurred. Gypsum can form in low pH conditions (Liu et al., 2015) where Ca is prone to form sulphide compounds in the presence of sulphuric acid (Antonijevic & Bogdanovic, 2004). The formation of gypsum aided in keeping the pH conditions in the desired range (pH 1-2), as Ca favoured the formation of $CaSO_4$ above that of Ca^{2+} seen in the speciation results (Table 4-2), thereby keeping pH stable, as there is less competition with hydrogen ions in solution.

Similar to the mineral dissolution behaviour of the carbonatite ore, the accumulation of covellite (7.42-10.79% for Sr and 0.25-0.65% for Sr_mag) during the chemical leaching process indicated that direct dissolution of Cu from $CuFeS_2$ during leaching of the silicate host mineral was less likely to occur. This is strengthened further by the formation of other Cu-intermediate species, bornite, chalcocite, digenite and djulerite for untreated Sr and bornite for Sr_mag. Covellite is, however, the only Cu mineral that increased in concentration during the leaching process, indicating that the

mineral is refractory in solution, which is also shown by the positive Gibbs free energy for Eq 24 (Doman & Alper, 1981). The solution pH for the untreated Sr minerals was in the desired range (pH 1-2) for extraction of Cu from the surface of the chalcopyrite mineral, as its can be seen from the Cu recovery curve. An alternative catalytic surface for ferric reduction through galvanic interaction with pyrite minerals, present in solution, aided the observed recovery behaviour further (Schaming, 2011; Khoshkhoo et al., 2014). The low pH conditions observed during mineral dissolution of the treated silicate mineral were sufficient for desired Cu recovery, however, at these low pH conditions (pH of 0.94) precipitation of ferric ion as jarosite occurred, which shows how readily ferric salts hydrolyse (Cordoba et al., 2008a); formation of gypsum during mineral dissolution of the Sr_mag samples also occurred at these conditions. The formation of these minerals, which are absent in the untreated mineral, lead to the lower recovery rates, as observed during mineral dissolution of the silicate ore treated with magnetite, as opposed to that of the untreated Sr mineral.

Table 4-5: Gibbs free energy of associated reaction equations at 85℃

Equation	**ΔG**
Eq18	-32.003
Eq20	-71.017
Eq21	-19.093
Eq22	-14.620
Eq23	-2.251
Eq24	1.966
Eq26	-17.127
Eq27	-35.154

4.4 Conclusion and recommendations

The purpose of this study was to evaluate the recovery of Cu from the chalcopyrite-bearing ores in a sulphuric acid solution with ferric sulphate as oxidant at fixed temperature conditions, with particular focus on the effects of magnetite (as an additive) on species formation during mineral dissolution and the influence on Cu recovery. Additionally, species formation and recovery from different samples streams from the same carbonate complex were compared.

Calcite-magnesium, along with dolomite for Cr and Gehlenite for Ct, played important roles during the mineral dissolution of Cu, as they were the main source of Ca released into solution. Lower concentrations of Ca at Ct resulted in lower pH compared to the Cr samples. At the alkaline pH conditions observed for both minerals, the solubility of metals are reduced, as seen from the formation of insoluble CuO species. The formation of gypsum also contributed to reduced recovery, as the chalcopyrite mineral was enclosed by a matrix mixture of gypsum, encapsulating undissolved minerals and hindering further dissolution. In the case of Ct, the formation of the ferric salts, further contributed to the formation of the passivation layer. Mineral dissolution in the presence of magnetite in a 1:1 solution reduced the initial Ca concentration in solution, thereby stabilising pH to the desired range (pH 1-2). At high H_2SO_4 concentrations recorded for the treated carbonatite minerals, gypsum formation occurred along with jarosite formation, although minimized; regardless, the passivation of $CuFeS_2$ was not reached during the 12 hours leaching period as the solubility of Cu was enhanced at these acidic conditions and dissolution was favourable.

The siliciclastic ore mainly contained different quartz minerals, which constituted 34.6% of the mineral concentration. A further 22.89% of the mineral was comprised of Cu sulphide minerals. Acidic pH conditions were recorded during mineral dissolution of the Sr and Sr_mag samples, as the initial pyrite was oxidised to form H_2SO_4 along with the large concentration of sulphide minerals and low Ca concentration favourable for solubility of hydronium ions in solution. At these low pH conditions (pH 1-2), dissolution of Cu was favourable; secondary formation of pyrite minerals further aided the recovery through galvanic interaction with chalcopyrite. Although still favourable for Cu dissolution (high recoveries of 15.78%), the pH conditions during leaching of Sr in the presence of magnetite favoured the formation of jarosite. The formation of gypsum was also favoured during dissolution in the presence of magnetite, as was the formation of additional magnetite, above that of pyrite, thus, lowering the effects of Galvanox interaction on the surface of the chalcopyrite-containing mineral.

It is recommended that a study is conducted over a wider temperature range, to incorporate the effects of magnetite on the dissolution behaviour of chalcopyrite-containing ores at lower temperature conditions. The study should, furthermore, compare the dissolution behaviour of the chalcopyrite-bearing minerals at static pH conditions, to determine whether addition of additives or injection of acids result in better recovery behaviour.

References

Acero, P., Cama, J., Ayora, C. & Asta, M., 2009. Chalcopyrite dissolution rate law from pH 1 to 3. *Geologica Acta,* 7(3), pp. 389-397.

Antonijevic, M. & Bogdanovic, G., 2004. Investigation of the leaching of chalcopyrite ore in acidic solutions. *Hydrometallurgy,* 73(2), pp. 245-56.

Aydogan, S., Ucar, G. & Canbazoglu, M., 2006. Dissolution kinetics of chalcopyrite in acidic potassium dichromate solution. *Hydrometallurgy,* 81(1), pp. 45-51.

Banerjee, P., Chakrabarti, B. & Das, A., 1990. Silver-catalysed hydrometallurgical extraction of copper from sulfide ores from Indian mines. *Hydrometallurgy,* 25(3), pp. 349-355.

Barlow, B., Nyembwe, K., Wanders, F. & Fosso-Kankeu, E., 2018. *Prediction of dissolution of copper from a chalcopyrite carbonatite ore of South Africa.* CapeTown, South Africa, s.n., pp. 99-103.

Barnes, S., Maier, W. & Ashwal, L., 2004. Platinum-group element distribution in the Main Zone and Upper Zone of the Bushveld Complex, South Africa. *Chemical Geology,* 208(1-4), pp. 293-317.

Berry, V., 1978. Galvanic interaction between chalcopyrite and pyrite during bacterial leaching of low grade waste. *Hydrometallurgy,* 3(4), pp. 309-326.

Beverskog, B. & Puigdomenech, I., 1996. Revised pourbaix diagrams for iron at 25-300 C. *Corrosion Science* , 38(12), pp. 2121-2135.

Boutroy, E. et al., 2014. Magnetite composition in Ni-Cu-PGE deposits worldwide and its application to mineral exploration. *Journal of Geochemical Exploration,* Volume 145, pp. 64-81.

Burkin, A., 1982. Composition and phase changes during oxidative acid leaching reactions. In: *Hydrometallurgical process fundamentals.* New York: Plenum Press, pp. 113-123.

Calvo, G., Mudd, G., Valero, A. & Valero, A., 2016. Decreasing ore grades in global metallic mining: A theoretical Issue or a global reality?. *Resources,* 5(4).

Cordoba, E., Munoz, J., Blazquez, M. & Ballester, A., 2008a. Leaching of chalcopyrite with ferric ion Part I: General aspects. *Hydrometallurgy,* 93(3-4), pp. 81-87.

Cordoba, E. et al., 2008b. Leaching of chalcopyirte with ferric ion Part II: Effect of redox potential. *Hydrometallurgy,* 93(3-4), pp. 88-96.

Dare, S., Barnes, S. & Beaudoin, G., 2012. Variation in trace element content of magnetite crystallized from a fractionating sulfide liquid. *Geochim Cosmochim Acta,* Volume 88, pp. 27-50.

Dare, S. et al., 2014. Trace elements in magnetite as petrogenetic indicators. *Mineralium Deposita,* 49(7), pp. 785-796.

Dixon, D., 2008. Galvanox: A novel galvanically-assisted atmospheric leaching technology for copper concentrates. *Canadian Metallurgical Quarterly,* 47(3), pp. 327-336.

Doman, R. & Alper, A., 1981. Refractory minerals. In: *Mineralogy: Encyclopedia of earth science.* Boston: Springer.

Fosso-Kankeu, E., Barlow, B., Lemmer, N. & Waanders, F., 2017. *Geochemical Speciation of Metal Ions in the Leachate of Tailings Treated with Synthetic Rain Water*. Parys, South Africa, s.n., pp. 19-23.

Gorbachev, V., Abzalov, V. & Yur'ev, B., 2007. Conversion of magnetite to hematite in iron-ore pellets. *Steel in Translation,* 37(4), pp. 336-338.

Hackl, R., Dreisinger, D., Peters, E. & King, J., 1995. Passivation of chalcopyrite during oxidative leaching in sulfate media. *Hydrometallurgy,* 39(1-3), pp. 25-48.

House, C., 1987. Potential-pH diagram and their application to hydrometallurgical systems. In: *Separation Processes in Hydrometallurgy.* Chichester: Ellis Horwood, pp. 3-19.

Khoshkhoo, M., 2014. *Chalcopyrite Disolution in Sulphate-Based Leaching and Bioleaching Systems,* s.l.: s.n.

Khoshkhoo, M., Dopson, M., Schukarev, A. & Sandstrom, A., 2014. Electrochemical simulatoin of redox potential development in boileaching of a pyritic chalcopyrite concentrate. *Hydrometallurgy,* 14(7), pp. 144-145.

Koleini, S., Aghazadeh, V. & Sandstrom, A., 2011. Acidic sulphate leaching of chalcopyrite concentrates in presence of pyrite. *Minerals Engineering,* 24(5), pp. 381-386.

Lamar, J. E., 1961. *Uses of Limestone and Dolomite,* Urbana: s.n.

Li, J. et al., 2010. Chalcopyrite leaching: the rate controlling factors. *Geochimica et Cosmochimica Acta,* 74(10), pp. 2881-2893.

Liu, K., Deng, M. & Mo, L., 2015. Influence of pH on the formation of gypsum in cement materials during sulfate attack. *Advances in Cement Research,* 27(8), pp. 487-493.

Lu, D., Wang, W., Xie, F. & Jiang, K., 2016. *Thermodynamic Analyses of Possible Chalcopyrite Dissolution Mechanism in Sulfuric Acidic Aqueous Solution,* Shenyang: s.n.

Mudd, G. & Weng, Z., 2012. Base Metals. In: J. L. Trevor M. Letcher, ed. *Materials for a Sustainable Future.* s.l.:Royal Society of Chemistry, pp. 11-59.

Namur, O. et al., 2010. Crystallization sequences and magma chamber processes in ferrobasaltic Sept Iles layered intrusion, Canada. *Journal of Petroleum Science and Engineering,* 51(6), pp. 1203-1236.

Nyembwe, K., Fosso-Kankeu, E. & Waanders, F., 2019. Structural, composition and mineralogical characterization of carbonatitic copper sulfide: Run of mine, concentrate and tailings. *International Journal of Minerals, Metallurgy and Materials,* 26(2), pp. 143-151.

Nyembwe, K., Fosso-Kankeu, E., Wanders, F. & Malenga, E., 2018. *Mineralogical observation made during the kinetic dissolution study of chalcopyrite mineral in sulphate media under free pH at room temperature.* Cape Town, s.n.

Pawlek, F., 1976. The influence of grain size and mineralogical composition on the leachability of copper concentrates. In: *Extractive Metallurgy of Copper.* 2 ed. s.l.:s.n., pp. 690-705.

Prince, D. & Warren, G., 1986. The influence of silver ion on the electrochemical response of chalcopyrite and other mineral sulfide electrodes in sulfuric acid. *Hydrometallurgy,* 15(3), pp. 303-324.

Salgado, P. et al., 2013. Fenton reaction driven by iron ligands. *Journal of Chilean Chemical Society,* 58(4), pp. 2096-2100.

Santos, A., Arena, F., Benedetti, A. & Bevilaqua, D., 2017. Effect of redox potential on chalcopyrite dissolution imposed by addition of ferrous ions. *Eclética Química Journal,* 42(1), pp. 40-50.

Schaming, J., 2011. *An investigation of leaching chalcopyrite ores.* Kingston, Ontario: Queen's University.

Skinner, H. & Jahren, A., 2003. Biomineralization. In: *Treatise on geochemistry.* s.l.:Elsevier, pp. 117-184.

Stiggov, B., 2013. *Field measurements of oxidation-reduction potentail (ORP),* Athens, GA: US Environmental Protection Agency.

Toplis, M. & Carrol, M., 1995. An experimental study of the influence of oxygen fugacity on Fe-Ti oxide stability, phase relations, and mineral— melt equilibria in ferro-basaltic systems. *Journal of Petrology,* 36(5), pp. 1137-1170.

Townsend, H., 1970. Potential-pH diagram at elevated temperature for the system Fe-H2O. *Corrosion Science,* 10(5), pp. 343-358.

Chapter 5: Conclusion and recommendations

Hydrometallurgical extraction is the desired leaching process for recovery of Cu from the surface of chalcopyrite, although extraction is hindered by the formation of a passivation film. The primary aim of the study was to comparatively evaluate the copper recovery rate from two different chalcopyrite mineral namely carbonatite and silicate. This aim was achieved by exposing the minerals to the same experimental conditions and allowing pH evolution to occur, rather than keeping pH stable. This aided in observing the effects of the gangue minerals present in each of the studied ores. The main approach involved treating samples of each of the chalcopyrite-containing ores with sulphuric acid in a ferrous sulphate medium of determined concentration. This was done to achieve the initial acidic pH suitable for the extraction of Cu from the minerals. The main parameters considered for assessing the extraction behaviour of copper from the chalcopyrite-containing minerals were solution temperature, ORP, Cl^- and SO_4^{2-} concentrations and solution pH. The solution temperature was varied over a wide range, from 25℃ up to 85℃, with increments of 20℃.

Desired extraction behaviour was obtained during mineral dissolution at lower temperature conditions for the carbonatite (ROM) host ore. pH evolution of the carbonatite mineral displayed alkaline behaviours, as acid consumption in solution occurred due to high concentration of Ca, which released in solution as a free hydrated ion, (Ca^{2+}). These ions competed with H^+ and resulted in pH neutralisation. This behaviour was enhanced by an increase in temperature, therefore revealing the tendency for calcium to thermodynamically form higher concentrations of free hydrated ions at elevated temperature conditions. Kinetic dissolution behaviour displayed the best recovery rates at lower temperature conditions, as these conditions were favourable for the formation of insoluble salt species of Ca ($CaSO_4$). This reduced the competition with H^+ ions, and allowed for the formation of acidic conditions in which the solubility of metals were increased. The Pourbaix diagram for Cu and Fe was used to explain the diffraction behaviour of the mineral residue sample. It indicated copper's tendency to form insoluble copper oxide species at elevated temperature conditions, further strengthening the observed recovery behaviour. The formation of gypsum was also thermodynamically favoured with a rise in temperature, increasing the likelihood for the surface of the mineral to be enclosed by a matrix mixture of gypsum. Although favourable at 25℃, extraction rates of copper decreased during the course of the leaching tests. This was as a result of the formation of gypsum, the presence of spinal calcium iron oxide, and the existence of elemental sulphur which all contributed to the passivation phenomenon.

As the clastic mineral contained high concentration (29.79%) of sulphide species, the pH behaviour was mostly acidic and, which was generally more stable compared to the carbonatite mineral. Initial concertation of pyrite aided in stabilising the pH behaviour, as oxidation of the Fe sulphide mineral contributed to higher concentrations of H_2SO_4 in solution. The formation of additional pyrite

improved the dissolution of Cu, as it provided an alternative catalytic surface for ferric reduction. The formation of an intermediate phase of covellite enhanced leaching as a secondary reaction between covellite and hydrogen ions promoted further formation of soluble free hydrate Cu ions. The greatest recovery rates for the clastic mineral were observed at 85°C, where 19.49% recovery of Cu was achieved after 12 hours dissolution. This corresponds with results of other studies, which found that extraction of Cu from chalcopyrite was most favourable at low pH (pH 1-2) and under higher temperature conditions.

The aim of the study was, furthermore, achieved by assessing the impact of an additive such as magnetite on the extraction behaviour of Cu from various chalcopyrite minerals at constant temperature. The effects of gangue minerals from different sample streams (ROM and tails) of the same carbonate mineral were also evaluated. The addition of magnetite in a 1:1 ratio to these carbonate sample streams resulted in the reduction of the initial concentration of Ca. The pH was stable at acidic conditions (pH 1-2) due to a reduction in the rate of acid consumption. There was accumulation of gypsum during the course of the leaching process; this was favoured by low pH conditions and relatively high levels of H_2SO_4. The accumulation of jarosite was also observed. Although gypsum and jarosite were present, the pH (and temperature) was in the desired range for enhancing solubility of the Cu. After 12 hours of leaching, no obvious passivation could be observed as Cu recovery was relatively high (12.84% and 20.94% from Cr and Ct respectively) and still increasing. Better recoveries observed for Ct compared to Cr are the result of lower initial concentrations of Ca enabling more acidic conditions and lower formation of gypsum. The concentrations of FeO(OH) and Fe_3O_4 accumulated at higher concentrations in the Ct mineral residue, allowing for lower formation of competing ferrous ion species. Higher jarosite concentration in the Cr mineral strengthened the observed recovery of both carbonate samples streams further. For the clastic mineral, the recovery was lower in the presence of magnetite. Unlike in the untreated mineral, pH levels were favourable for jarosite formation (pH <1). Residue characterisation revealed the formation of gypsum and magnetite and lower concentration of pyrite – all contributing to lower recovery rates compared to untreated siliciclastic mineral (15.78% compared to 19.49%).

In this study pH evolution was allowed to take place such as to effectively evaluate to what extent the gangues from various minerals can affect the dissolution of chalcopyrite. It is recommended that with the knowledge of the effects of gangues observed in this study, that static (controlled) pH tests be implemented. This should be conducted over the same temperature range, to evaluate the recovery of copper from both minerals under acidic conditions. The study also recommends investigating magnetite as an additive over a wider temperature range, and at different concentrations, for further analysis of the effect of addition of additives on copper recovery; as the impact of passivation was not significant after 12 hours leaching in the presence of magnetite. It is also advised that leaching experiments are conducted for an extended period of time, to evaluate the effects of further

accumulation of gypsum and jarosite on the recovery rate of Cu. Furthermore, the effects of other additives, such as pyrite or silver, on the specific chalcopyrite-bearing minerals, should also be considered.

Appendix A: Titration equations

Chloride ion concentration

$$\boldsymbol{T_c = \frac{(V_t \times 1000)}{(V_s)}} \quad \text{(Eq 30)}$$

Tc = Total chloride concentration

Vs = volume of the solution

Vt = volume of the titrant

Total Alkalinity

$$\boldsymbol{T_{al} = \frac{(V_{H_2SO_4} \times 1000)}{(V_s)}} \quad \text{(Eq 31)}$$

Tal = total alkalinity

VH2SO4 = volume of sulphuric acid titrant

Total Acidity

$$\boldsymbol{T_{ac} = \frac{(V_t \times 1000 \times CF)}{(V_s)}} \quad \text{(Eq 32)}$$

CF = correction factor

Tac = total acidity

Appendix B: Experimental equipment

Figure B- 1: Hanna Instruments 8424 pH meter

Figure B- 2: Hanna Instruments 83099 COD and Multiparameter Photometer

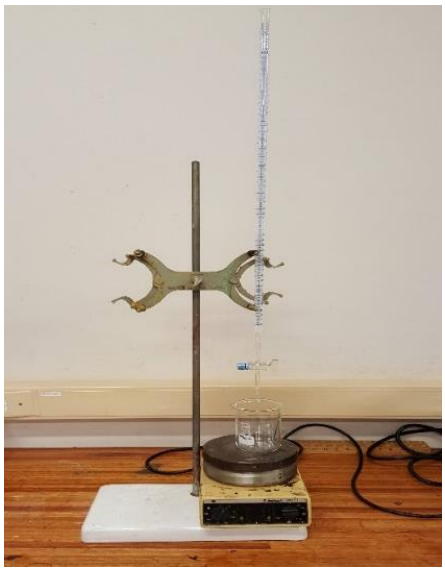

Figure B- 3: Titration equipment (beaker, burette & magnetic stirrer)

Figure B- 4: Example of tight seal plastic container (carbonatite ROM)